NTNU – Trondheim
Norwegian University of
Science and Technology

Modeling wax thickness in single-phase turbulent flow

Kjetil Kandal Botne

Earth Sciences and Petroleum Engineering
Submission date: June 2012
Supervisor: Jon Steinar Gudmundsson, IPT

Norwegian University of Science and Technology
Department of Petroleum Engineering and Applied Geophysics

Abstract

Oil and gas transport is today a vital part of the industry. Oil cooled during transport in pipelines may precipitate paraffin wax. Precipitated wax may deposit on pipe walls and cause flow restrictions. Deposition models are used to understand and predict deposition of solids. A deposition model can help predict wax problems before a pipe line is set into operation. If the amount of deposited wax is predicted it can help operators to develop removal plans and strategies.

A total of 21 wax deposition experiments performed by others were digitized and evaluated. The logarithmic deposition-release model showed a good match with 18 of the experiments. The experiments tested the effect of varying flow rate, temperature or both. Most experiments behaved as expected when flow rate and temperature were varied.

The deposition-release model consists of two coefficients, k_1 and k_2. Both coefficients were evaluated against wall shear stress for the varying rate experiments. The coefficients in the varying temperature series were evaluated against the temperature driving force. Linear trends between most coefficients and physical parameters were found. These linear trends lead to the development of four models that predict wax deposition. The models use either wall shear stress, the temperature driving force or both as an input. All models produce similar results. Each model was based on an experimental series.

A study of a real pipeline with wax deposition was also investigated. Temperature and viscosity calculations matched well with values used in the study. The study reported calculated wax thickness based on measurements of pressure drop. The pressure drop method was evaluated and explained. The method does not consider an altered pressure drop due to increased pipe roughness and non-evenly distribution of deposits. Both of these effects will increase the pressure drop. It was found that neglecting these will cause the calculated thickness to be overestimated. Because of the overestimation of thickness it was hard to get an accurate match with models.

Sammendrag

Transport av olje og gass er i dag en viktig del av industrien. I oljer som kjøles under transport i rørledninger kan vil utfelles parafin voks. Utfelt voks kan avsettes på rørveggene og vil føre til restriksjoner for oljestrømmen. Avsetningsmodeller brukes i dag for å forutse problemer med voks før en rørlinje tas i bruk under produksjon. Dersom mengden av avsatt voks kan forutsees, vil dette hjelpe operatører med å utvikle planer for fjerning av voks. Voksen kan da bli fjernet før det oppstår store problemer.

Totalt 21 voks avsetnings eksperimenter utført av andre har blitt digitalisert og vurdert. Den logaritmiske avsetnings og ta vekk modellen viste seg å passe godt med 18 av disse eksperimentene. Eksperimentene ble testet for varierende strømningsrate, varierende temperatur eller begge disse. De fleste eksperimentene oppførte seg som forventet når strømningsrate og temperatur ble endret.

Avsetnings og ta vekk modellen består av to koeffisienter, k_1 og k_2. Begge koeffisientene ble vurdert mot vegg skjær spenning for eksperimentene med varierende strømningsrate. Koeffisientene for den varierende temperatur serien ble vurdert mot temperaturen drivkraften. Det ble observert lineære trender mellom de fleste koeffisientene og fysiske parametere. Disse lineære trendene førte til utviklingen av fire modeller som kan forutse voksavsetning. Hver modell tilhører sine eksperimenter, men er relativt like. Disse modellene trenger enten vegg skjær spenning, temperatur drivkraft eller begge disse som input. All modellene produserer relativt like resultat.

En studie av en ekte undervanns rørledning har også blitt undersøkt. Temperatur og viskositetsberegninger stemte godt overens med data fra studien. Studien rapporterte voks tykkelse basert på målinger av trykk tap i rørledningen. Trykktapsmetoden er blitt forklart og vurdert. Metoden tar ikke hensyn til økt ruhet i rørledningen som følge av voksavsetning. Den tar heller ikke hensyn til at voksen ikke er spred jevnt utover i hele røret. Begge disse effektene vil øke trykktapet i rørledningen. Om disse to sees bort i fra vil beregninger på vokstykkelse gi et overestimert anslag på vokstykkelsen.

Preface

This master thesis was submitted as a fulfillment of the TPG 4905 Petroleum Technology – Petroleum Production master thesis. TPG 4905 is a compulsory subject in the 10th semester in Petroleum Production at the Norwegian University of Science and Technology (NTNU). The topic for the master thesis was discussed and developed in collaboration with my supervisor Professor Jon Steinar Gudmundsson at the Department of Petroleum Engineering and Applied Geophysics at NTNU. The work of the thesis was carried out from January to June 2012.

I would like to thank professor Gudmundsson for excellent guidance and good discussions throughout the semester. All inputs have been appreciated. I would also like to thank my fellow students for discussions and inputs.

Table of contents

1. Introduction

Wax deposition in oil and gas production is one of the major flow assurance challenges the industry faces today. Wax deposition is mostly a temperature driven process which means that subsea pipelines are especially vulnerable. Increased production in deeper waters and artic environment makes prevention of wax deposition very important. Wax precipitates from oil when it is cooled and the wax may deposit on pipeline walls. Wall deposits can lead to severe problems and need to be removed in an efficient way. It is difficult to perform accurate deposition measurements on real pipelines. Models are often developed and tuned with help from flow loop experiments. A model developed from deposition experiments could be scaled up to field data and used to predict deposition of solids.

The main part of this thesis is a continuation of my semester project called "Modeling wax deposition with deposition-release models". In the semester project the exponential and logarithmic deposition-release models were investigated. The models were tested against deposition experiments presented by Rosvold (2008). The logarithmic deposition-release model proved to be the most accurate model to these experiments. In this thesis the logarithmic deposition-release model was tested further against other flow experiments. The model was matched to the experiments and evaluated. The physical dependencies of the model were then investigated.

The focus of the work has been on the use of deposition-release models for build-up of wax deposits with time. The vast literature of paraffin wax deposition was not reviewed. Instead, the emphasis has been on the theses and other works that present data; laboratory data and field data. A lot of time has been used to digitize the published data properly. The digitized data tables are not included in the thesis itself. Instead, the thesis contains at the back cover a CD-disc with the data used. The data will also be made available on the home page of my supervisor Professor Jon Steinar Gudmundsson with the link http://www.ipt.ntnu.no/~jsg/studenter/diplom/diplom.html .

The second part of the thesis investigated a study with deposition data from a real subsea pipeline. The wax thickness calculated from pressure drop was explained and evaluated. Other parameters like viscosity and temperature were also evaluated.

2. Paraffin wax and wax related problems

Deposition of paraffin wax is a major issue in the oil industry. Wax precipitates from both crude oil and condensate when temperature falls below a certain value. As oil temperature decreases further, more wax will precipitate. If wax precipitates it may deposit in pipes and equipment causing flow issues. Wax deposition is mainly a problem in pipelines and in production equipment. Deposited wax in pipelines may cause increased pressure drop, decreased production and lead to clogged pipes. Deposited wax may also damage production equipment or make it less efficient.

Wax molecules are mostly long chain n-alkanes, and weight% of 1-15 is considered typical in both crude oil and condensates (Aske 2011). These n-alkanes normally have a carbon number between C_{20} and C_{40} (Gudmundsson 2010). When oil is cooled below a certain temperature, wax will start to precipitate. This temperature is called the wax appearance temperature (WAT), and it is normally found around 30-40 °C (Gudmundsson 2010). The term cloud point temperature is another term used to describe the WAT. Below the cloud point there is another temperature called the pour point temperature. When the pour point is reached the paraffin wax will become a soft solid (a gel).

Normal ways of preventing wax deposition in pipelines includes heating or insulation, pigging and chemical injection. Active heating is expensive and limited by distance, especially for subsea pipelines. Insulation is common on long land pipelines (Gudmundsson 2010). Pigging is the most common removal technique on subsea pipelines. Pigging removes deposited wax mechanically by scraping it of the wall. In a startup phase pigging is usually performed when wax thickness reaches 2-3 mm (Labes-Carrier 2002). This criterion is set to avoid incidents with a stuck pig. Chemical additives may prevent agglomeration of wax molecules and prevent wax from depositing on the wall (Gudmundsson 2010).

3. Wax deposition mechanisms and deposition models

3.1 Diffusion, aging and shear removal

When oil is transported in a pipeline and the surroundings are cooler than the oil we get heat transfer. Heat is transferred from the hot oil to the cooler surroundings. Most subsea pipelines have sea water temperature below the oil temperature. The velocity profile at the wall in turbulent flow is determined by the universal velocity profile. The velocity profile is also the base for the temperature profile at the wall (Gudmundsson 2010). Since wax precipitation is a function of temperature, the concentration of wax molecules is also dependent on temperature. The concentration profile for wax depends on both the temperature profile and the velocity profile.

A normal transport pipe will have bulk temperature above the solution temperature. The lowest temperature will be at the pipe wall. When temperature drops below the WAT wax starts to precipitate out of solution. Since the temperature varies from the wall and towards the bulk, the degree of precipitation also varies. The lower the temperature the more wax precipitates. The difference in temperature causes a concentration profile, which again causes molecular diffusion. The molecular diffusion will cause particles in solution to move towards the wall. The lowest temperatures are found at the wall and consequently the lowest concentrations of wax are also found at the wall. When particles in solution reach the pipe wall they may deposit on the metal surface or onto an existing layer of wax.

The presence of precipitated wax molecules in the oil leads to a more complicated deposition process (Akbarzadeh and Zougari, 2008). For the most part this has been neglected in wax deposition studies due to its complexity. This might be acceptable in laminar flow, but in turbulent flow eddies carrying wax particles can penetrate the boundary layer (Akbarzadeh and Zougari, 2008). The wax molecules are carried with turbulent eddies and if these hit the wall, wax molecules may deposit.

Deposited wax is not pure wax and often contains some part of trapped oil. The amount of trapped oil inside the wax deposits is sometimes called wax porosity. The wax porosity gives the fractional amount of trapped oil in the deposit. Wax deposition experiments gave a porosity of up to 90 % for soft deposit and 50-72 % for hard deposits (Lund 1998). Aging or internal diffusion is a process that causes deposits to harden. Over time some of the trapped

oil can be replaced by wax molecules through diffusion. This will decrease the porosity of the deposits and cause them to become harder (Akbarzadeh and Zougari, 2008). This process is called aging. Harder deposits can become more difficult to remove from the pipeline. Hard deposits can increase the danger for a stuck pig accident in a pipeline.

Moving fluid will give a shear force at the wall when flowing through a pipe. This shear force may break off deposit from the wall (Akbarzadeh and Zougari, 2008). The phenomenon is also called sloughing. The shear stress can also make it hard for molecules to deposit on the wall. The wall shear stress in a pipe is given by the equation:

$$\tau_w = \frac{1}{8} f \rho_{oil} {u_{oil}}^2 \tag{3.1}$$

Where τ_w is the wall shear stress, f is the friction factor, ρ_{oil} is the density of oil and u_{oil} is the oil velocity. The wall shear stress is proportional to the velocity squared. An increase in velocity will cause a bigger increase in the wall shear stress. Increased shear stress will cause more stress on deposited wax and may also prevent more wax from depositing. An increase in wax thickness will reduce the effective diameter of a pipe. With constant rate the diameter reduction will cause increased velocity and increased wall shear stress.

3.2 Theoretical model

A lot of models use a theoretical basis in order to model deposition of wax. Physical models can start out with a thermodynamic approach or with some physical assumptions. A comparison of mechanisms in single-phase models was shown by Akbarzadeh and Zougari (2008). This comparison can be seen in Figure 1. Molecular diffusion as deposit mechanism is used in all of the models. The molecular diffusion can be estimated through different heat and mass transfer correlations. The latest models shown in Figure 1 also implements shear removal and aging.

In order to utilize deposition models some have been implemented in simulation software. Rosvold (2008) did a review of two deposition models and compared them against single-phase flow loop data. These models are called the RRR model and the Matzain model and are found in the OLGA simulating software. The Matzain model proved to be the most accurate because it implements the use of shear removal. One problem was the extensive tuning necessary in order to match the Matzain model with the flow loop data. Studies by Labes-

Carrier et al. (2002) and Bansal et al. (2012) compared real field data with simulation data. Both studies emphasized the importance in having accurate experimental fluid and wax data in order to get good results.

3.3 Deposition-release model

Another approach to the deposition modeling is to model flow loop results through a semi-empirical method. The deposition data is first matched with a mathematical model. Physical parameters that effect the deposition are then fitted to the mathematical model. The semi-empirical model approach is investigated in this thesis. One such method is to use the deposition-release model proposed by Gudmundsson (2010). The deposition release model says that growth in deposition thickness equals to the rate of deposition minus the rate of removal. Mathematically it would look like this (Bott 1995):

$$\frac{dx}{dt} = x_D - x_R \tag{3.2}$$

Where dx/dt is the growth of deposit thickness, x_D is the deposition rate and x_R is the removal rate.

If the removal rate becomes equal to the deposition rate the growth in thickness will stop. An exponential deposition release model has been showed to work well for different types of deposition situations by Gudmundsson (1981). In the study by Botne (2011) the exponential and logarithmic deposition release models were compared to flow loop data from Rosvold (2008). The logarithmic model was matched very well to seven out of eight experiments.

Possible deposition trends are shown in Figure 2. The shape of the logarithmic model is similar to the logarithmic curve in Figure 2. The basic equation for this curve is:

$$\frac{dx}{dt} = k_1 {k_2}^{-x} \tag{3.3}$$

Where dx/dt is the growth of deposition thickness, x is deposit thickness, k_1 and k_2 are coefficients. When the deposit thickness, x, is zero the k_2^{-x} equals 1. With k_2^{-x} equal to 1, the initial deposition rate $(dx/dt)_{x=0}$ is decided by k_1. When deposit thickness increase the value of k_2^{-x} will go towards zero and the deposit will stop growing. The k_1 coefficient is the initial deposition, while the k_2 coefficient controls the asymptotic deposition. If transferred to Eq. 3.2 the k_1 is the deposition rate and k_2 controls the removal of deposits.

All flow loop data used was presented as the deposition thickness with time. Equation 3.3 can be integrated and rearranged into:

$$x = \frac{1}{ln\ k_2} \ln[1 + (k_1 \ln k_2)t] \tag{3.4}$$

Where t is the time, x is the deposit thickness and k_1 and k_2 are the same as before. The full derivation of this can be seen in Appendix 2. Equation 3.4 will give the deposit thickness at a given time.

4. Experiments

A total of 21 different lab experiments have been evaluated using the logarithmic deposition-release model. The experimental data were given in four different theses. All the experimental data were from single-phase turbulent experiments and have been analyzed using the same method. The experiments were given as plots showing increase in wax thickness with time. All wax thickness measurements were performed by measuring the pressure drop and calculating the wax thickness. The wax deposition data have been digitized using the method described in Appendix A. The digitized deposition data were analyzed and coefficients in the logarithmic deposition-release model were found. The method used to find the model coefficients are given in Appendix C. Detailed information about each experiment is given below.

4.1 Rosvold deposition experiments

These experiments were presented in a master thesis by Rosvold (2008). The experiments were also presented by Hoffmann and Amundsen (2010). The experimental data were modeled and analyzed in my previous project (Botne 2011). The experiments were performed at Statoil's multiphase flow loop laboratory in Porsgrunn. A total of eight deposition experiments were given by Rosvold (2008). The flow loop used was 5.55 m long and had an inner diameter of 52.58 mm. Details about the rig are given in Table 1. All experiments were run with an outside cooling temperature of 10 °C. The experimental rig was operated at atmospheric pressure (Rosvold 2008). Duration of the experiments were between 70 and 320 hours.

The fluid used in the experiments was a North Sea condensate with wax content of about 4.5 weight % (Hoffman and Amundsen 2010). The only fluid data reported by Rosvold (2008) was the wax appearance temperature of 45 °C. A WAT of about 30 °C was reported by Hoffman and Amundsen (2010) for the same experiments. This value was determined through several tests that all came up with a WAT of about 30 °C. A WAT of 26 °C at atmospheric conditions was given in another study of a North Sea gas condensate by Labes-Carrier et al. (2002). The wax content of this condensate was similar at 4.4 %. Using this information it was decided to base calculations on a WAT of 30 °C. All fluid properties are given in Table 2.

4.1.1 Data and experiments

Five experiments tested the effect of varying rate on deposition and kept oil inlet temperature constant. These five experiments are named Rosvold A-E and details are given in table Table 3. The oil temperature was 20 °C for all these experiments. The varying rate experiments are shown graphically in Figure 3. Four experiments tested the effect of oil temperature on deposition and kept flow rate constant. The constant rate was kept at 21 m^3/h. These experiments are named Rosvold F-H and also contain the Rosvold D experiment. The Rosvold D experiment was part of both experimental series. Details from these four experiments are given in Table 4. The varying temperature series are shown graphically in Figure 4.

4.1.2 Use of model

The experiments with varying rate (Rosvold A-E) were performed with a rate between 5 and 25 m^3/h. The rates correspond to flow velocities between 0.66 and 3.31 m/s. A typical fluid velocity for oil in a pipeline would be from 2 m/s to 4 m/s (Gudmundsson 2009). More detailed data about these experiments are given in Table 3. The best match between the model and the five experiments are given in Figure 5 and 6. All five experiments show a pretty good match with the deposition-release model. The coefficients k_1 and k_2 used to model the flow rate experiments are given in Table 5.

The four experiments with varying oil temperature had an oil temperature between 15 and 40 °C. Details from these experiments are given in Table 4. A comparison between the experiments and the model is shown in Figure 7 and 8. The experiments Rosvold D and Rosvold G show a great match with the model. The Rosvold F experiment shows a good match with the model. The model does not fit very well with the Rosvold H experiment. The logarithmic deposition-release does not model the asymptotic level of the Rosvold H experiment very well. That might be because of the big difference between oil and cooling temperature. The coefficients k_1 and k_2 used to model the temperature experiments are given in Table 6.

4.1.3 Coefficient analysis

The experiments are evaluated against the varying parameters. No clear tendency in the k_1 values for the varying rate experiments is seen, values are given in Table 5. The k_2 value on

the other hand show a clear trend of increase with increasing rate. The k_1 values for the varying temperature experiments seem to decline with increasing oil temperature, seen in Table 6. The exception is the Rosvold D experiment which shows a much bigger k_1 value than the others. When evaluating the k_2 coefficients the values seem to increase with increasing oil temperature. Again, the exception is the Rosvold D experiment.

The coefficients in the model were analyzed against physical parameters by Botne (2011). For the varying rate experiments it was found that the k_1 coefficient showed a linear trend against $1/\tau_w$. Coefficient k_1 is plotted against $1/\ \tau_w$ in Figure 9. The trend was observed for Rosvold experiments B, C and E. The k_2 coefficient showed a linear trend with ${\tau_w}^2$. The plot between k_2 and ${\tau_w}^2$ is shown in Figure 10. The linear trend is good for Rosvold experiments A-D while Rosvold E is a bit further from the trend. If k_1 is a linear function of $1/\ \tau_w$ then $k_1 = k_3 + k_4/\ \tau_w$. If k_2 is proportional to ${\tau_w}^2$ then $k_2 = k_5\ {\tau_w}^2$. The new constants or coefficients k_3, k_4 and k_5 are introduced. The same trends are observed if τ_w is replaced with Re in Figure 9 and 10. Using these new constants Eq. 3.3 can be rewritten to:

$$\frac{dx}{dt} = \left(k_3 + {k_4}/{\tau_w} \right) ({k_5 {\tau_w}^2})^{-x} = \frac{k_3 + {k_4}/{\tau_w}}{{k_5}^x {\tau_w}^{2x}} \qquad 4.1$$

where $k_3 = -0.321$, $k_4 = 2.55$ and $k_5 = 39.2$.

The varying temperature experiments are performed with the same flow rate. The coefficients are therefore only evaluated against a temperature dependent parameter. A coefficient called the temperature driving force, ΔT^+, was introduced by Gudmundsson (2010). The temperature driving force is calculated by $\Delta T^+ = (T_c - T_{wall})/T_{oil}$. T_c is the cloud point temperature (WAT), T_{wall} is the inner wall temperature and T_{oil} is the oil temperature. The ΔT^+ is calculated using wall temperatures given by Hoffmann and Amundsen (2010). The four k_1 coefficients are plotted against ΔT^+ in Figure 11. A linear trend between three of the coefficients is seen. Coefficient k_2 for the varying temperature series are plotted against $1/\ \Delta T^+$ in Figure 12. A linear trend between three of the coefficients is observed. The Rosvold D experiment does not match either of the observed trends. The linear trends suggest that k_1 is proportional to ΔT^+, $k_1 = k_3\ \Delta T^+$. The trend also suggests that k_2 is proportional to $1/\ \Delta T^+$, $k_2 = k_4/\ \Delta T^+$. Constants k_3 and k_4 does not have the same values as above. Eq. 3.3 can be rewritten to:

$$\frac{dx}{dt} = k_3 \Delta T^+ \left({}^{k_4}/_{\Delta T^+}\right)^{-x} = \frac{k_3 \Delta T^+}{\left({}^{k_4}/_{\Delta T^+}\right)^{x}} = \frac{k_3 (\Delta T^+)^{1+x}}{{k_4}^{x}} \qquad 4.2$$

where $k_3 = 5.72 \times 10^{-2}$ and $k_4 = 1.31 \times 10^{2}$.

4.1.4 Particle mass transfer coefficient

The particle mass transfer coefficient was calculated and compared to values of k_1. The particle mass transfer coefficient was calculated using the friction velocity and dimensionless mass transfer coefficient. Using data from Rosvold (2008) a parameter called the particle relaxation time was calculated. Assuming different wax particle sizes the flow regime of particles was determined to be in the diffusion regime (Gudmundsson 2010). The diffusion regime established the size of the dimensionless mass transfer coefficient. A more detailed description of particle mass transfer coefficients and how they were calculated is found in Appendix D.

Values of k_1 for the varying flow rate experiments were compared to the particle mass transfer coefficients in Table 7. For comparison the k_1 values were changed from mm/h to m/s. The values of the k_1 coefficients were much lower than the calculated particle mass transfer coefficients. How k_1 coefficients and particle mass transfer coefficients change with flow rate are shown in Figure 13. The particle mass transfer coefficients increased with increasing flow rate. As mentioned above only three k_1 coefficients behaved similar when flow rate increased. These three k_1 values decreased with increasing flow rate. The mass transfer coefficients and k_1 coefficients show opposite trends for increasing flow rate.

4.2 Hernandez deposition experiments

Extensive research on wax deposition has been carried out at the University of Tulsa. The experiments were part of the Tulsa University Paraffin Deposition Projects (TUPDP) and were presented by Hernandez (2002). Many flow loop experiments were done and tested to determine dependencies on several effects by Hernandez (2002). Some of the dependencies tested were shear stress, aging, temperature gradient, flow regime and fluid properties. The test rig was 50 m long and had an inner diameter of 43.6 mm. Duration of the experiments were about 25 hours. Detailed rig information is given in Table 8.

4.2.1 Data and experiments

A total of six experiments from Hernandez (2002) had the desired properties. The experiments are named Hernandez A-F. These experiments tested the effect of shear stress and temperature gradient. To test the effect of shear the flow rate was varied. The fluid used in the experiments was a single-phase condensate from Shell's Gordon Banks field in the Gulf of Mexico. The fluid had a WAT of 34.44 °C and a wax content of 0.5 wt. %. Key fluid parameters are given in Table 9. All experiments were performed under turbulent flow conditions. A digitized version of all six experiments as they were given by Hernandez (2002) can be seen in Figure 14.

4.2.2 Use of model

All six series were run with the same oil temperature of 29.4 °C, but the flow rate and cooling temperature were varied. The difference between oil and cooling temperature outside the pipe was called ΔT ($\Delta T = T_{oil} - T_{cool}$). Hernandez experiments A-C were performed with ΔT = 16.7 °C and Hernandez D-F were performed with ΔT = 8.3 °C. The flow rates were 1000, 1500 or 1800 BPD for one experiment per cooling temperature. These flow rates correspond to a flow velocity between 1.24 and 2.23 m/s. Detailed data for each experiment is given in Table 10 and 11.

The best match between deposition-release model and the Hernandez A-C is given in Figure 15. It is clear that all three experiments show a fairly good match with the model. The best match between the model and Hernandez D-F experiments is shown in Figure 16 and 17. The D-F series are performed with a low ΔT and show some instability. Not all experiments follow the expected logarithmic trend. The model is quite good for Hernandez experiments D and F. But it struggles with the asymptotic level seen in Hernandez E.

4.2.3 Coefficient analysis

Coefficients k_1 and k_2 used to model all six experiments are given in table 12. Since these series have varying rate (velocity) and temperature (cooling) the effect of these parameters were investigated. Coefficient k_1 increase when ΔT increases from 8.3 °C to 16.7 °C. It is harder to see a definitive trend when varying the rate. Based on the three experiments Hernandez A-C the coefficient k_2 increase with increasing rate. No specific trend on coefficient k_2 is observed between experiments D-F.

The flow rate dependency and the temperature dependency were investigated at the same time. This is possible because the same flow rates were tested for the same ΔT. The coefficient k_1 for all six experiments is plotted against $\Delta T^+/\tau_w$ in Figure 18. The temperature driving force (ΔT^+) and wall shear stress (τ_w) has been explained above. A linear trend is observed between at least four of the k_1's and $\Delta T^+/\tau_w$. If k_1 is plotted against ΔT^+/Re the same linear trend is observed. Coefficient k_2 plotted against $\tau_w^2/\Delta T^+$ also show a possible linear trend between four of the points. This is shown in Figure 19.

The wall temperature needed in the calculation of the temperature driving force is not given by Hernandez (2002). Instead of the wall temperature the cooling temperature outside the pipe (T_{cool}) was used. The difference between T_{wall} and T_{cool} may not be significant for a thin steel pipe. If τ_w is replaced with Reynolds number the same linear trend is seen. The linear trends show that k_1 might be proportional to $\Delta T^+/\tau_w$ and k_2 might be proportional to $\tau_w^2/\Delta T^+$. Coefficients can be rewritten as $k_1 = k_3\, \Delta T^+/\tau_w$, and $k_2 = k_4\, \tau_w^2/\Delta T^+$. The wall shear stress could be replaced by Reynolds number with altered values of k_3 and k_4. These new constants do not have the same values as the constants used above. Eq. 3.3 can be rewritten as:

$$\frac{dx}{dt} = \left(k_3 \frac{\Delta T^+}{\tau_w}\right)\left(k_4 \frac{{\tau_w}^2}{\Delta T^+}\right)^{-x} = \frac{k_3}{{k_4}^x}\ \frac{{\Delta T^+}^{1+x}}{{\tau_w}^{1+2x}} \qquad 4.3$$

where $k_3 = 0.483$ and $k_4 = 0.871$.

4.3 Lund deposition experiments

Experiments were also performed by the University of Tulsa prior the TUPDP that Hernandez (2002) was a part of. The predecessor of the TUPDP was a Joint Industry Project titled "Paraffin Deposition Prediction in Multiphase Flowlines and Wellbores". Experiments performed in this project were presented by Lund (1998). Three experiments presented by Lund (1998) were comparable to the data in this thesis. These three series are presented in Figure 20. The fluid used by Lund (1998) was a crude oil from Mobile Oil Co.'s South Pelto field in the Gulf of Mexico. The fluid had a WAT of 49 °C and a wax content of 5 wt %. Fluid parameters are given in Table 13.

4.3.1 Data and experiments

The three experiments from Lund (1998) were performed with different cooling temperatures. The experiments are named Lund A-C. Experiments were performed in the same rig as used by Hernandez (2002). The rig is 50m long and has an inner diameter of 4.36 cm (1.715 inches). More rig properties are given in Table 8. The oil temperature in these experiments was kept constant at 40.6 °C. The outside cooling temperature was varied and ΔT (= T_{oil} – T_{cool}) of 8.3 °C, 16.7 °C and 25 °C was reported. All three series were performed with a flow rate of 1500 BPD which corresponds to 1.85 m/s. The duration of the experiments was about 24 hours.

4.3.2 Use of model

The three experiments are compared with the logarithmic deposition-release model in Figure 21. Lund experiment A with a ΔT of 8.3 °C shows some instability below 5 hours. The pressure drop method gives a negative deposition, seen in Figure 20. This trend cannot be modeled by the deposition-release model. One possible explanation of this phenomenon is that the initial deposition is smoother than the original pipe. The pressure drop decrease compared to a clean pipe and gives negative thickness. The measured deposition thickness for experiment A after about 24 hours is well matched by the model, as seen in Figure 21. The model correlates well with Lund experiments B and C as seen in Figure 21.

4.3.3 Coefficient analysis

All Lund experiments were performed with the same flow rate and therefore have the same Reynolds number and velocity. Coefficients k_1 and k_2 used to model these three experiments are given in Table 15. These experiments cannot be checked for any rate dependent parameters. The temperature dependence can be evaluated since the cooling temperature was varied. The general trend of coefficient k_1 is an increase with increasing ΔT, seen in Table 15. The given coefficient for Lund experiments A may not be valid because of the instability of the experiment. Coefficient k_2 seem to decrease with increasing ΔT, as seen in Table 15. No information about wall temperature is given, and it cannot be calculated with the given data. As for the Hernandez experiments the temperature driving force (ΔT^+) was therefore calculated using the outside cooling temperature.

Coefficient k_1 is plotted against ΔT^+ in Figure 22. A linear trend is observed, although the Lund A experiment may not be valid as mentioned above. When coefficient k_2 is plotted against $1/\Delta T^+$ the same linear trend is observed. Coefficient k_2 vs. $1/\Delta T^+$ is seen in Figure 23. The trend indicates that k_1 might be a linear function of ΔT^+ and k_2 might be a linear function of $1/\Delta T^+$. The wall shear stress may change slightly due to differences in deposit roughness, but this parameter is not given by Lund (1998). The linearity between k_1 and ΔT^+ can be given by $k_1 = k_3 + k_4\Delta T^+$. The linearity between k_2 and $1/\Delta T^+$ may be given by $k_2 = k_5 + k_6/\Delta T^+$. The new constant values vary from the ones given earlier. Since the temperature dependence is the only parameter checked, equation 3.3 is altered to:

$$\frac{dx}{dt} = (k_3 + k_4\Delta T^+)(k_5 + \frac{k_6}{\Delta T^+})^{-x} = \frac{(k_3 + k_4\Delta T^+)}{(k_5 + \frac{k_6}{\Delta T^+})^x} \qquad 4.4$$

where $k_3 = -4.34\text{x}10^{-2}$, $k_4 = 0.194$, $k_5 = -5.83$ and $k_6 = 9.02$.

4.4 Venkatesan deposition experiments

Venkatesan (2004) presented some turbulent single-phase deposition data in his doctoral thesis. Some of these experiments were comparable with this work. All digitized experiments are given in Figure 24. The fluid used by Venkatesan (2004) was a mixture of 50:50 (by weight) kerosene and a mineral oil. A paraffin wax was added to this mixture to make it waxy. The wax content of the model oil was 3 wt. % and the WAT was 23.1 °C. Properties of fluid and equipment used in the experiments are given in Table 16.

4.4.1 Data and experiments

Four experiments by Venkatesan (2004) were digitized and evaluated. The test rig used was 8 feet (2.44 m) long and had an internal diameter of 0.876 inches (22.3 mm). Oil temperature in the experiment was kept constant at 25.6 °C. The cooling temperature was 4.4 °C and was also kept constant in all experiments. The experiments are named Venkatesan A-D. All experiments were run with different flow rates between 10 and 25 gpm (gallons/minute). This corresponds to flow velocities between 1.62 and 4.06 m/s. The corresponding Reynolds numbers are given in Table 17. All experiments were run for about 20 hours.

4.4.2 Use of model

The four experiments are compared to the logarithmic deposition-release model in Figure 25. The model corresponds well to the Venkatesan experiments A-C. The logarithmic model struggles with the shape of the curve in the Venkatesan experiment D. Experiment D is the experiment with the highest flow rate. The initial deposition of the Venkatesan D experiment is matched well by the model. But the asymptotic part does not fit very well with the model. Increased flow rate will increase the wall shear stress. If the wall shear stress becomes too big the deposition may go from a logarithmic to an exponential deposition trend.

4.4.3 Coefficient analysis

Coefficients k_1 and k_2 are given in Table 18. Both oil temperature and cooling temperature were constant in all four experiments. The temperature driving force is equal in all the series. The flow rate was varied resulting in different flow velocities and Reynolds numbers. The coefficients are therefore only evaluated against velocity parameters. The general trend seen is that k_1 seems to decrease with increasing flow rate, as seen in Table 18. Coeffient k_2 seem to increase with increasing flow rate, as seen in Table 18. A problem is that the coefficient k_2 is a lot bigger in Venkatesan experiments C and D than for the A and B experiments. This big increase is only observed for the Venkatesan experiments.

When coefficient k_1 is plotted against 1/Re a linear trend is seen in Figure 26. The wall shear stress is not calculated because of limited data given by Venkatesan (2004). Reynolds number is used as the rate dependent parameter instead. The linear trend applies for three of the four coefficients. This linear trend shows that k_1 might be a linear function of 1/Re. The linear trend corresponds to $k_1 = k_3 + k_4/Re$. Coefficient k_2 is plotted against Re^2 in Figure 27. No linear trend is seen between the coefficients. A possible exponential shaped trend is seen, but this is not clear. The big difference between k_2 values are difficult to match with any velocity dependent parameter. Because of the difficulty in determining k_2 no new rewrite of Eq 3.3 is proposed.

5. Real pipeline study

A wax deposition study using data from a real subsea pipeline in Indonesia was presented by Singh et al. (2011). Field data was compared to deposition data from a simulator called TUWAX by Singh et Al. (2011). Two different models were investigated in the TUWAX simulator. The Film Mass Transfer (FMT) model and the Equilibrium model (EM). The study showed that the FMT model gave a higher deposition rate than the EM. Both models were tested against viscosity, fraction of trapped oil in deposits, thermal conductivity, aging and shear stress. After tuning these parameters the models were compared to field deposition data. Both models under predicted the deposition rate compared to the field data.

This thesis will evaluate the field data used in the study by Singh et al. (2011). Potential problems and possible sources of error will be investigated. All experimental data presented earlier used pressure drop measurements to estimate wax deposition thickness. The same method was used by Singh et al. (2011) to evaluate deposition in the real pipeline. Properties of the fluid and the pipeline are given in Table 20. The measured wax deposition will also be compared against the logarithmic deposition-release model.

5.1 Wax thickness estimated from pressure drop

The measured pressure drop in the pipeline increase from about 200 to 300 psi (13.8 to 20.7 bar) during a week of operation (Singh et al. 2011). When the pipeline is pigged the pressure drop is reduced back to about 200 psi. If paraffin wax deposits on the pipeline wall the pipeline diameter will decrease. The Darcy-Weisbach (Gudmundsson 2009) equation says that the frictional pressure drop is:

$$\Delta p = \frac{f}{2}\frac{L}{d}\,\rho u^2 = \frac{f}{2}\frac{L}{d}\,\rho\left(\frac{4q}{\pi d^2}\right)^2 = \frac{8f}{\pi^2}\frac{L}{d^5}\,\rho q^2 \qquad 5.1$$

where Δp is the pressure drop, f is the friction factor, L is the pipe length, d is the pipe diameter, ρ is the fluid density, u is the fluid velocity and q is the volume flow. We can see that pressure drop in Eq. 5.1 is inversely proportional to pipe diameter to the power of five. A change in pipe diameter will have a great effect on the frictional pressure drop. When pipe diameter decreases the pressure drop will increase.

Singh et al. (2011) used the change in diameter due to wax deposition to quantify the increased pressure drop. Blasius correlation with Reynolds number is used to estimate friction factor, f = 0,316/Re. The Blasius correlation is used for hydraulically smooth pipes and turbulent flow. The increase in pressure drop caused by reduction of diameter is given by Singh et al. (2011) as:

$$\Delta p = \frac{0{,}0158 L \mu^{0{,}25}}{(2r)^{0{,}25}} \rho^{0{,}75} \left(\frac{u_0}{(2r)^2} (2r_0)^2 \right)^{1{,}75} \quad 5.2$$

where μ is the viscosity, u_0 is the velocity in a clean pipe, r_0 is the radius of a clean pipe and r is the effective radius of the pipe. Then a parameter κ is defined as:

$$\kappa = \frac{\Delta P}{{u_0}^{1{,}75}} = \frac{0{,}0158 L \mu^{0{,}25}}{(2r_i)^{4{,}75}} \rho^{0{,}75} (2r_i^0)^{3{,}5} \quad 5.3$$

By measuring the pressure drop, calculating κ and comparing κ with κ_0 for a clean pipe, wax deposition thickness is calculated:

$$\frac{\kappa}{\kappa_0} = \frac{(2r_0)^{4{,}75}}{(2r)^{4{,}75}} \quad 5.4$$

The $r = r_0 - x$, where x is the deposit thickness. Solved for deposit thickness it looks like this.

$$x = r_i^0 \left(1 - \left(\frac{\kappa}{\kappa_0} \right)^{1/4{,}75} \right) \quad 5.5$$

The entire detailed derivation is found in Appendix E. The wax thickness calculated by Singh et al. (2001) using this method is found in Figure 28. The figure show how the wax thickness builds up with time after running a cleaning pig through the pipe.

5.2 Wax thickness and temperature in the pipeline

The measured wax thickness is about 13-15 mm after 7 days as seen in Figure 28. The pigging frequency is about once a week (Singh et al. 2011). This is also seen on run 1-5 in Figure 28 which stop at about 7 days. Run 6 and 7 in Figure 28 show a duration of about 25

days. In order to avoid a stuck pig incident the recommended maximum wax layer thickness is 2-3 mm (Labes-Carrier et al. 2002). The 13-15 mm layer of wax is well above this recommended maximum. Samples from the pig trap showed that the amount of wax to oil in deposits were around 25 % Singh et al. (2011). The wax porosity in the deposits should be about 75 % .

The pipeline inlet temperature is about 73.9 °C (165 °F) and the measured outlet temperature is between 26.7 and 29.4 °C (80-85 °F) (Singh et al. 2011). The theoretical outlet temperature can be calculated using this equation (Gudmundsson 2009).

$$T_{out} = T_{sea} + (T_{in} - T_{sea}) exp\left[\frac{-U\pi d}{mC_p} L\right] \qquad 5.5$$

T_{out}, T_{in} and T_{sea} is the outlet, inlet and sea temperature, U is the thermal conductivity of the pipe, d is the pipe diameter, L is the pipe length, m is the mass rate and C_p is the heat capacity. All parameters except the heat capacity were given by Singh et al. (2011).

The temperature along the pipeline is calculated using Eq. 5.5 and is given in Figure 29. The temperature development is shown for a C_p of 2000 and 2300 J/kg.K. The C_p of 2000 J/kg.K gives and outlet temperature of 27.46 °C, while the C_p of 2300 J/kg.K will give an outlet temperature of 28.63 °C. Both of these are in the range reported by Singh et al. (2011). A HYSYS temperature simulation is also shown for the pipeline in Figure 29. The simulated temperature matches the calculated profiles well. The outlet temperature is similar to the one seen in the C_p = 2000 J/kg.K curve.

The amount of wax precipitated in the oil will increase when the oil temperature decreases. The solid wax fraction precipitation curve reported by Singh et al. (2011) is given in Figure 30. This figure was digitized and turned into a function which gives weight % of solid wax for a specified temperature. This function was used to plot the maximum amount of precipitated wax along the temperature profile. This plot is seen in Figure 31. The maximum amount of precipitated wax is given in volume per day.

A maximum precipitated wax amount of 550 m^3/d is calculated for the C_p of 2000 J/kg.K. The wax amount is about 500 m^3/d when C_p is 2000 J/kg.K. The initial buildup rate after pigging

was reported to be 3-4 mm/day by Singh et al. (2011). A 4 mm wax layer in the pipe will give a deposit volume of about 87 m^3. If the deposit porosity of about 75 % is taken into account the amount of pure wax is lower. About 5 % of the theoretical precipitated amount of wax will deposit if a 4 mm wax layer with 75 % porosity is assumed. The calculation shows that the theoretical amount of "available" wax is much greater than the amount of deposited wax. Even though the amount of wax is available, does not necessarily mean that it will deposit.

5.3 Measured viscosity

The viscosity of the crude oil was measured in a laboratory using a rheometer by Singh et al. (2011). The measured viscosity is shown in Figure 32. The viscosity was measured for different shear rates and decreasing temperature. The figure also show the viscosity estimated by the TUWAX simulator. The simulator does not account for the precipitated wax in the crude. When wax precipitates from the crude it shows signs of becoming a non-Newtonian fluid. Non-Newtonian fluids are fluids that do not follow the linear law that says shear stress is equal to viscosity multiplied by the velocity gradient ($\tau = \mu (du/dy)$) (White 2008). The viscosity used by Singh et al. (2011) in calculations was 10 mPa.s.

The shear rate in the fluid was calculated as a function of viscosity using two different methods. The shear rate is seen in Figure 33. One method uses boundary layer calculations while the other uses definition of viscosity and wall shear stress. The full calculations behind both methods are given in Appendix F. A weakness for both methods is the assumption of Newtonian fluid properties. The two methods give very similar shear rates for a given viscosity. The calculated shear is in the range of 50 – 1000 s^{-1}. This match well with the shear rates plotted in Figure 32.

The measured pressure drop in a clean pipe is about 13.8 bar (200 psi) (Singh et al. 2011). It is assumed that the measured pressure drop in a clean pipe is the frictional pressure drop. The theoretical viscosity which gives a pressure drop of 13.8 bar is 11.5 mPa.s (cp) using equation 5.1. The viscosity is not a direct part of equation 5.1, but comes in through Re in the friction factor. A viscosity of 11.5 mPa.s gives a shear rate between 300 and 400 s^{-1} from Figure 33. This viscosity and shear stress will give an approximate temperature of 35 °C in Figure 32.

This is a fairly good match with the approximated average temperature of 40 °C from the C_p = 2000 J/kg.K series in Figure 29.

5.4 Roughness and even distribution of deposits

The calculated wax thickness from pressure drop uses the assumption of a smooth pipe. The Blasius friction factor correlation used is valid for Reynolds numbers < 100 000 and smooth pipes. The Re of the pipeline is about 29 500, well below the criterion. But a possible increase in pipeline roughness due to depositions of wax is not accounted for. An increased roughness will increase the friction factor and increase the pressure drop. If the pressure drop increase due to increased roughness it will overestimate the deposition thickness. The actual thickness will be less than the calculated thickness.

If given pipe roughness is multiplied by a factor of ten (0.5 mm), the theoretical pressure drop increase with 15 % (with μ = 11.5 mPa.s). This is calculated using the Haaland friction factor calculation which accounts for roughness (Gudmundsson 2009). A study of the Valhall offshore pipeline matched wax amount and wax roughness to measured pressure drop (Marshall 1990). In order to explain the pressure drop, the roughness needed to be around the same size as the thickness of deposits. If wax roughness increases to 2 mm, the pressure drop will increase with about 50 %. A wax roughness of that size will greatly affect the measured pressure drop.

The calculation of deposit thickness from pressure drop also assumes evenly distribution of deposits in the pipeline. A wax deposition simulation was run in the simulation software called HYSYS. Temperatures, pressure, flow rate and pipe specifications found in Table 20 were used as an input. The wax solubility showed in Figure 30 was also specified in HYSYS. The wax model used in HYSES was the AEA model. The HYSYS simulation show wax deposition along the pipeline and is given in Figure 34. According to the simulation most of the wax will deposit when wax precipitation starts. The precipitation will occur after about 3 km. A similar wax simulation, from TUWAX, given by Singh et al. (2011) is shown in Figure 35. The TUWAX simulation shows no deposition in the first 3 km with a deposit peak around 13 km. The predicted precipitation in Figure 31 also starts at around 3-4 km.

A calculation showing the effect of non-evenly distributed deposits was done. A 5 mm wax layer evenly distributed in the entire pipeline gives a theoretical pressure drop of 15.7 bar. We assume that the same amount of wax (volume) is deposited in 1/3 of the pipeline. Wax evenly distributed in 1/3 of the pipeline will increase the pressure drop to 16.4 bar. If wax only deposits in 1/9 of the pipeline the pressure drop will increase to 24 bar. This development is shown in Figure 36 where the pipe is divided into 27 equally long segments. Deposit in segment 10-18 is 1/3 of the pipe, while segment 13-15 is 1/9 of the pipe. The deposition is showed in the middle of the pipe in Figure 36. The total pressure drop is not affected by the location of the non-evenly distributed wax deposits.

If the a wax thickness layer of 10 mm is assumed the theoretical pressure drop will be 18.5 bar. Assuming deposits in 1/3 of the pipe will increase the pressure drop to 23 bar. The effect of non-evenly distributed deposition will increase with increasing wax thickness. The increased pressure drop will overestimate the wax thickness. The effect of increased roughness and non-evenly distributed deposition will both cause an increase in pressure drop. The estimated wax thickness may be too great. That might explain why the TUWAX simulations (Singh et al. 2011) under predicts the thickness of wax.

5.5 Deposition-release model

The calculated wax thickness showed in Figure 28 was digitized and coefficients in the deposition-release model were found. The comparison between calculated thickness and the model is shown in Figure 37. The figure shows a very good match between the calculated thickness and the model. Coefficient values used in the model are $k_1 = 0.25$ and $k_2 = 1.11$. The k_1 value is comparable to some of the experiments while the k_2 value is a bit lower than the values in the experiments. The lower k_2 will lead to a larger asymptotic deposit.

The wall shear stress of the real pipeline was calculated to 4.64 N/m^2 and the temperature driving force is 0.75 (assuming $T_{oil\_average} = 40$ °C). The temperature driving force was calculated using the surrounding temperature instead of wall temperature. The Hernandez A experiment mentioned earlier has similar $\tau_w = 4.72$ N/m^2 and $\Delta T^+ = 0.736$. The coefficient values for Hernandez A experiment are $k_1 = 0.0644$ and $k_2 = 10$. The real pipeline shows a higher initial deposition and a lower asymptotic value than the experiment. The experiment is

also compared to the real pipeline in Figure 40. The amount of wax deposited is much greater for the real pipeline than the experiment.

6. Discussion

6.1 Experiments with varying rate

A claim stated by Gudmundsson (2010) suggests that "The initial rate of deposition and the asymptotic deposition both decrease with increased flow rate". This phenomenon is based on both experiments and literature reviews. The statement can be transferred to the logarithmic deposition-release model. If the initial deposition decreases it will lead to a decreased value of coefficient k_1. If the asymptotic deposition decreases the value of coefficient k_2 will increase. The expected trend says that an increase in flow rate should decrease the k_1 value and increase the k_2 value.

Rosvold experiments A-E have increasing flow rate. No definitive trend is observed when evaluating k_1 values in Table 5. If Rosvold experiments A and D is excluded the stated claim seems correct. Rosvold experiment A was hard to digitize, especially the initial deposition. Experiments B, C and E show a decrease in initial rate with increased flow rate. The k_2 values are more stable and increase with increasing rate as seen in Table 5. Experiment B, C and E confirm the statement that increased flow rate will decrease initial deposition. All five experiments confirm that the asymptotic level decreases with decreased flow rate.

The Hernandez experiments contain two series of experiments with increasing rate. Model coefficients are given in Table 12. Hernandez experiments A-C have increased flow rate from A to C (1000-1800 BPD) with constant cooling temperature. The initial deposition (value of k_1) for experiment C is higher than experiment B. This is also seen in Figure 4 where initial deposition rate of experiment C is higher than experiment B. The k_2 values increase with increased flow rate for Hernandez experiments A-C. Experiments A and B confirm the decreased initial deposition with increasing flow rate. All three experiments (A-C) confirm the decreased asymptotic level with increasing flow rate.

The other Hernandez experiments are D-F and were performed with constant cooling temperature. Experiments D-F also increase flow rate from 1000-1800 BPD. Model coefficients are given in Table 12. Not all of these experiments show the expected deposition trend. Experiment D seems more linear and experiment E seems to fit the exponential trend in Figure 2. A low temperature driving force ($\Delta T^+ = 0.453$) may cause some instability. Hernandez experiment E and F confirm that the initial deposition decrease with increased

flow rate. Experiments D and F confirm that increased flow rate decreases the asymptotic level. Experiment E shows a low asymptotic level due to the exponential shape of the deposition curve.

The Venkatesan experiments A-D were performed with increasing flow rate, from 10-25 gpm. The model coefficients are given in Table 18. Except for Venkatesan experiment B the k_1 values decrease with increased flow rate. Experiment A, C and D confirms that initial deposition will decrease with increased flow rate. The k_2 values increase with increased flow rate for all experiments except experiment B. Again experiment A, C and D confirms that the asymptotic level will decrease with increasing flow rate. Experiments C and D, with the highest flow rate, show a deposition curve more like the exponential curve than the logarithmic curve. This might indicate that when flow rate is high the deposition curve is more similar to an exponential curve.

6.2 Experiments with varying temperature

Another claim by Gudmundsson (2010) states that "The initial rate of deposition and the asymptotic deposition both increase with increased difference between solution cloud point and wall temperature". Some experiments evaluated vary the oil temperature and some vary the cooling temperature on the outside wall. An increase in oil temperature will increase the wall temperature. We expect an increase in oil temperature to decrease the value of k_1 and increase the value of k_2. A decrease in outside cooling temperature will decrease the wall temperature. Therefore we expect a decreased cooling temperature to increase the value of k_1 and decrease the value of k_2.

The experiments presented by Rosvold (2008) increased the oil temperature to test the varying temperature effect on wax deposition. Rosvold experiments D and F-H increase the oil temperature and model coefficients are given in Table 6. Increasing the oil temperature leads to an increase in wall temperature. Experiments F-H show decreased initial deposition rate and decreased asymptotic level with increased oil temperature. These three confirm the statement by Gudmundsson (2010). The Rosvold D experiment does not fit the trend shown by the others. The Rosvold D experiment was part of both the varying rate and temperature experiments. The D experiment did not fit the expected trend for either of these experiments.

The experiments performed by Hernandez (2002) were performed with two different cooling temperatures. The Hernandez experiments A-C were performed with a ΔT ($\Delta T = T_{oil} - T_{cool}$) of 16.7 °C. The Hernandez experiments D-F were performed with a ΔT of 8.3 °C. The A-C experiments have a lower cooling temperature than the D-F experiments. Consequently the wall temperature is lower for experiments A-C than for experiments D-F. All values of k_1 are higher for experiments A-C than for experiments D-F. The trend is observed in both Table 12 and Figure 14. The trend confirms Gudmundsson's claim that decreased wall temperature will lead to a higher initial deposit rate. An increased k_2 value with decreased ΔT is observed for experiments A and D (similar rate) and experiments B and C (similar rate). It is not the case between experiments C and F. Two out of three series confirms that an increased ΔT increases the asymptotic deposition.

The experiments performed by Lund (1998) also vary the cooling temperature to test the temperature effect on deposition. Lund experiments A-C were performed with a ΔT ($\Delta T = T_{oil} - T_{cool}$) of 8.3, 16.7 and 25 °C. The lowest cooling temperature is for the 25 °C experiment. An increased ΔT gives a higher value of k_1 in Table 15. But the k_1 value for Lund experiment A may not be valid since the model does not match the experiment. The Lund A experiment showed a negative initial deposition. The k_2 values decrease with increasing ΔT. The Gudmundssen statement is confirmed for both initial rate and for asymptotic deposition level.

6.3 Evaluating experiments and model

The general idea behind a deposition model is that it should predict the amount of deposits. Physical dependencies of coefficients k_1 and k_2 need to be established if the deposition-release model is going to do this. The experiments evaluated were tested for effects of varying rate, varying temperature or both. The varying rate experiments were evaluated against wall shear stress. The varying temperature experiments were evaluated against the dimensionless temperature driving force.

The wall shear stress in the Venkatesan experiments could not be calculated and these were evaluated against Reynolds number. Reynolds number is a direct function of pipe diameter. This could cause issues if a model is scaled up to fit a field size pipeline. The wall shear stress is only dependent on diameter through the Reynolds number in the friction factor. The original formula for temperature driving force used the wall temperature (Gudmundsson

2010). The Rosvold experiments were the only ones with a given wall temperature (Hoffmann and Amundsen 2010). In the other experiments the wall temperature was replaced with the outside cooling temperature.

The Rosvold A-E experiments have varying flow rate. Experiment B, C and E confirmed the expected trend for initial deposition (k_1) for increasing rate. Coefficient k_1 from these three experiments show a linear trend with $1/\tau_w$ seen in Figure 9. All five experiments (A-E) confirmed the statement regarding asymptotic level with increased rate. Coefficient k_2 for all five experiments show a possible linear trend with τ_w^2 in Figure 10. Rosvold experiment E with the highest flow rate is the point furthest from this trend. Based on these findings Eq. 3.3 is rewritten to Eq. 4.1.

The Rosvold experiments D and F-H were tested for varying oil temperature. When oil temperature increase the temperature driving force is decreased. The decreased temperature driving force means we expect a smaller amount of deposit. The expected trend was shown for experiments F-H while the D experiment did not match. Coefficient k_1 from experiments F-H show a linear trend with ΔT^+ in Figure 11. Coefficient k_2 from experiments F-H show a linear trend with $1/\Delta T^+$ in Figure 12. Based on these trends Eq. 3.3 was rewritten to Eq. 4.2.

The experiments by Hernandez (2002) made it possible to evaluate both varying rate and varying temperature at the same time. A possible linear relationship between k_1 and $\Delta T^+/\tau_w$ is seen in Figure 18. The same trend is seen if τ_w is replaced with Re. The only experiment which is off from this trend is the Hernandez D experiment. Another possible linear relationship is observed between k_2 and $\tau_w^2/\Delta T^+$ in Figure 19. The linear relationship is quite good for Hernandez experiments A-C. The same trend as seen in Figure 19 is seen if τ_w is replaced by Re. The linear relationships propose a rewrite of Eq. 3.3 to Eq. 4.3.

Experiments by Lund (1998) were only performed at different cooling temperatures. Coefficient k_1 seems to be a linear function of ΔT^+ in Figure 22. As mentioned before the initial rate of Lund A experiment may not be valid. The k_2 values plotted against $1/\Delta T^+$ show a linear relationship in Figure 23. Coefficient k_1 seem to be a linear function of ΔT^+ and k_2 seem to be a linear function of $1/\Delta T^+$. The linear relationship put into Equation 3.3 will change it to Equation 4.4.

The experiments performed by Venkatesan (2004) only tested the rate dependence. The rate parameter tested was Reynolds number, not enough data were given to calculate wall shear stress. Coefficient k_1 seem to be a linear function of 1/Re in Figure 26. The k_2 coefficient does not seem to be a linear function of Re^2, shown in Figure 27. Since no relationship between the coefficient k_2 and a flow parameter was established a new equation will not be proposed. But the linear dependency between k_1 and 1/Re show the same trend as seen above.

The evaluations of coefficients k_1 and k_2 and physical properties show the same trends. Coefficient k_1 seems to be dependent of the following rate parameters $1/\tau_w$, $\Delta T^+/\tau_w$ or Re. The k_2 coefficient for changing rates seems to be dependent on parameters τ_w^2 or $\tau_w^2/\Delta T^+$. In the Hernandez experiments, ΔT^+ is a constant when cooling temperature does not change. For changing temperatures, coefficient k_1 seems to be dependent on ΔT^+ or $\Delta T^+/\tau_w$. Coefficient k_2 seems to depend on $1/\Delta T^+$ or $\tau_w^2/\Delta T^+$ when temperatures change. For the Hernandez experiment τ_w is constant with constant rate. The only experiments which did not fit the experimental trends were the k_2 coefficients in the Venkatesan experiments.

The models based on the experiments are tested in Figure 39. The input data were wall shear stress of 4.64 N/m^2 and a ΔT^+ of 0.75. Both of these are numbers from the real pipeline study. The Rosvold Rate model is based on the integrated version of Eq. 4.1, while the Rosvold Temperature model is based on the integrated version of Eq. 4.2. The Hernandez Rate & Temperature model is based on the integrated version of Eq. 4.3. The Lund temperature model is based on the integrated version of Eq. 4.4. It is clear that all four models produce quite similar results. The Hernandez model considers both the wall shear and temperature driving force which is an advantage. The Lund model shows higher wax deposition than the others.

Some of the differences between the four experiments are rig pipe length, rig pipe diameter, wax appearance temperature and wax content of fluid. A comparison of these parameters is given for all experiments in Table 19. The Hernandez (2002) and Lund (1998) experiments were performed in the same rig. The fluid used by Lund had a higher wax content and WAT than the fluid used by Hernandez. A higher wax content in a fluid means that it is more wax available for deposition. A high wax appearance temperature means that wax will appear earlier in a cooling process. The WAT is usually higher for oils with higher wax content.

One would expect thicker wax deposits from oils with higher wax content. The Hernandez B experiment and Lund B experiment were performed with the same flow rate and the same ΔT. The flow rate was 1500 BPD and ΔT ($=T_{oil} - T_{cool}$) was 16.7 °C. These two experiments are compared in Figure 38. As expected the Lund B experiment with higher wax content have a higher initial deposition and higher asymptotic level. The Lund B experiment has a higher value of k_1 and a lower value of k_2. The same thing is observed between the Hernandez E experiment and the Lund A experiment from Table 12 and 15. These were also performed with the same flow rate and ΔT.

The diameter in the experiments varies between 23.1 and 52.58 mm. The length of the rigs varies from 2.44 to 50 m, a bigger difference than for the diameter. An increase in diameter and length increases the deposition area in the pipe. An increase in deposition area will decrease the deposit thickness if volume of deposit is constant. According to Eq. 5.5 the outlet temperature will decrease if diameter and length increases. A decreased outlet temperature will lead to more precipitation and possibly thicker deposits.

The Venkatesan experiments were performed in the rig with the smallest diameter and shortest length. One experiment from each thesis is compared in Figure 38. All compared experiments have a flow velocity between 1.62 and 1.92 m/s and a ΔT^+ between 0.62 and 0.82. The Venkatesan experiment show higher wax deposit than the other experiments seen in Figure 38. The other three experiments have more similar deposit thickness. It seems like a decrease in pipe diameter and length will cause thicker deposits in laboratory experiments.

The particle mass transfer coefficient was calculated for the Rosvold experiment A-E with increasing flow rate. The coefficients were compared to the k_1 coefficients in Table 7. It is seen that the model coefficient k_1 is a lot smaller than the mass transfer coefficient. The k_1's are smaller by a factor of about 10^{-2}. The initial deposition rate (k_1) decreases with increasing rate. The particle mass transfer coefficient increases with increasing flow rate due to increased friction velocity. A potential decrease in the dimensionless mass transfer coefficient with increased flow rate is not being accounted for. Increased shear stress caused by increased flow rate might move wax particles away from the wall. The particle mass transfer does not consider changes in temperature.

6.4 Real pipeline study

The real pipeline study was investigated and modeled with the deposition-release model. The measured wax thickness after one week of operation (13-15 mm) is well above the recommended thickness. The calculated temperature drop in the pipe matched well with outlet temperatures given by Singh et al. (2011). The temperature drop was also matched with HYSYS calculations seen in Figure 29. The maximum potential wax precipitation in the pipeline was calculated using temperature drop. The calculations showed that about 5 % of the maximum amount of precipitated wax deposited. The amount of precipitated wax to deposited wax may help explain why the particle mass transfer coefficient had a much bigger value than the k_1 coefficients in the Rosvold experiments.

The pressure drop calculations gave an average viscosity of 11.5 mPa.s. The corresponding shear rate was found from Figure 33. Using viscosity and shear rate the temperature was found to be around 35°C from Figure 32. The calculated average using temperature drop from Figure 29 was around 40 °C. The calculated shear rates may be too high because of the assumption of Newtonian fluids. If wax molecules make the fluid more viscous the shear rate will decrease. A decreased shear rate will give a temperature closer to the 40 °C average. The calculated viscosity of 11.5 mPa.s is close to the 10 mPa.s viscosity used by Singh et al. (2011)

The wax thickness calculated from pressure drop measurements were explained earlier and in Appendix E. Some of the assumptions made in the calculations may not be correct. The Blasius friction factor is for smooth pipes and does not consider changes in roughness by the wax deposit. The effect of increased roughness on friction factor may be calculated by the Haaland friction factor correlation. A wax roughness of the same size as the deposit thickness was shown by Marshall (1990). A roughness of 2 mm will increase the calculated pressure drop with about 50 % compared to a clean pipe. If this is the case the given wax thickness is too great.

Another assumption was that the wax deposits were evenly distributed along the pipeline. The HYSYS simulation in Figure 34 shows that most wax deposits between 3-5 km. The TUWAX simulation in Figure 35 also shows an uneven distribution of deposits. These are indications that wax do not deposit evenly in the pipe. Calculations show that if the actual deposit area is less than the entire pipe, the measured pressure drop will increase. The way

non-evenly distributed deposits will affect the pressure drop is seen in Figure 36. As the deposited layer increase in thickness the effect of the non-evenly distributed deposits on the pressure drop will increase. Non-evenly distributed deposits will cause the calculated wax thickness to be too great.

The assumptions of constant pipe roughness and evenly distributed deposits are likely to overestimate the thickness of deposited wax. The actual amount of deposit should be less than the reported amount. Other evidence of this is that the wax modeling by Singh et al. (2011) underestimated the thickness of wax. The wax thickness calculated by Singh et al (2011) is compared to one of the Hernandez experiments in Figure 40. The Hernandez experiment had similar wall shear stress and temperature driving force as the real pipeline. The pipeline show much thicker deposits and bigger deposit growth than the Hernandez experiment.

A comparison between the deposition-release models and the calculated wax thickness is shown in Figure 41. All four models clearly under predict the calculated wax thickness. Some part of this difference may be caused by difference in diameter and the high wax content of the oil from the real pipeline. It is important to be able to scale up the models to fit the dimensions of a full size pipeline. This has not been possible in the current work. Some of the difference may simply be caused by the overestimation of wax thickness by Singh et al. (2011).

7. Conclusion

- A total of 21 experiments were digitized and evaluated and 18 of them show a good match with the logarithmic deposition-release model. Changes in temperature and flow rate causes changes in initial deposition rate and asymptotic deposition level. Most experiments behaved as expected when temperatures and rates were varied.

- The deposition-release model consists of two coefficients, k_1 and k_2. The value of k_1 and k_2 was determined for all 21 experiments. The coefficients were then matched against physical parameters. The rate dependency was determined by the wall shear stress (τ_w) and the temperature dependency was determined by the temperature driving force (ΔT^+). Data from one experiment was not enough to calculate wall shear stress and Reynolds number was used instead.

- The experiments varied either the temperature, flow rate or both of these. Linear trends between coefficients k_1 and $1/\tau_w$, ΔT^+, $\Delta T^+/\tau_w$ or $1/Re$ was shown. The k_2 coefficient showed linear trends with τ_w^2, $1/\Delta T^+$ or $\tau_w^2/\Delta T^+$. These linear trends were used to rewrite the model equations and include the physical dependencies. The models were then tested for a given wall shear stress and temperature driving force. The models gave quite similar results when compared.

- A real pipeline wax deposition study was investigated. The temperature and viscosity calculations matched well with the calculated values. The reported wax thickness was calculated from measured pressure drop. The pressure drop method assumed wax roughness equal to pipe roughness and evenly distributed deposits. Other studies and simulations show that these assumptions may not be correct. The wax thickness calculated from pressure drop is likely to be overestimated. The reported wax thickness was also compared to an experiment with similar properties. The comparison also showed that reported thickness may be too great.

8. Recommendations

- The logarithmic deposition-release model needs to be developed further. It should be evaluated against more experimental data and field data if available.

- Investigate at which values of τ_w and ΔT^+ the logarithmic trend will go towards a more exponential trend.

- Experiments which vary the pipe diameter and length could be performed to help scale up models.

- Experiments performed with different fluids in the same rig could help determine how wax content influences the deposition-release model.

9. Nomenclature

A [m^2] – Inner area of flow pipe

C_p [J/kg.K] – Specific heat capacity

d [m] – Inner diameter of flow pipe

du/dy [s^{-1}] – Shear rate

f – friction factor

k [m] – Pipe roughness

k_1, k_2 …k_6 – Constants and coefficients in the deposition-release model

L [m] – Pipe length

m [kg/s] – Mass rate

q [m^3/h] – Flow rate

r [m] – Pipe radius

Re – Reynolds number, dimensionless

t [h] - time

T_{out} [°C] – Outlet temperature

T_{in} [°C] – Inlet temperature

T_{sea} [°C] – Sea temperature (surrounding temperature)

T_c [°C] – Cloud point temperature, also known as WAT

T_w [°C] – Wall temperature

T_{oil} [°C] – Oil temperature

T_{cool} [°C] – Cooling temperature in experiments

u [m/s] – Flow velocity

U [W/m^2/K] – Thermal conductivity

x [mm] – wax thickness

Δp [Bar] – Pressure drop

ΔT – Difference between oil and cooling temperature in experiments

ΔT^+ – Dimensionless deposition temperature driving force (Gudmundsson 2010)

κ – Term used by Singh et al(2011)

ρ [kg/m^3] – Density of gas condensate

τ_w [N/m^2] – Wall shear stress

μ [Pas] – Viscosity of oil

Some of the formulas used in this thesis:

$$A = \frac{\pi}{4} d^2$$

$$u = \frac{q}{A}$$

$$Re = \frac{\rho u d}{\mu}$$

$$\Delta T^+ = \frac{T_c - T_{wall}}{T_{oil}} \, , T_w = T_{cool} \; is \; used \; in \; some \; calculations$$

Blasius friction factor:

$$\frac{0.316}{Re^{0.25}}$$

Haaland friction factor

$$\sqrt{\frac{1}{f}} = -1.8 log \left[\left(\frac{6.9}{Re} \right) + \left(\frac{k}{3.75d} \right)^{1.11} \right]$$

10.References

1. Akbarzadeh, K. and Zougari, M. (2008): Introduction to a Novel Approach for Modeling Wax Deposition in Fluid Flows. 1. Taylor-Couette System, Ind. Eng. Chem. Res. 2008, 47, pp 953-963.

2. Aske, N., Statoil ASA (2011): Wax Control, Guest Lecture in TPG 4135 Processing of Petroleum, 7 March, http://www.ipt.ntnu.no/~jsg/undervisning/prosessering/gjester/LysarkAske2011.pdf

3. Bansal, R., Ravishankar, B., Dr Sharma, SS., Afzal, K. et al. (2012): Dynamic Simulation for Optimising Pigging Frequency for Dewaxing, SPE Oil and Gas India Conference and Exhibition, 28-30 March 2012, Mumbai, India, SPE 153935, 8pp.

4. Botne, K.K. (2011): Modeling wax deposition with deposition-release models, Specialization Project, Department of Petroleum Engineering and Applied Geophysics, Norwegian University of Science and Technology, Trondheim, 38pp.

5. Bott, T.R. (1995): Fouling of Heat Exchangers, Chemical Engineering Monographs Vol. 26.

6. Edmonds, B., Moorwood, T., Szczepanski, R. and Zhang, X. (2007): Simulating Wax Deposition in Pipelines for Flow Assurance, 8th International Conference on Petroleum Phase Behavior and Fouling, Energy and Fuels 2008, pp 729-741.

7. Gudmundsson, J.S. (1981): Particulate Fouling, Fouling of Heat Transfer Surfaces, Somerscales, E.F.C. and Knudsen J.G. (eds.), Hemisphere Publishing Corporation, Washington, 357-387

8. Gudmundsson, J.S. (2010): Flow Assurance, Solids in Oil and Gas Production (First Draft), Department of Petroleum Engineering and Applied Geophysics, Norwegian University of Science and Technology, Trondheim.

9. Gudmundsson, J.S. (2009): Kompendium TPG 4135, Prosessering av Petroleum, Grunnleggende enhetsoperasjoner i produksjon av olje og gass, Department of

Petroleum Engineering and Applied Geophysics, Norwegian University of Science and Technology, Trondheim, 185pp.

10. Hernandez, O.C. (2002): Investigation of Single-Phase Paraffin Deposition Characteristics, M.Sc. Thesis, the University of Tulsa, 172pp.

11. Hoffman, R. and Amundsen, L. (2010): Single-Phase Wax Deposition Experiments, Energy & Fuels, Vol. 24, pp 1069-1080.

12. Labes-Carrier, C., Rønningsen, H.P., Kolnes, J., Leporcher, E. (2002): Wax Deposition in North Sea Gas Condensate and Oil Systems: Comparison Between Operational Experience and Model Prediction, SPE Annual Technical Conference and Exhibition, 29 September-27 October, San Antonio, Texas, SPE 77573, 12pp.

13. Lund, H.J. (1998): Investigation of Paraffin Deposition During Single Phase Flow in Pipelines, M.Sc. Thesis, the University of Tulsa, 158pp.

14. Marshall, G.R. (1990): Cleaning the Valhall Offshore Oil Pipeline, Offshore Technology Conference, 2-5 May 1988, Houston, SPE 17880-PA, pp 275- 278.

15. Rosvold, K. (2008): Wax Deposition Models, M.Sc. Thesis, Department of Petroleum Engineering and Applied Geophysics, Norwegian University of Science and Technology, Trondheim, 104 pp.

16. Singh, A., Lee, H., Singh, P., Sarica, C. (2011): SS: Flow Assurance: Validation of Wax Deposition Models Using Field Data from a Subsea Pipeline, the Offshore Technology Conference, 2-5 May 2011, Houston, Texas, OTC 21641, 19pp.

17. Venkatesan, R. (2004): The Deposition and Rheology of Organic Gels, Doctoral Thesis in Chemical Engineering, the University of Michigan, 225pp.

18. White, F.M. (2008): Fluid Mechanics, Sixth Edition, Published by McGraw-Hill.

11.Tables

Table 1: Porsgrunn wax rig data. Ref Rosvold (2008)

Parameter	**Value**
Oil Pipe, ID	52,58 mm
Oil Pipe, OD	60,56 mm
Water Pipe, ID	131,33 mm
Water Pipe, OD	0,1397 m
Tank Volume	300 l
Epoxy coating pipe diameter	51,7 mm
Differential pressure length	5,55 m
Water jacket length	5,31 m
Fluid	A waxy gas- condensate

Table 2: Fluid parameters in Rosvold experiments. Ref Hoffman and Amundsen (2009)

Constant rate parameters	**Value**
Oil density, ρ	809 kg/m3
Viscosity, μ	2,00E-03 Pas
WAT (Cloud point temperature),Tc	30 °C
Wax content	4,5 wt. %

Table 3: Details about Rosvold's varying rate experiments.

Experiment	Rosvold A	Rosvold B	Rosvold C	Rosvold D	Rosvold E
Rate of condensate [m^3/h], q	**5**	**10**	**15**	**21**	**25**
Fluid velocity [m/s], u	0,66	1,32	1,98	2,78	3,31
Reynolds Number, Re	13836	27672	41508	58111	69179
Wall temperature[°C], Tw	11,9	12,7	13,5	14,4	15,0
Temperature driving force, ΔT+	0,91	0,87	0,83	0,78	0,75

Table 4: Details about Rosvold's varying oil temperature experiments.

Experiment	Rosvold F	Rosvold D	Rosvold G	Rosvold H
Condensate temperature [°C], Tcond	**15**	**20**	**30**	**40**
Rate of condensate [m^3/h], q	21	21	21	21
Wall temperature[°C], Tw	12,1	14,4	19,4	24,7
Temperature driving force, ΔT+	1,19	0,78	0,35	0,13

Table 5: Coefficients in deposition-release model on Rosvold's varying rate experiments.

Experiment	Rosvold A	Rosvold B	Rosvold C	Rosvold D	Rosvold E
Rate of condensate [m^3/h], q	**5**	**10**	**15**	**21**	**25**
Condensate temperature [°C], Tcond	20	20	20	20	20
k_1	0,21	0,45	0,23	0,29	0,07
k_2	40	210	580	1050	2000

Table 6: Coefficients in deposition-release model on Rosvold's varying temperature experiments.

Experiment	Rosvold F	Rosvold D	Rosvold G	Rosvold H
Condensate temperature [°C], Tcond	**15**	**20**	**30**	**40**
Rate of condensate [m^3/h], q	21	21	21	21
k_1	0,07	0,29	0,03	0,01
k_2	80	1050	360	1000

Table 7: Coefficient k_1 (Rosvold's flow rate series) compared to particle mass transfer coeff.

Experiment	Rosvold A	Rosvold B	Rosvold C	Rosvold D	Rosvold E
Rate of condensate [m^3/h], q	**5**	**10**	**15**	**21**	**25**
Fluid velocity [m/s], u	0,66	1,32	1,98	2,78	3,31
k_1 [mm/h]	0,21	0,45	0,23	0,29	0,07
k_1 [m/s]	5,75E-08	1,24E-07	6,47E-08	7,94E-08	1,91E-08
Mass transfer coeff [m/s], h (h+ = 10^{-4})	1,68E-06	3,09E-06	4,40E-06	5,91E-06	6,88E-06
Mass transfer coeff [m/s], h (h+ = 10^{-3})	1,68E-05	3,09E-05	4,40E-05	5,91E-05	6,88E-05

Table 8: Details about wax rig in Hernandez and Lund's experiments. Ref Hernandez (2002)

Rig Data	**Values**
Oil Temp	40-160 °F
Glycol Temp (Cooling)	40-160 °F
Oil Flow rate	0-2000 BPD
Glycol Flow rate	0-2500 BPD
Inner Diam	43.6 mm
Length	50 m

Table 9: Fluid details from Hernandez experiments. Ref Hernandez (2002)

Constant fluid parameters	**Values**
WAT (Cloud point temperature), Tc	34.44 °C
API Density	42 °
Fluid density, ρ	816 kg/m^3
Fluid viscosity, μ	3.10 mPa.s
Wax content	0.5 wt %

Table 10: Velocity parameters from Hernandez experiments.

Experiment #	**Flow rate [BPD]**	**ΔT [°C]**	**Velocity [m/s]**	**Re**	**τw [Pa]**
Hernandez A	1000	16,67	1,24	14206	4,72
Hernandez B	1500	16,67	1,86	21309	9,81
Hernandez C	1800	16,67	2,23	25571	13,69
Hernandez D	1000	8,33	1,24	14206	4,73
Hernandez E	1500	8,33	1,86	21309	9,82
Hernandez F	1800	8,33	2,23	25571	13,69

Table 11: Temperature parameters from Hernandez experiments.

Experiment #	Flow rate [BPD]	ΔT [°C]	Toil [°C]	Tcool [°C]	ΔT+
Hernandez A	1000	16,67	29,44	12,77	0,736
Hernandez B	1500	16,67	29,44	12,77	0,736
Hernandez C	1800	16,67	29,44	12,77	0,736
Hernandez D	1000	8,33	29,44	21,11	0,453
Hernandez E	1500	8,33	29,44	21,11	0,453
Hernandez F	1800	8,33	29,44	21,11	0,453

Table 12: Model coefficients from Hernandez experiments.

			Model coefficients	
Experiment #	Flow rate [BPD]	ΔT [°C]	k_1	k_2
Hernandez A	1000	16,67	0,0644	10
Hernandez B	1500	16,67	0,0466	60
Hernandez C	1800	16,67	0,0485	250
Hernandez D	1000	8,33	0,0105	50
Hernandez E	1500	8,33	0,0173	500
Hernandez F	1800	8,33	0,0136	95

Table 13: Fluid details from Lund's experiments. Ref Lund (1998)

Constant Fluid paramters	Value
WAT	49 °C
Density	850 kg/m^3
Wax content	5 wt %

Table 14: Details from Lund's experiments.

Experiment #	ΔT [°C]	Toil [°C]	Tcool [°C]	Flow rate [BPD]	Velocity [m/s]	ΔT+
Lund A	8,33	40,6	32,27	1500	1,85	0,412
Lund B	16,67	40,6	23,93	1500	1,85	0,617
Lund C	25	40,6	15,6	1500	1,85	0,823

Table 15: Model coefficients from Lund's experiments.

Experiment #	ΔT [°C]	k1	k2
Lund A	8,33	0,034	16
Lund B	16,67	0,0815	9
Lund C	25	0,1137	5

Table 16: Rig and fluid data from Venkatesan's experiments. Ref Venkatesan (2004)

Rig and fluid data	Value
Rig Pipe Length	8 ft (2.44 m)
Rig Pipe Diameter	0.876 in (22.25 mm)
WAT	23.1 °C
Oil Wax content	3 wt %

Table 17: Details from Venkatesan's experiments.

Experiment #	Oil flow [gpm]	Flow velocity [m/s]	Re	Toil [°C]	Tcool [°C]	ΔT+
Venkatesan A	10	1,62	7350	25,56	4,4	0,728
Venkatesan B	15	2,43	11025	25,56	4,4	0,728
Venkatesan C	20	3,25	14700	25,56	4,4	0,728
Venkatesan D	25	4,06	18375	25,56	4,4	0,728

Table 18: Model coefficients from Venkatesan's experiments.

Experiment #	Oil flow [gpm]	k1	k2
Venkatesan A	10	3,7159	250
Venkatesan B	15	0,6847	200
Venkatesan C	20	0,995	10000
Venkatesan D	25	0,5503	30000

Table 19: Different rig and fluid parameters between the experiments.

Experiments	Rosvold	Hernandez	Lund	Venkatesan
Pipe length [m]	5.3	50	50	2.44
Pipe diameter [mm]	52.58	43.6	43.6	22.25
Cloud point temerature (WAT) [°C]	30	34.44	49	23.1
Wax content [wt %]	4.5	0.5	5	3

Table 20: Pipeline and fluid properites for Real pipeline. Ref Singh et al (2011)

Pipeline properties and fluid properties	
Inner diameter, d [m]	0,3048
Length [m]	23000
Thermal Conductivity, U [W/m2/K]	22
Pipe roughness, k [µm]	50
Flow rate, Q [BPD]	55000
Flow velocity, u [m/s]	1,39
Fluid density, ρ [kg/m3]	800
Fluid viscosity, µ [mPas]	11,5
Reynolds number, Re	29489
Friction factor (clean pipe), f	0,024
Arrival pressure,p [bar]	24,1
Wall shear stress, τw [Pa]	4,64
ΔT+	0,75
Wax content in oil [wt. %]	17
Inlet temperature pipeline [°C]	74
Outlet temperature pipeline [°C]	26.7-29.4

12.Figures

no.	model	pub. year	mechanisms	ref no.
1	Burger et al.	1981	MD, SD	1
2	Majeed et al.	1990	MD	2
3	Svendsen	1993	MD	3
4	Brown et al.	1993	MD, SD	4
5	Hsu et al.	1995, 1998	MD	5, 6
6	Rygg et al.	1998	MD	7
7	Creek et al.	1999	MD	8
8	Singh et al.	2000, 2001	MD, ID, gelation	9, 10
9	MSI	2000	MD, kinetic, crystallization	11
10	Solaimany et al.	2001	MD, SR	12
11	Banki et al.	2002	MD	13
12	Lindeloff	2002	MD, SD	14
13	Azevedo	2003	MD, SD	15
14	Fasano et al.	2004	MD	16
15	Ramirez et al.	2004	MD, SR, ID	17
16	Hernandez et al.	2004	MD, SR, ID	18
17	this work	2006	MD, SD, SR, ID, PD, and inertia	

[a] MD molecular diffusion; SR shear removal (sloughing); SD shear dispersion; ID internal diffusion (aging); PD particle diffusion.

Figure 1: An overwiew of deposition models in litterature. Ref Akbarzadeh and Zougari (2008).

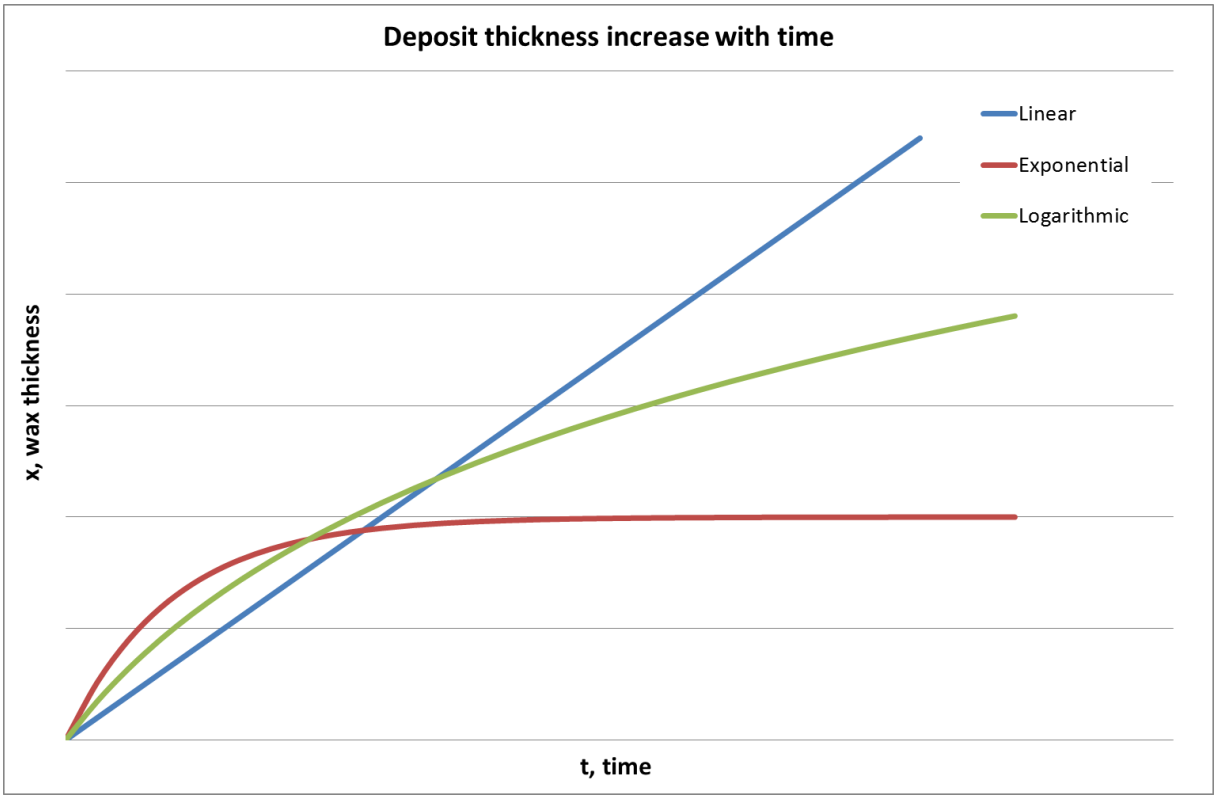

Figure 2: Possible buildup trends of deposits seen in experiments.

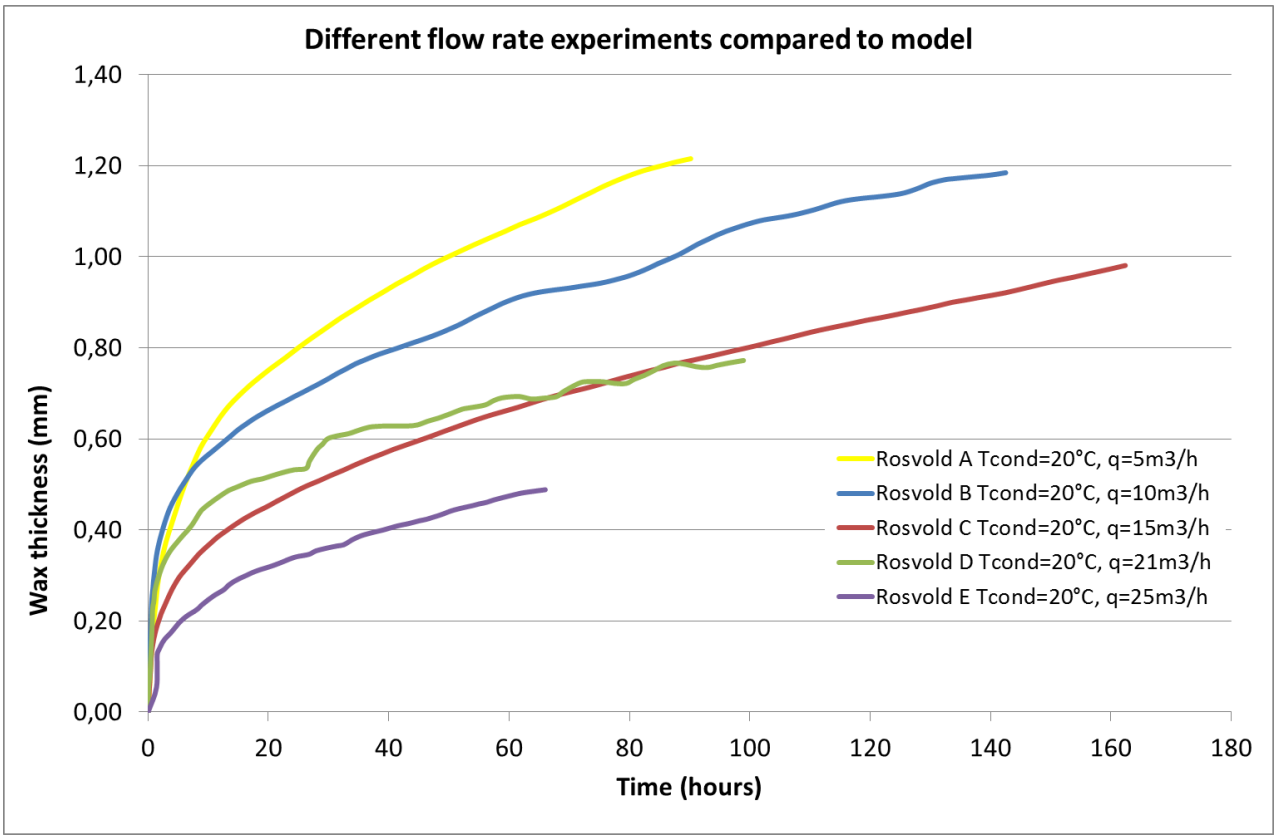

Figure 3: Wax thickness vs. time for Rosvold's digitized flow rate experiments.

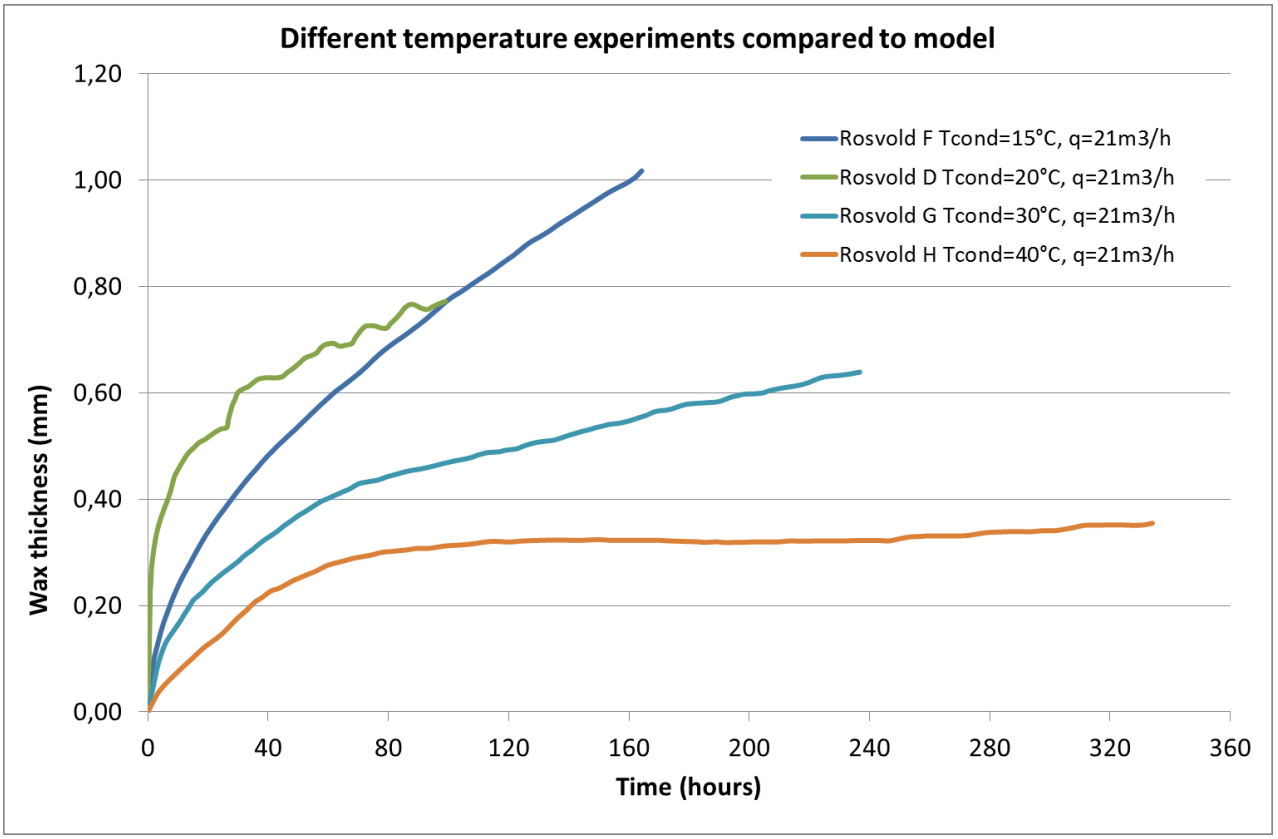

Figure 4: Wax thickness vs. time for Rosvold's digitized temperature experiments.

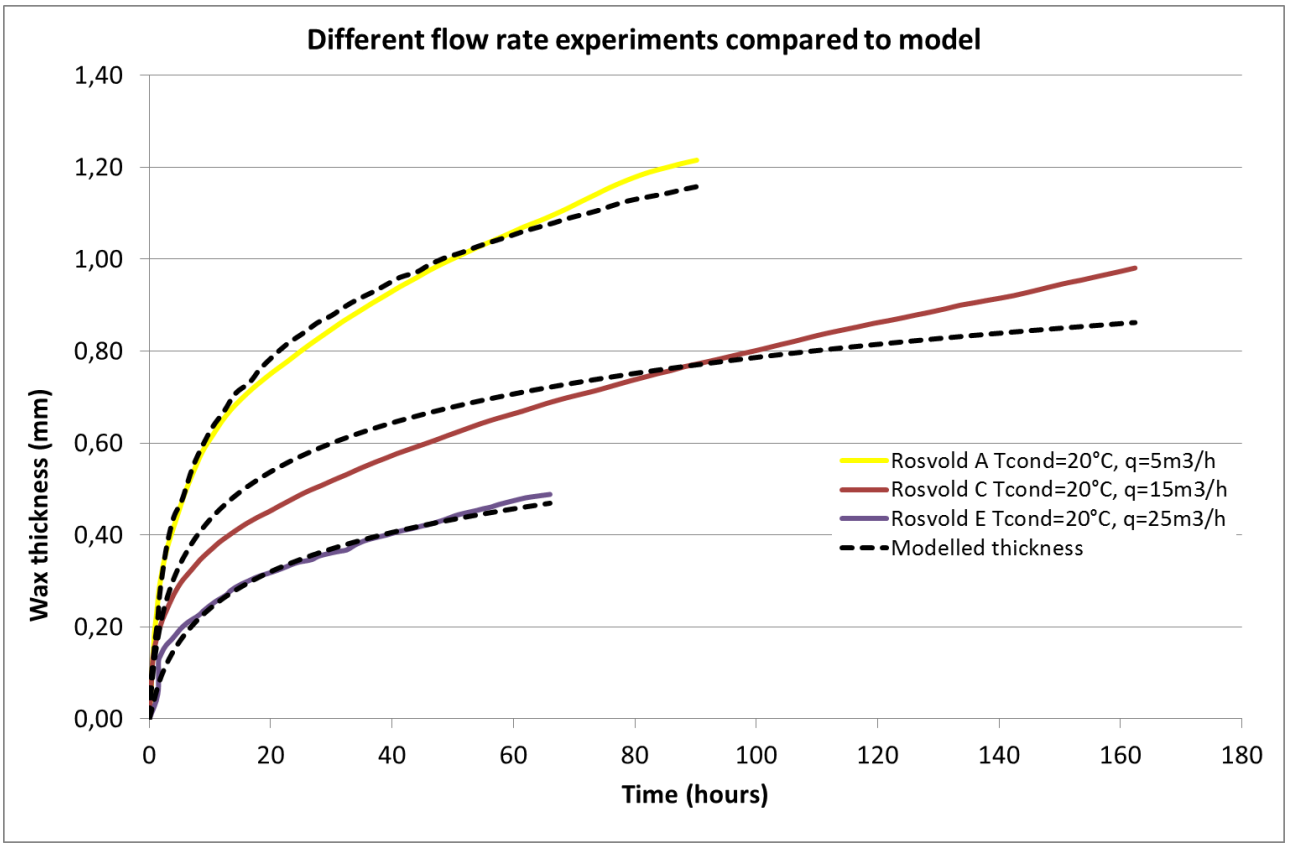

Figure 5: Wax thickness and match with model for Rosvold's digitized flow experiments.

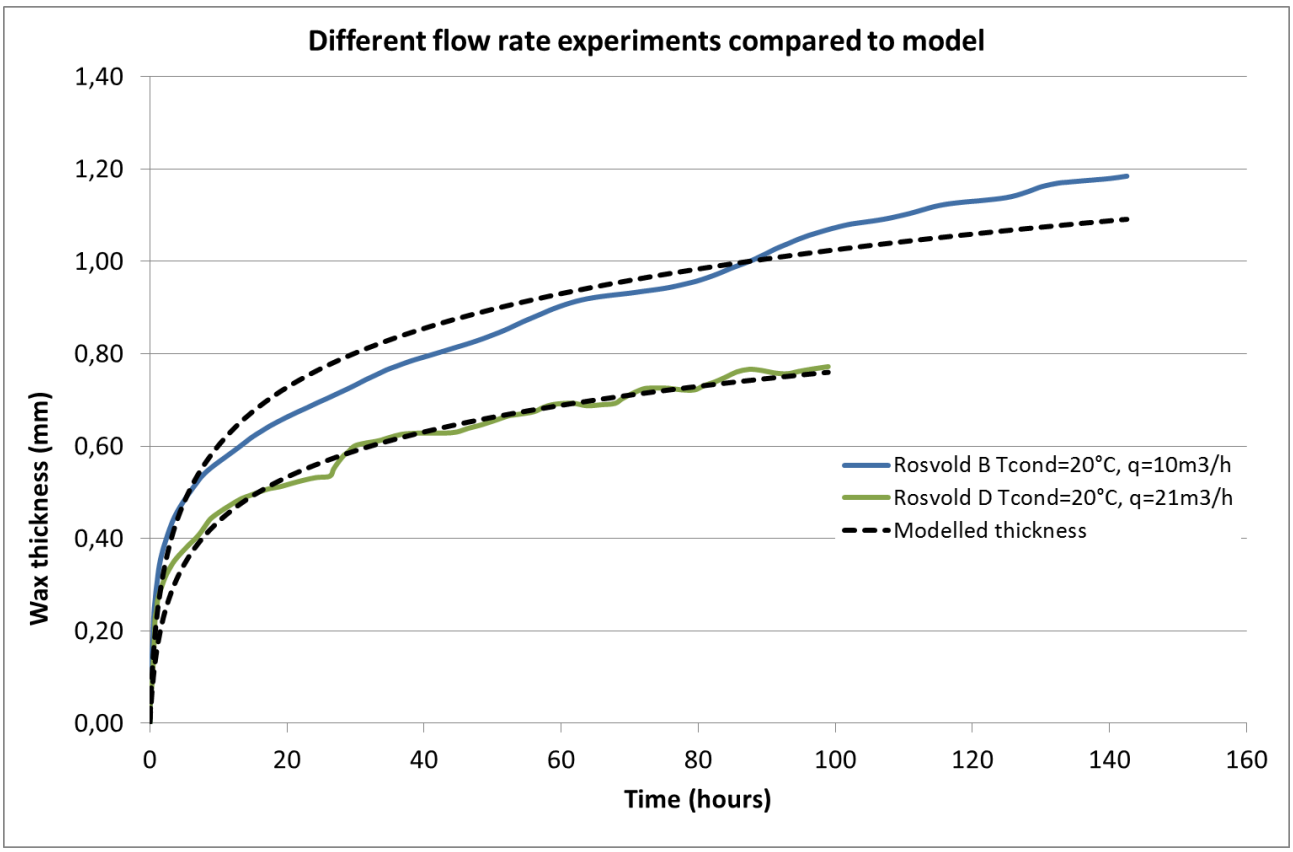

Figure 6: Wax thickness and match with model for Rosvold's digitized flow experiments.

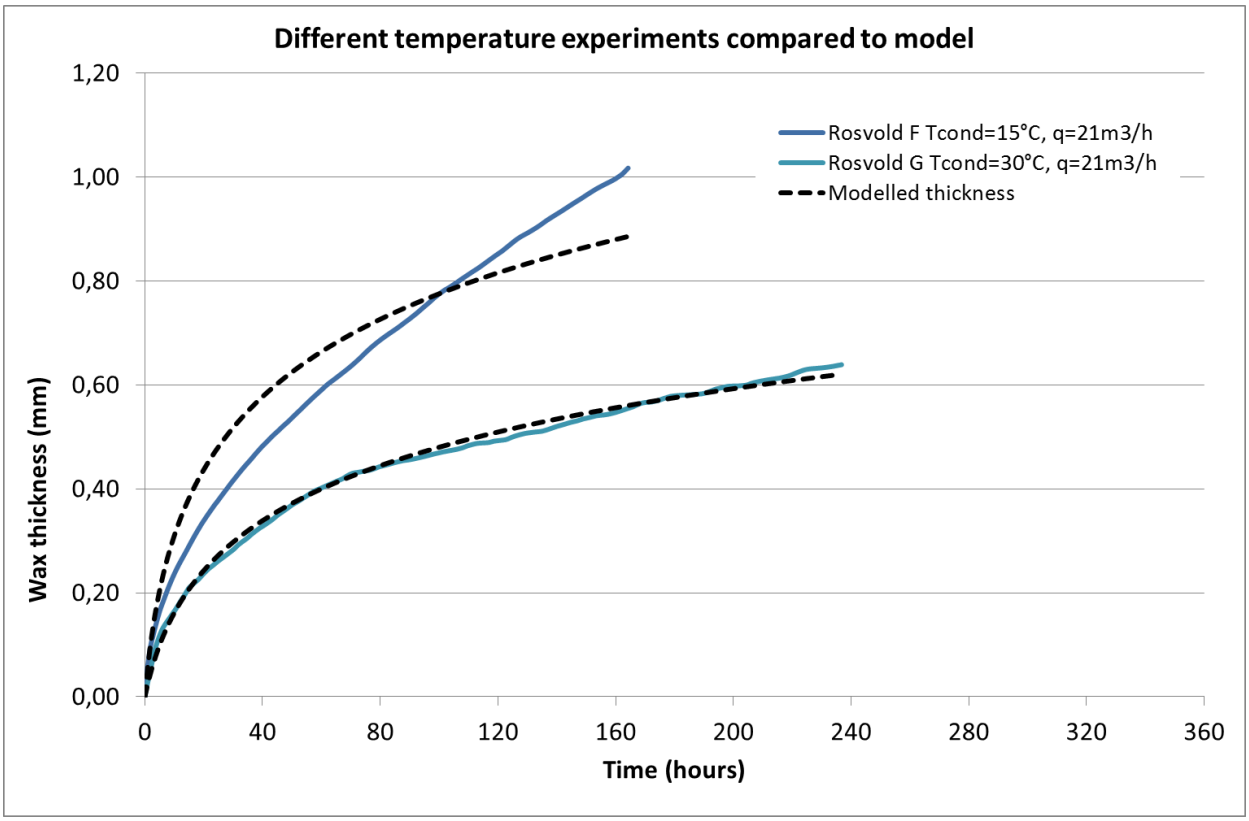

Figure 7: Wax thickness and match with model for Rosvold's digitized temperature experiments.

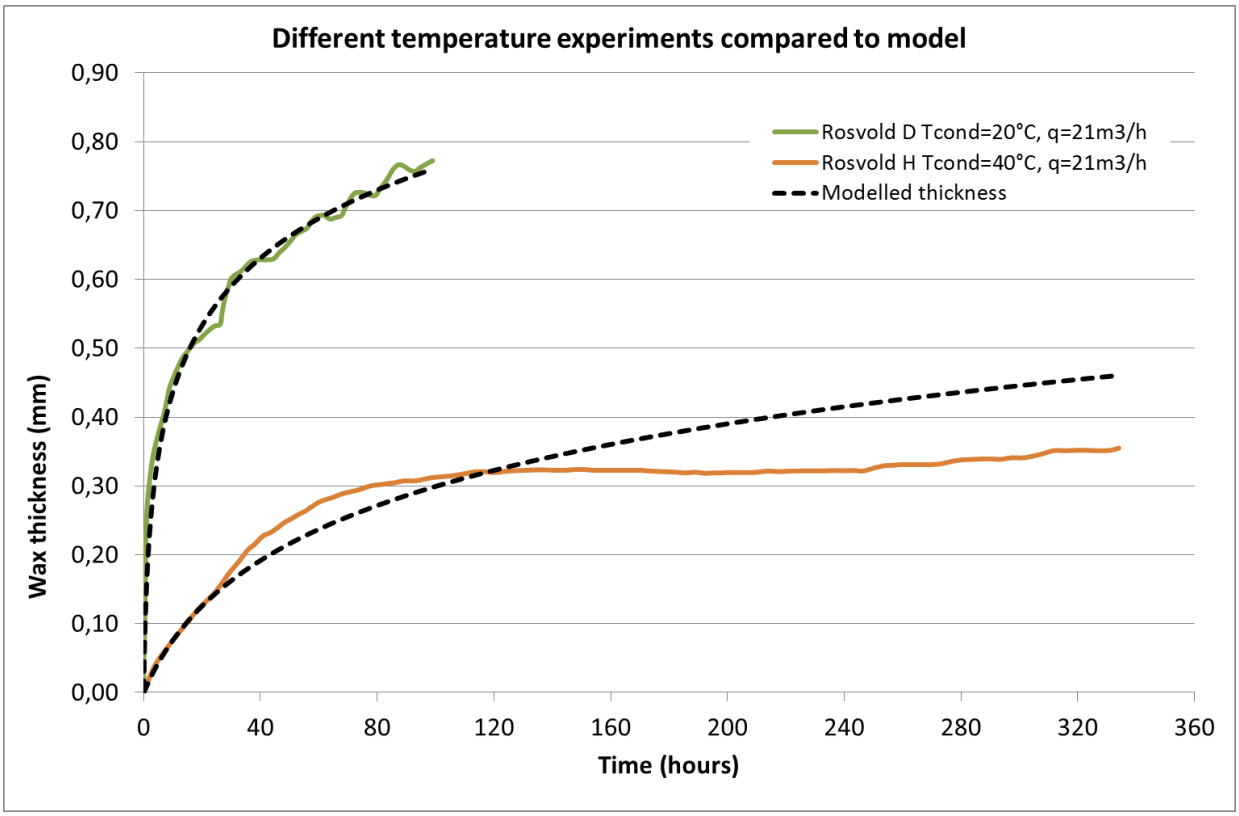

Figure 8: Wax thickness and match with model for Rosvold's digitized temperature experiments.

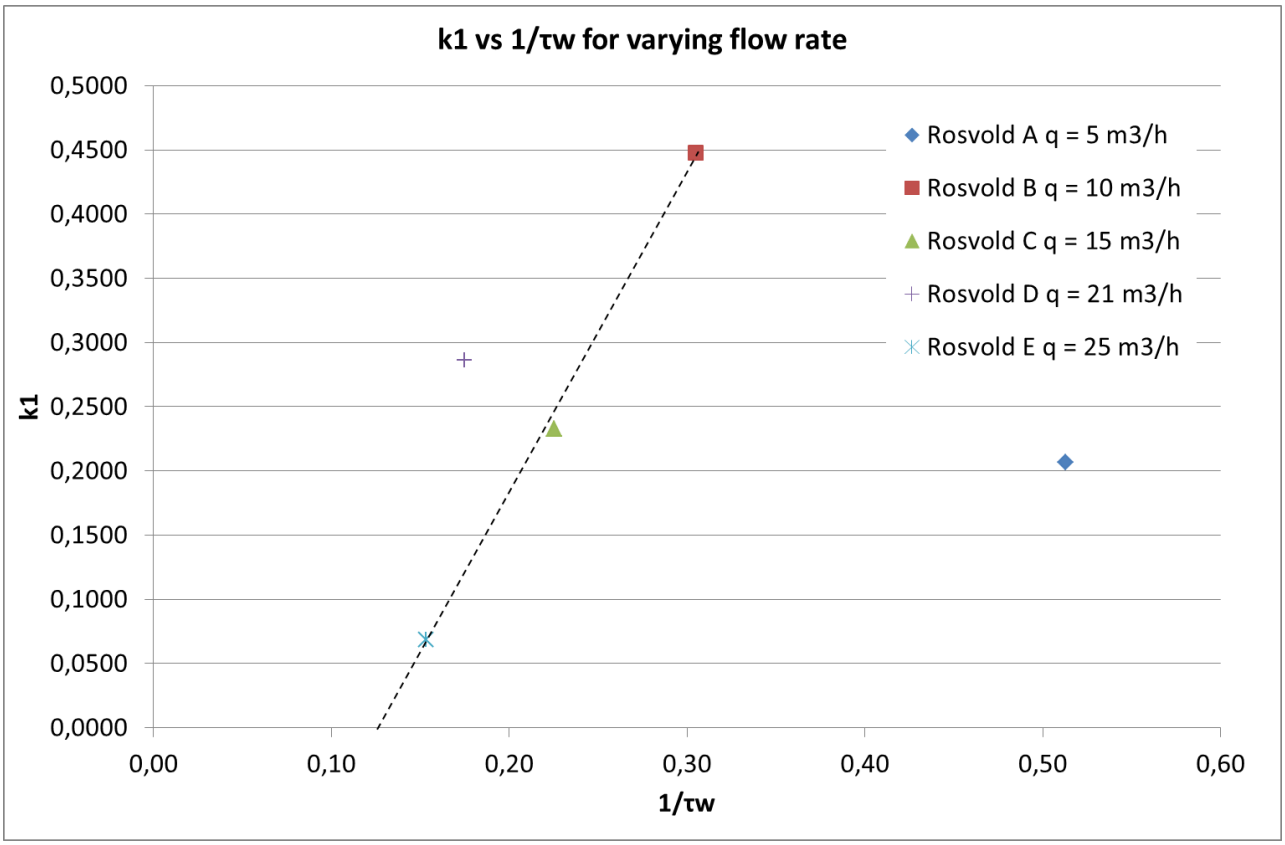

Figure 9: Constant k1 vs. 1/Re for varying flow rate series from Rosvold.

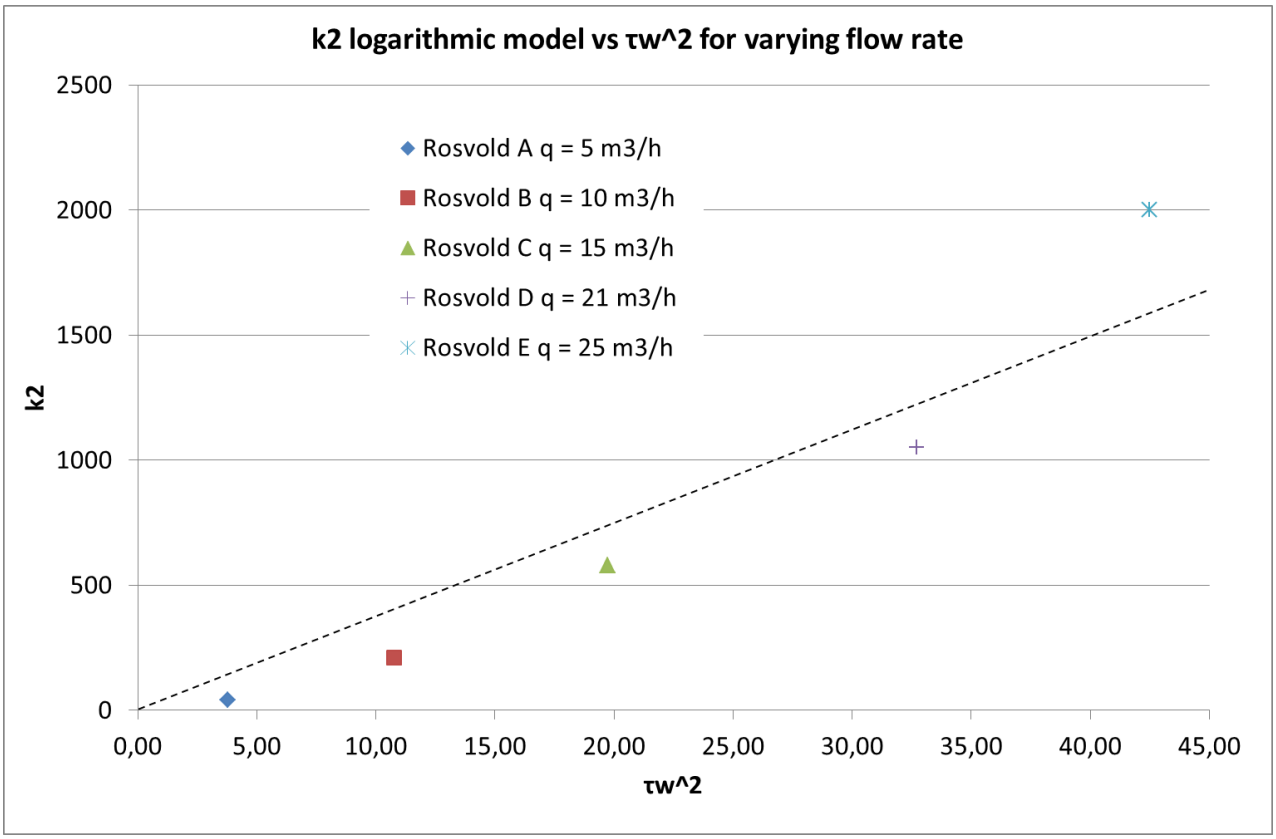

Figure 10: k_2 vs. Re^2 for varying flow rate series from Rosvold.

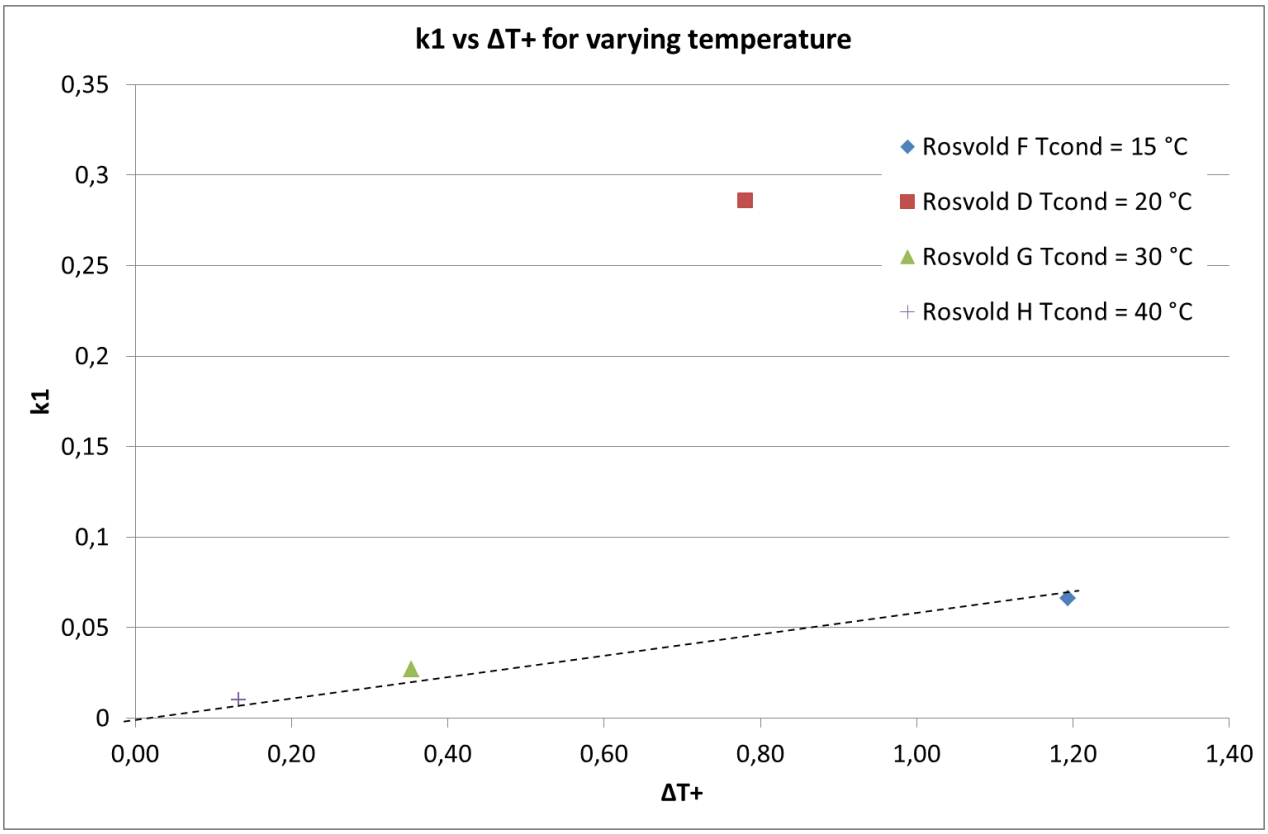

Figure 11: k_1 vs. ΔT^+ for varying temperature series from Rosvold.

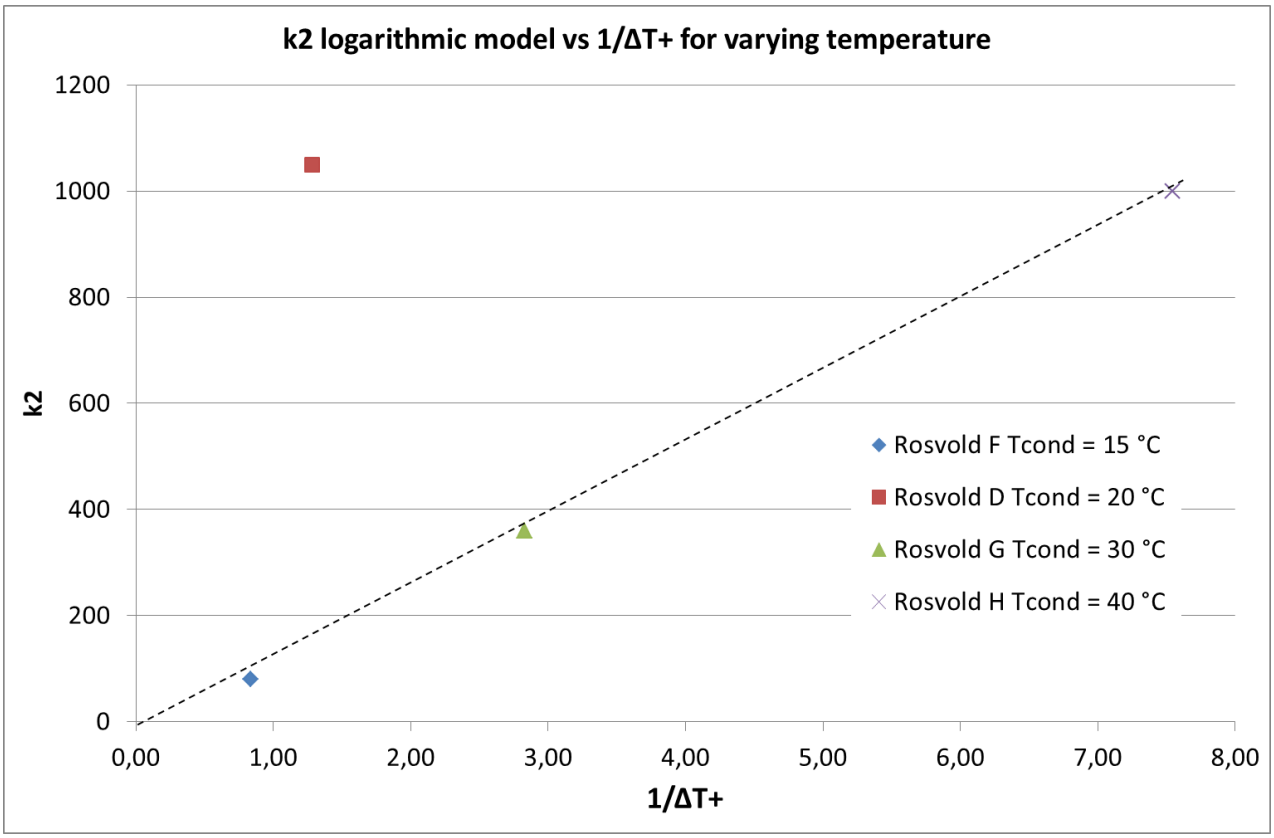

Figure 12: k_2 vs. $1/\Delta T^+$ for varying temperature series from Rosvold series.

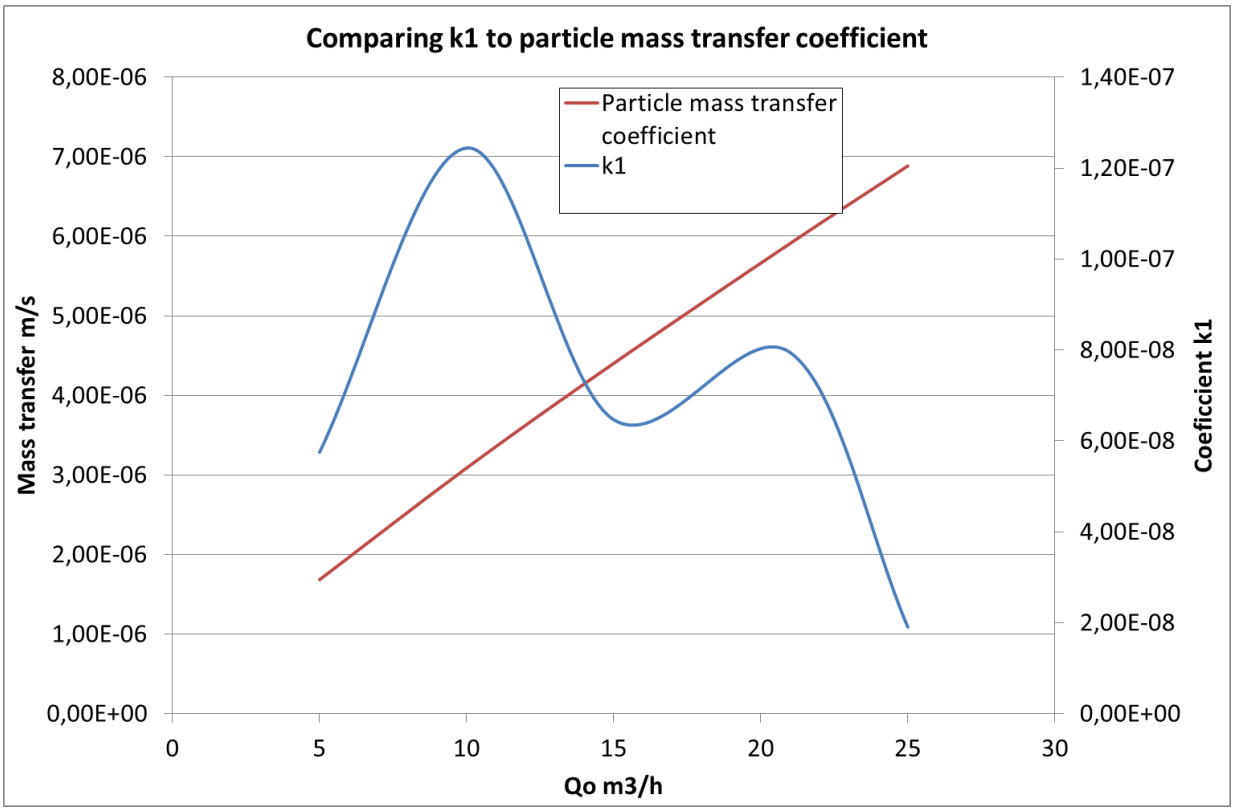

Figure 13: Coefficient k_1 (Rosvold's flow rate series) compared to particle mass transfer coefficient.

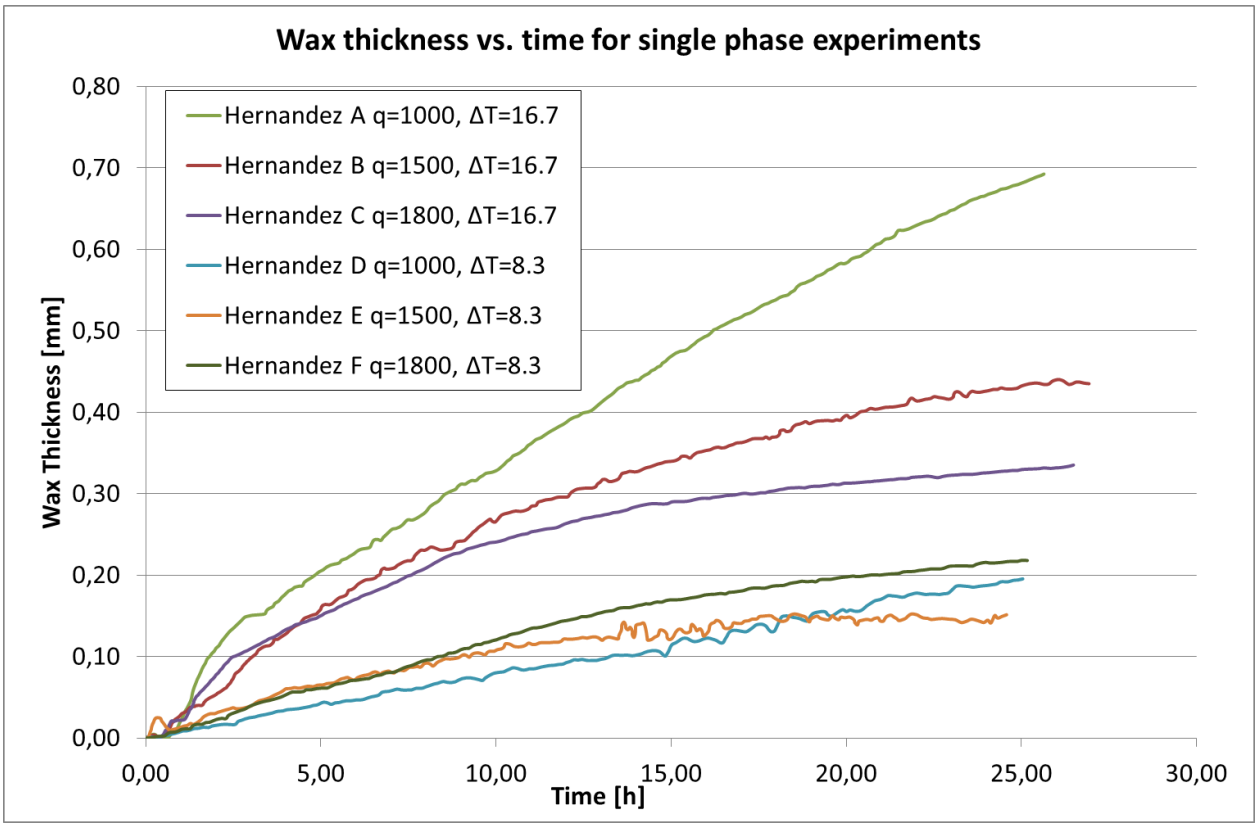

Figure 14: Wax thickness vs. time for Hernandez digitized experiments.

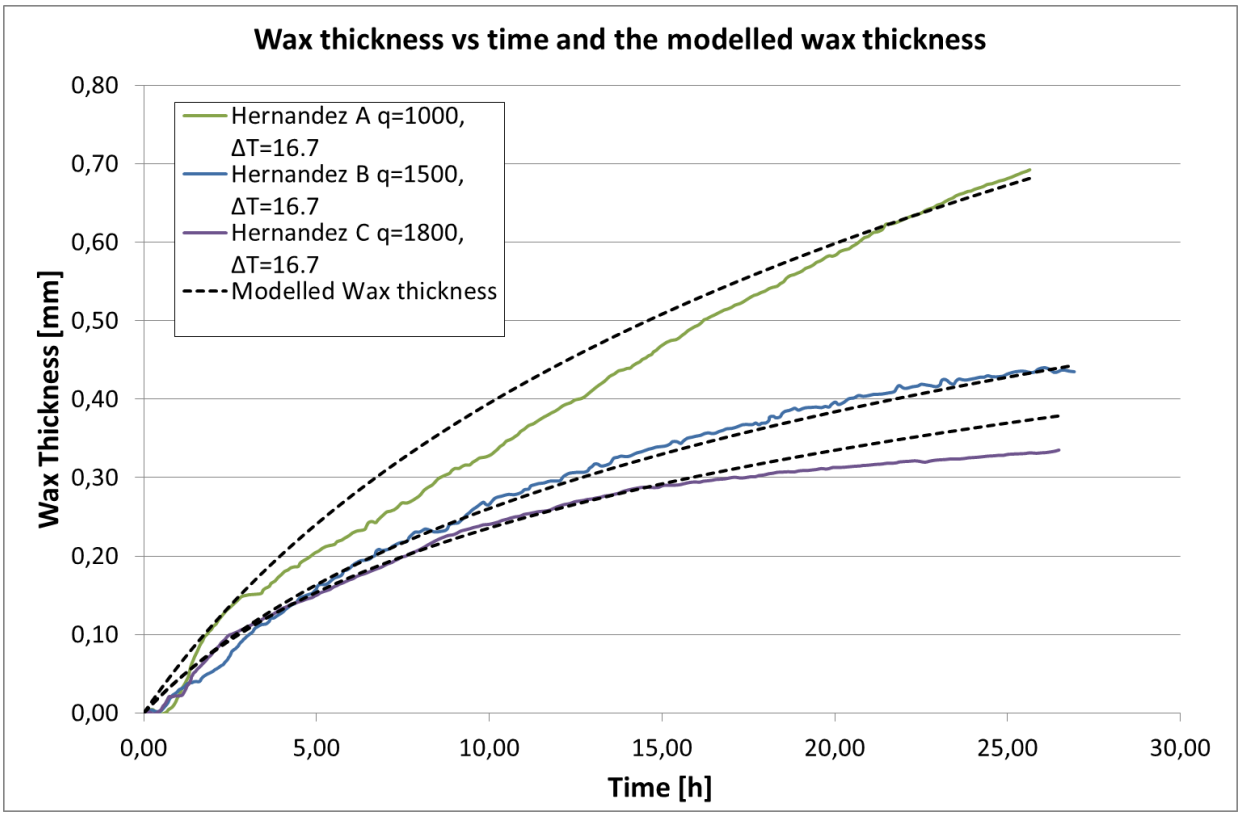

Figure 15: Wax thickness vs. time and best fit with deposition release model for Hernandez digitized experiments.

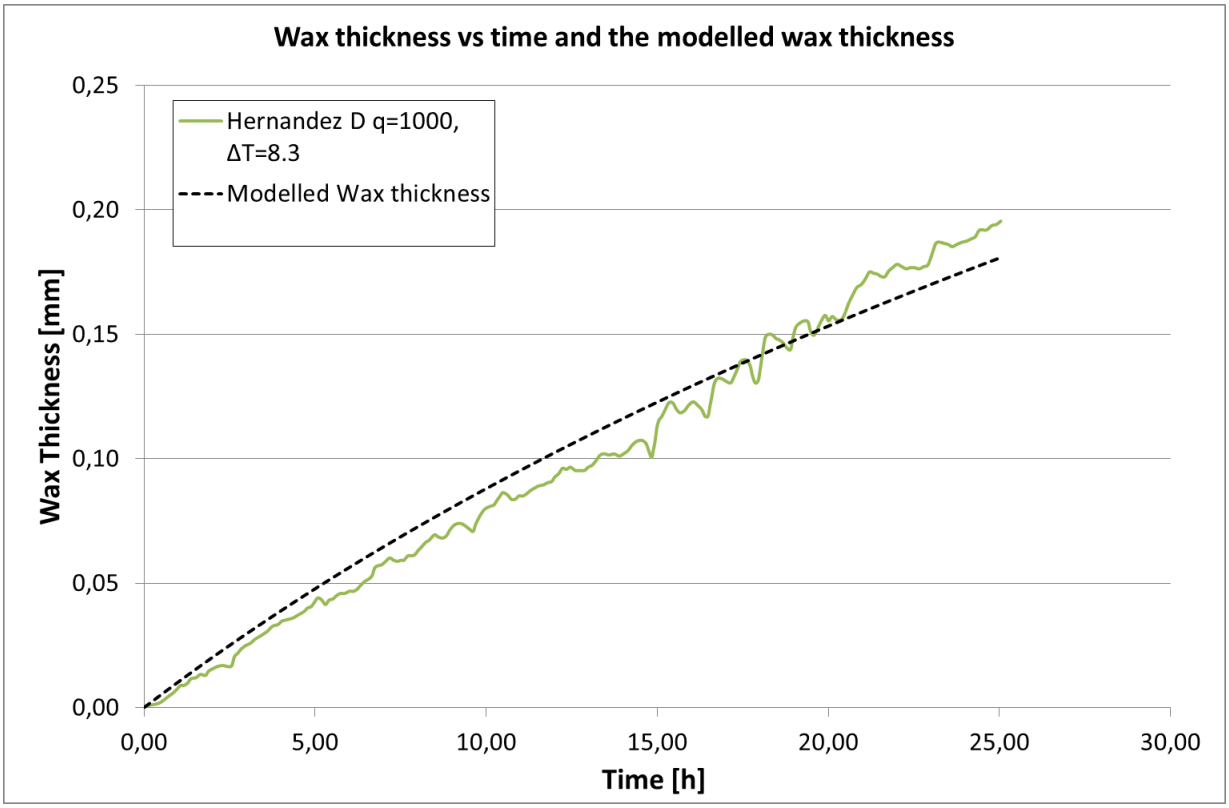

Figure 16: Wax thickness vs. time and best fit with deposition release model for Hernandez digitized experiments.

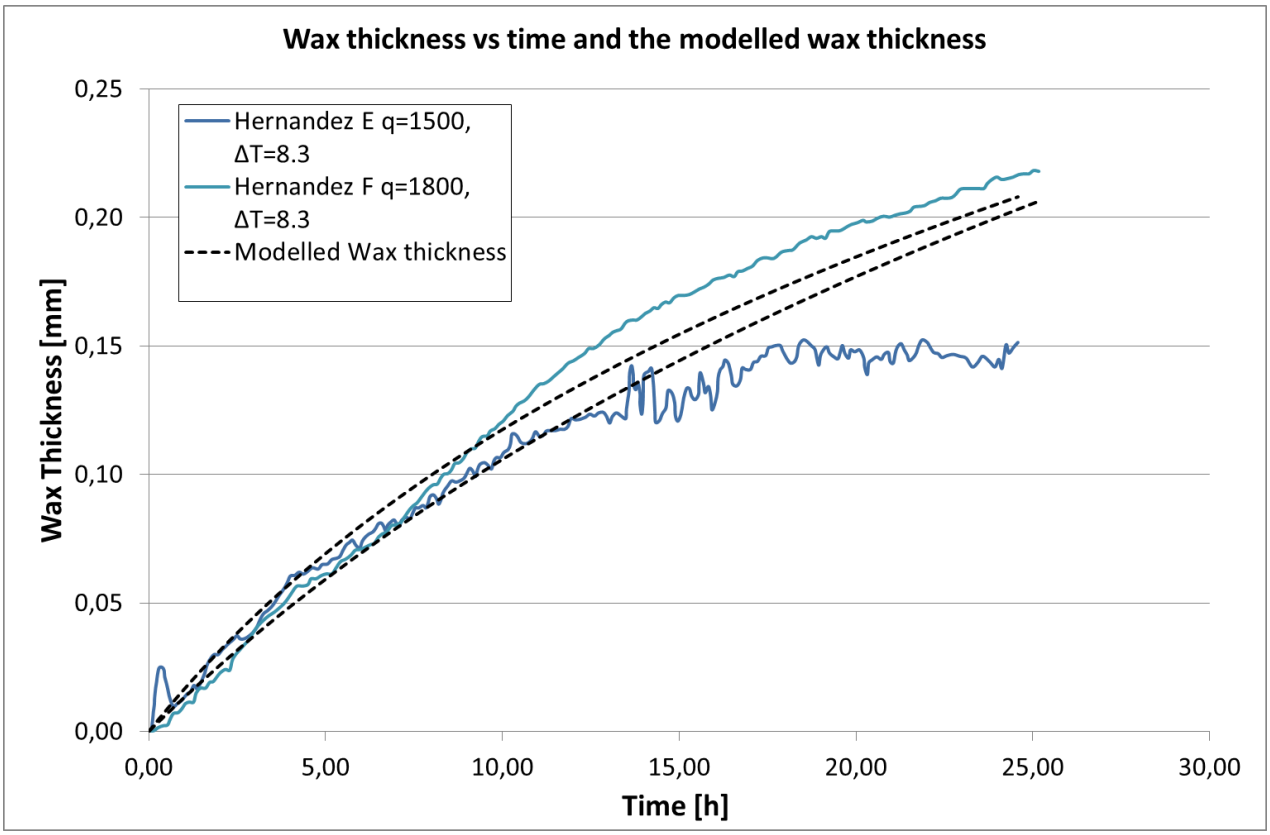

Figure 17: Wax thickness vs. time and best fit with deposition release model for Hernandez digitized experiments.

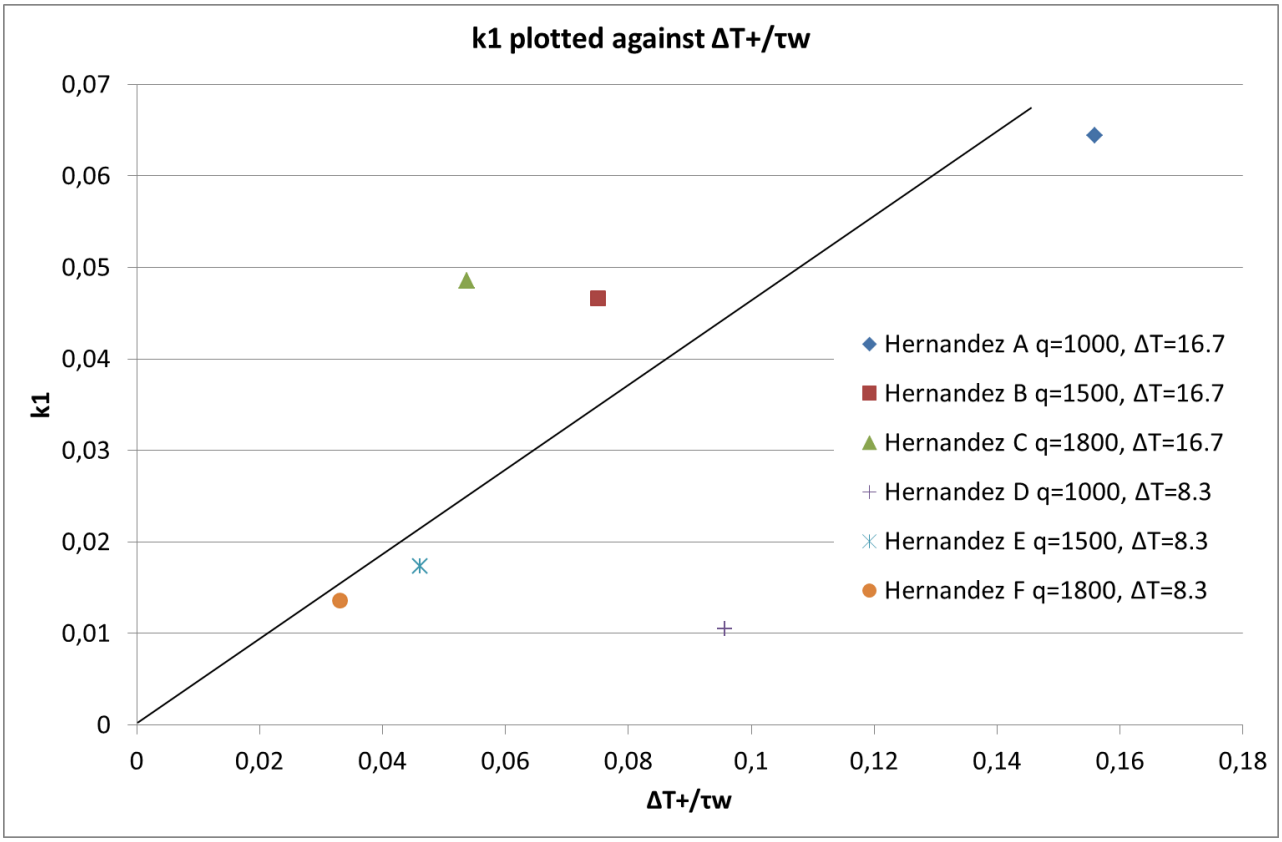

Figure 18: Coefficient k_1 plotted against $\Delta T^+/\tau_w$ from Hernandez series.

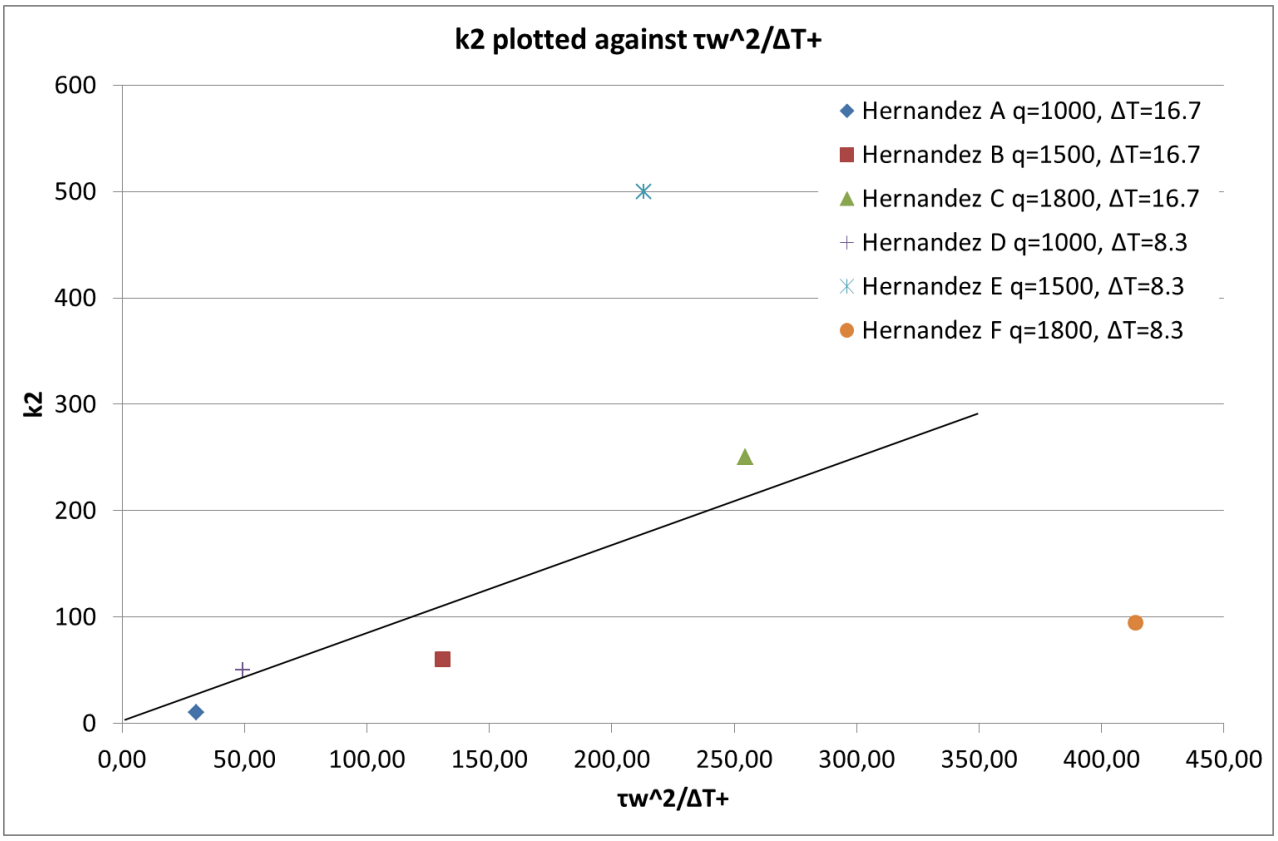

Figure 19: Coefficient k_2 plotted against $\tau_w^2 / \Delta T^+$ from Hernandez series.

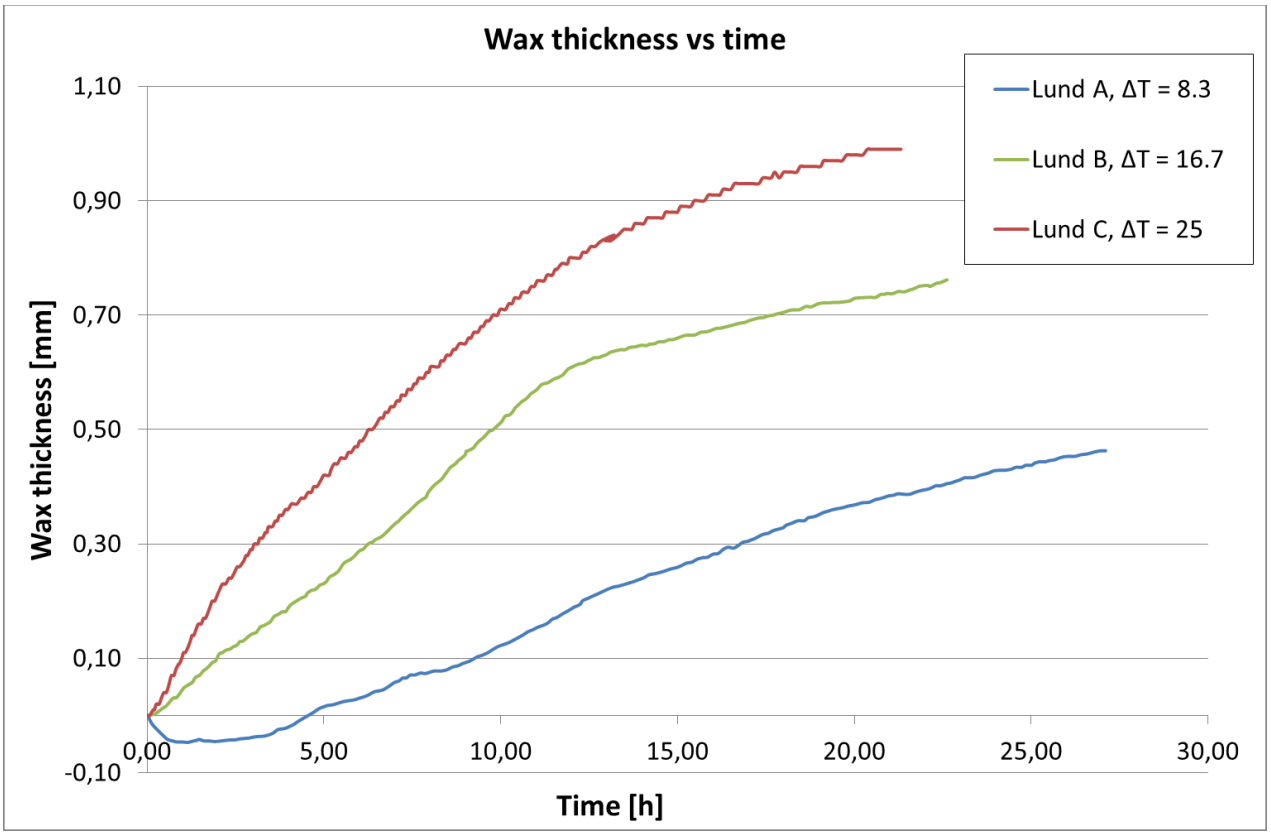

Figure 20: Wax thickness vs. time for Lund digitized experiments.

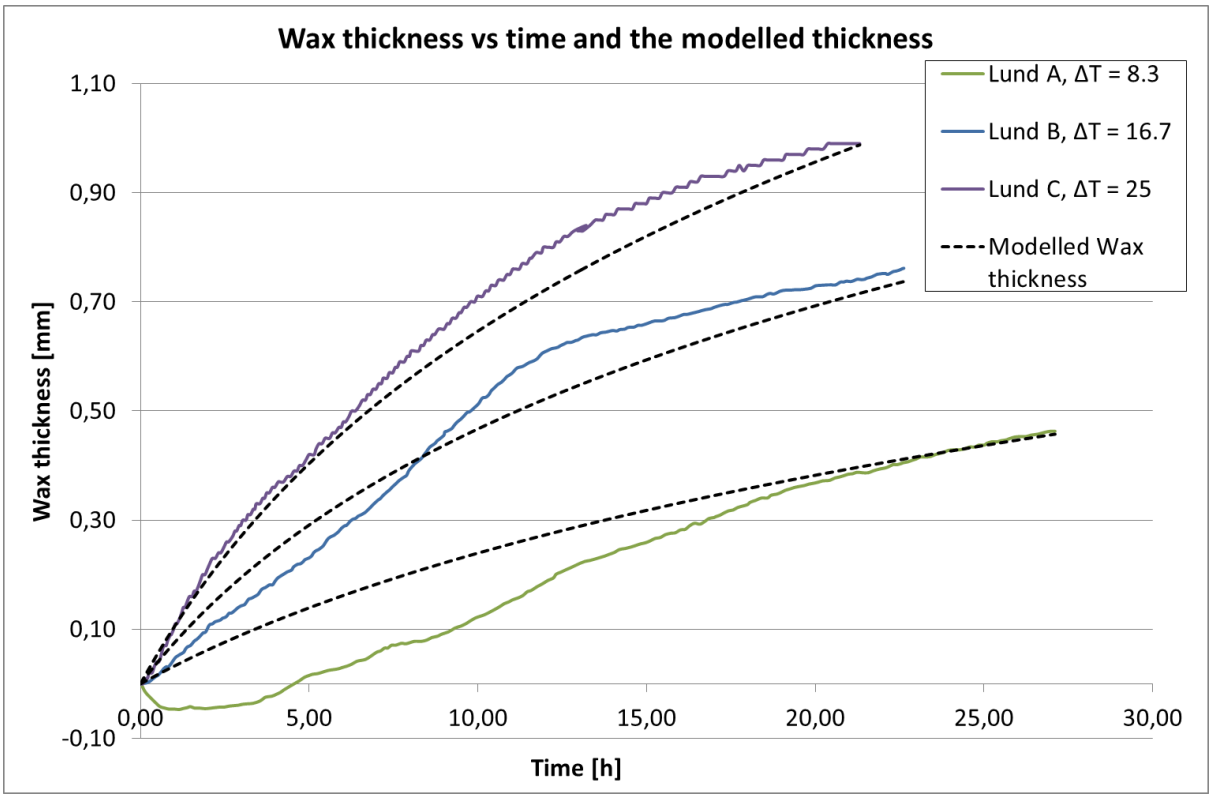

Figure 21: Wax thickness and match with model for Lund digitized experiments.

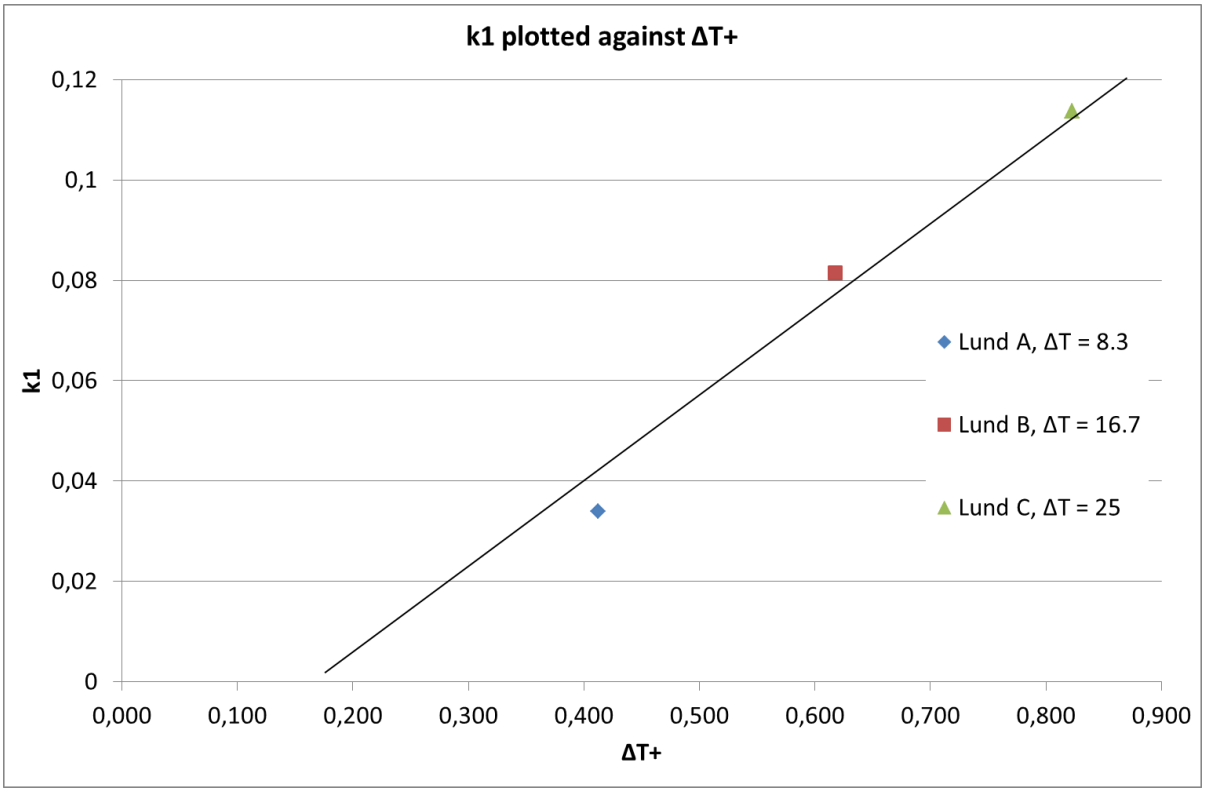

Figure 22: Coefficient k_1 plotted against ΔT^+ from Lund's series.

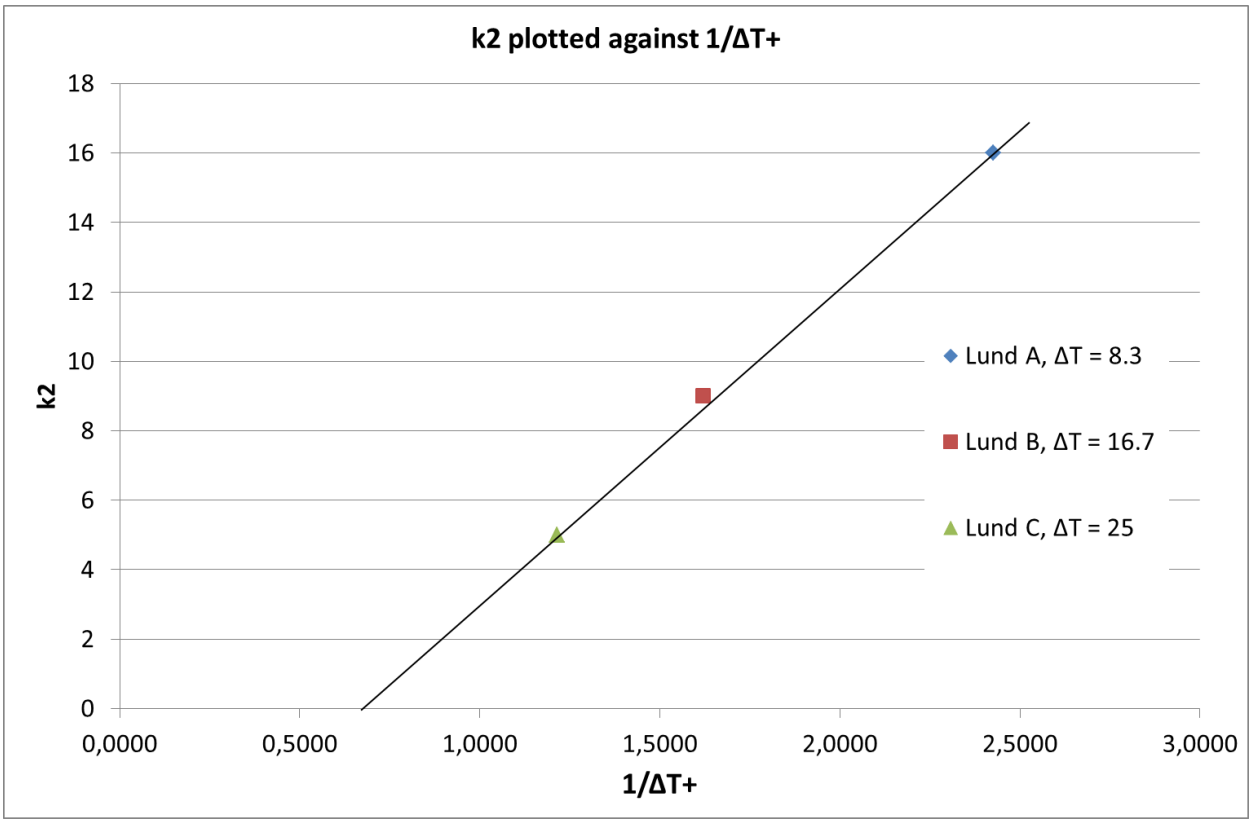

Figure 23: Coefficient k_2 plotted against 1/ ΔT^+ for Lund's series.

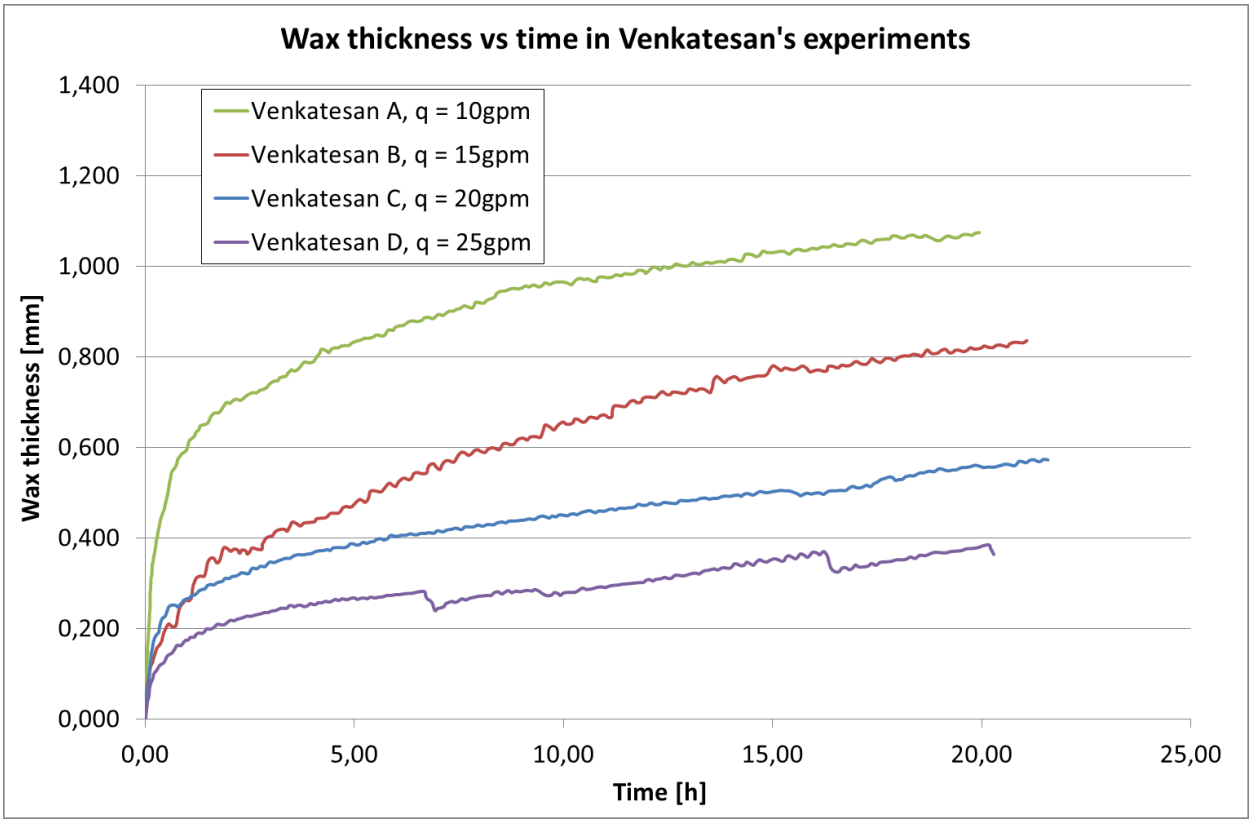

Figure 24: Wax thickness vs. time for Venkatesan's digitized experiments.

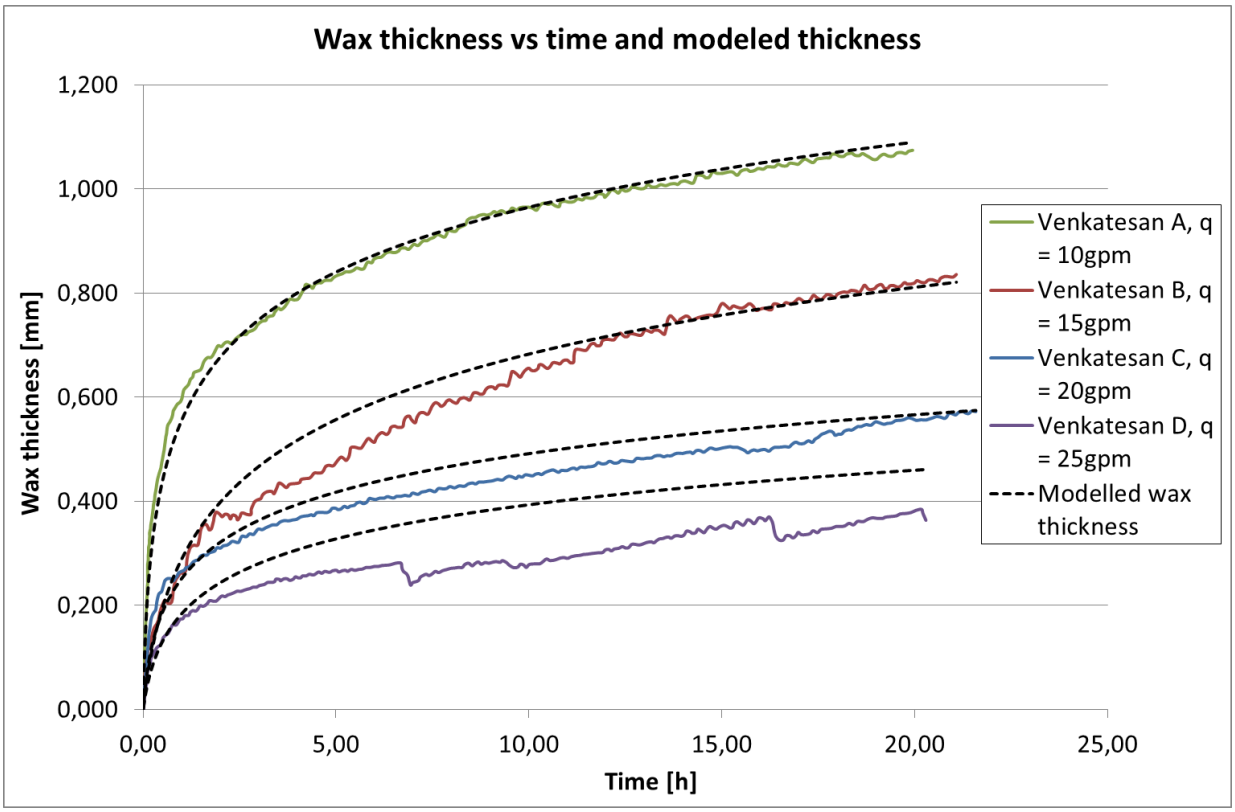

Figure 25: Wax thickness and match with model for Venkatesan's digitized experiments.

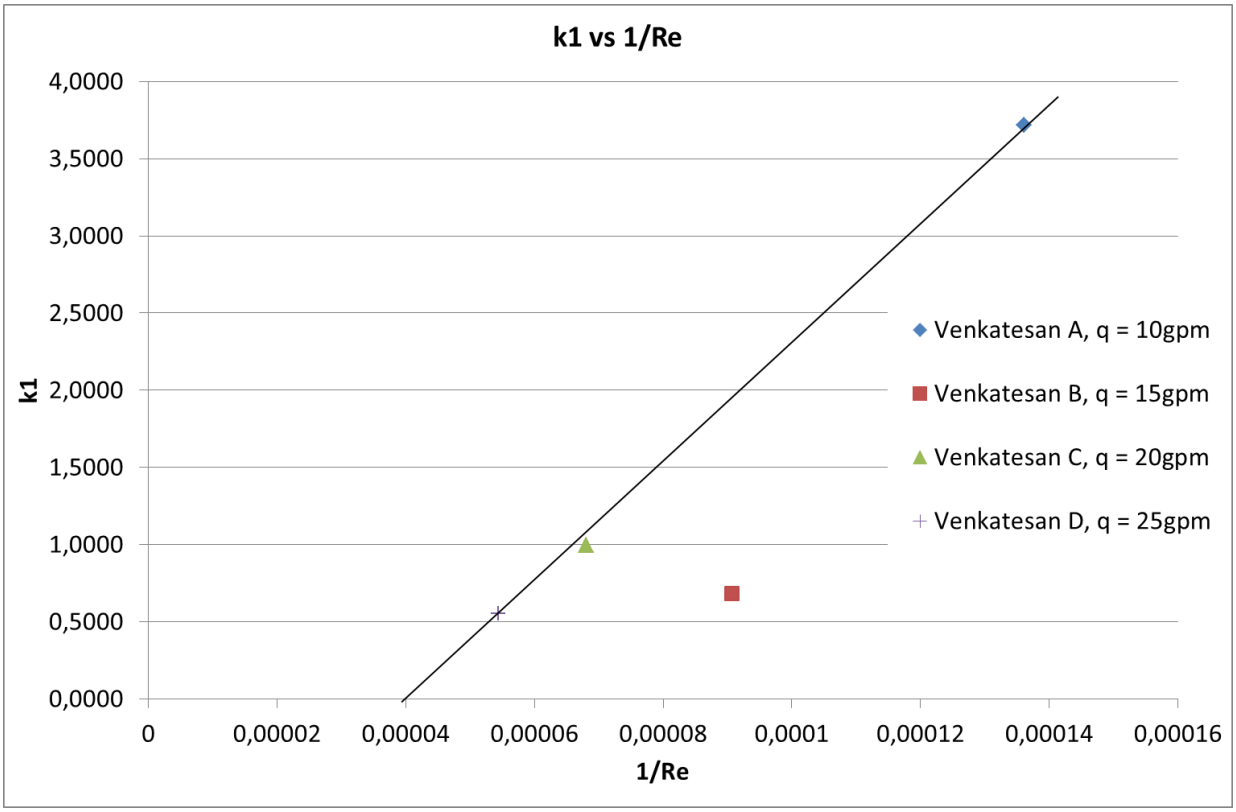

Figure 26: Coefficient k_1 plotted against 1/Re from Venkatesan's series.

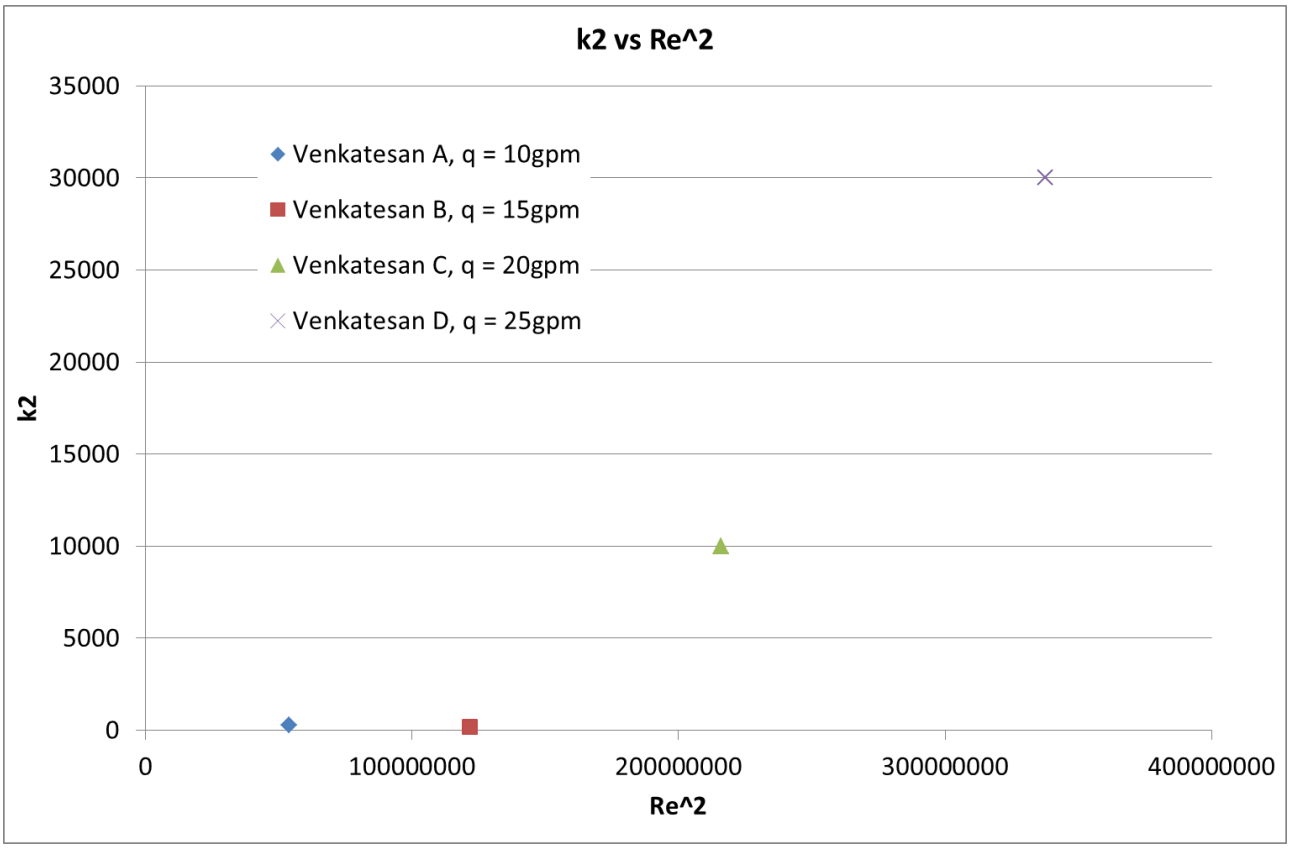

Figure 27: Coefficient k_2 plotted against Re^2 from Venkatesan's series.

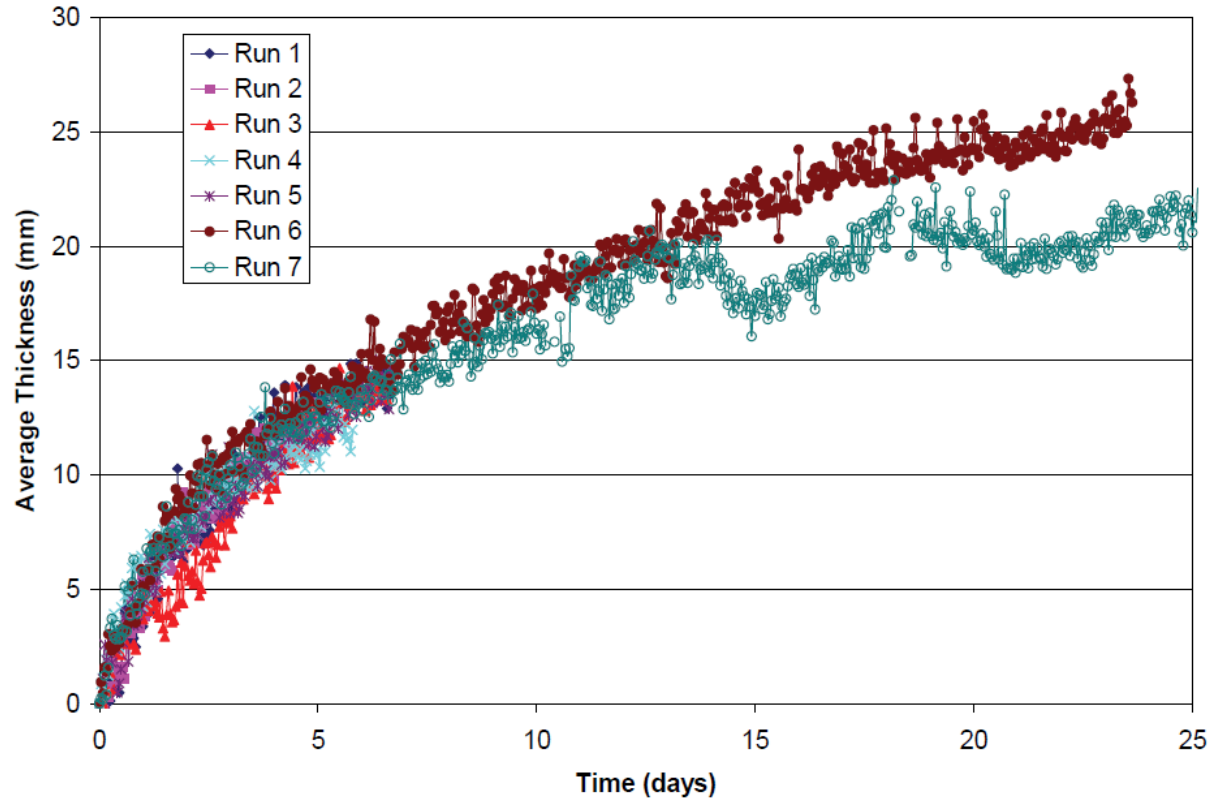

Figure 28: Wax thickness vs time for real pipeline. Ref Singh et al. (2011).

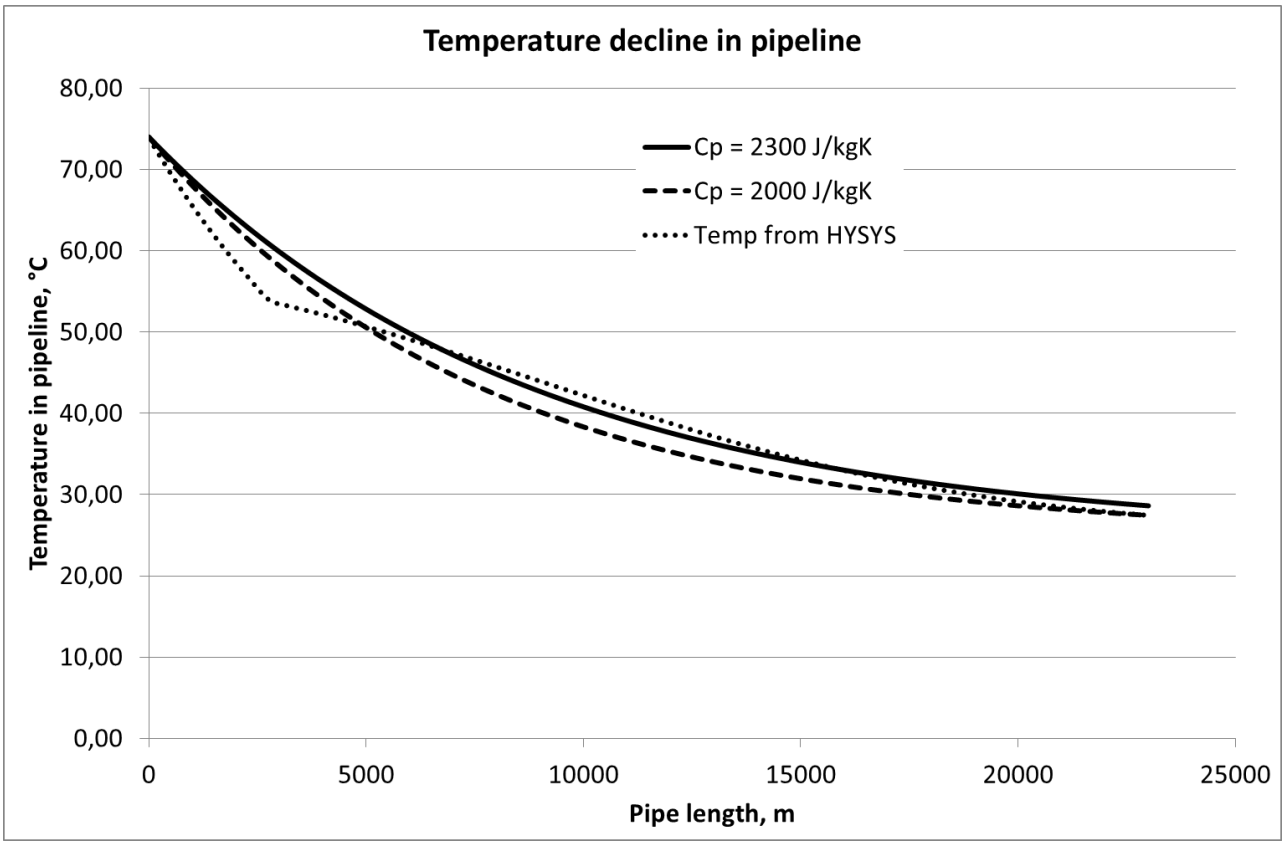

Figure 29: Pipeline temperature vs pipe length for two different heat capacities and a HYSYS simulation.

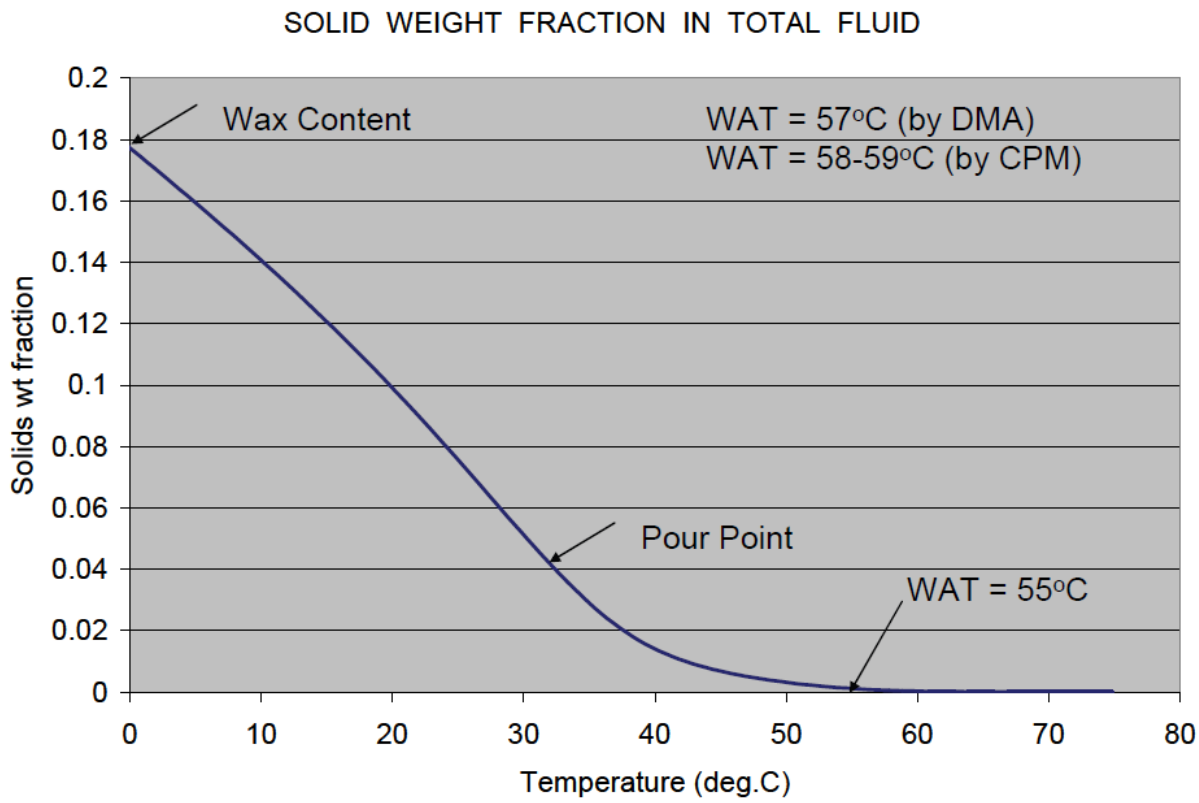

Figure 30: Solid weight fraction vs. temperature. Ref Singh et al. (2011).

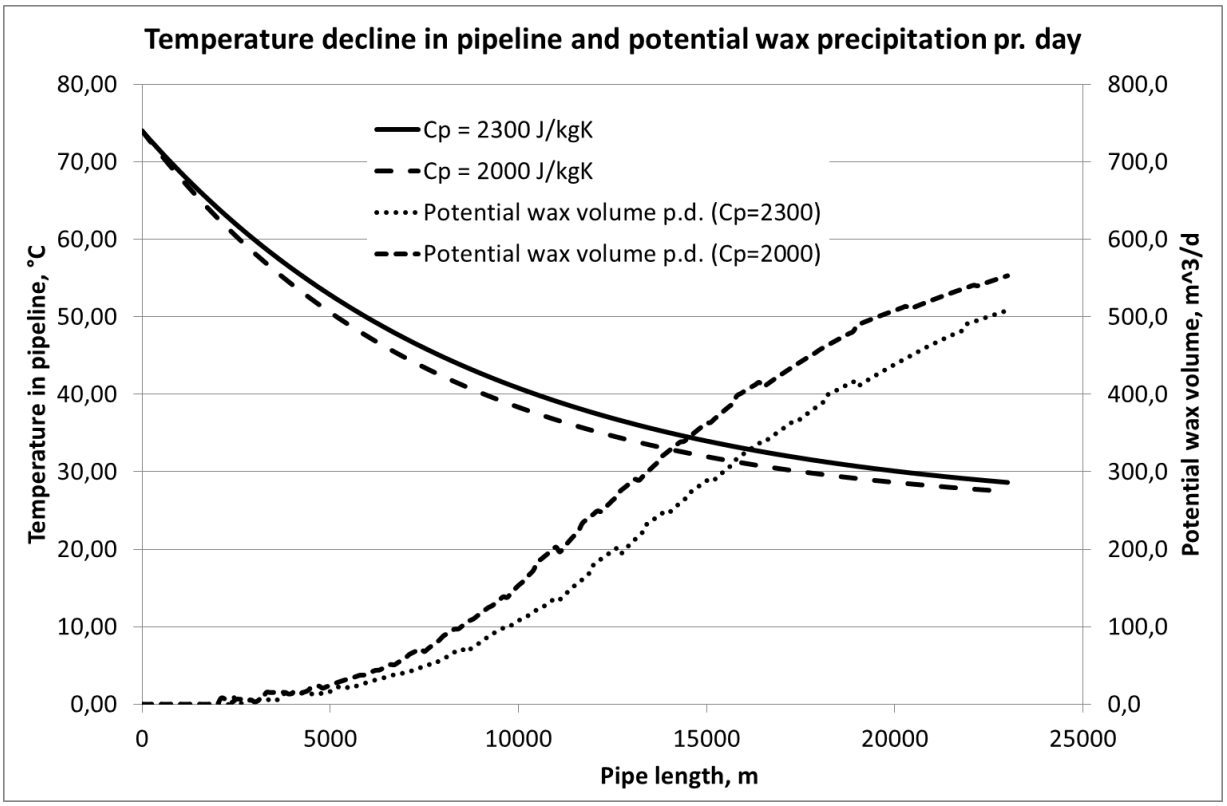

Figure 31: Temperature decline and potential precipitated wax volume vs pipe length.

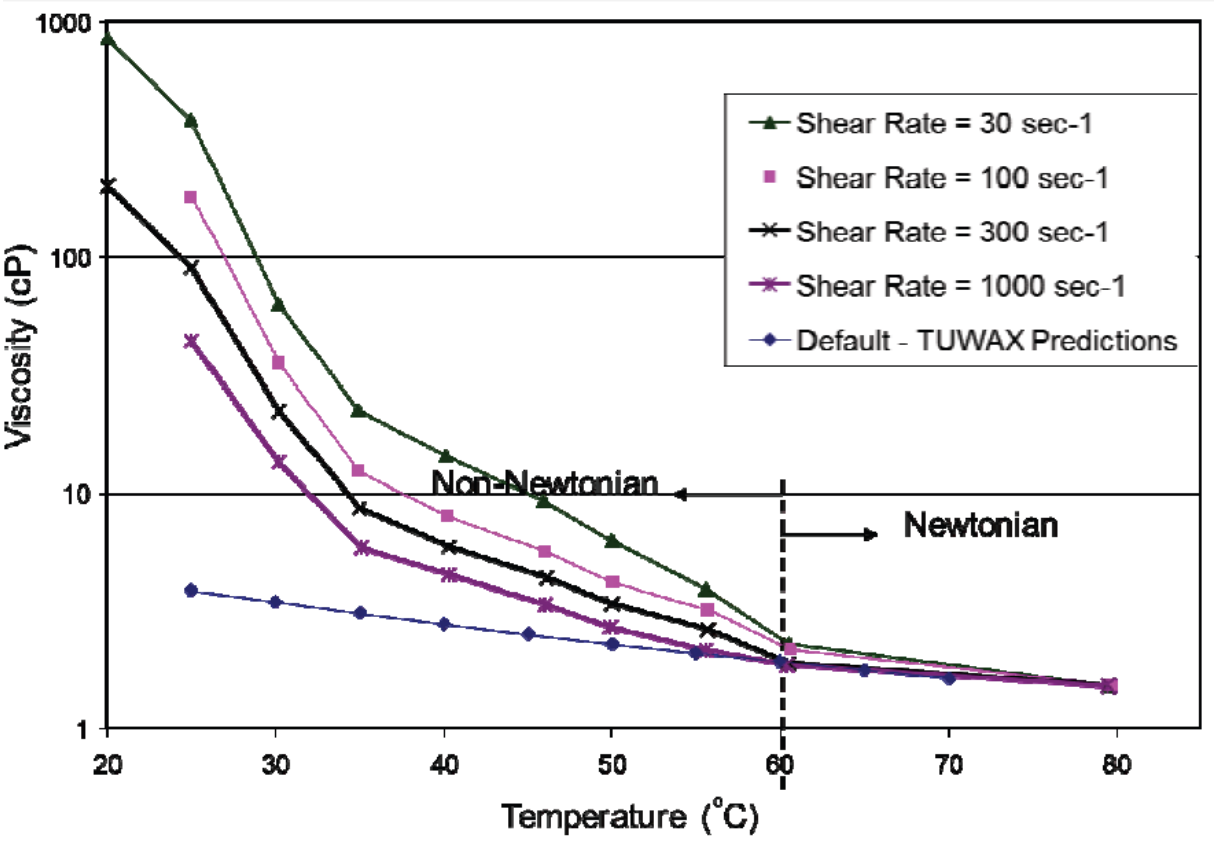

Figure 32: Viscosity and shear rate against temperature. Ref Singh et al. (2011).

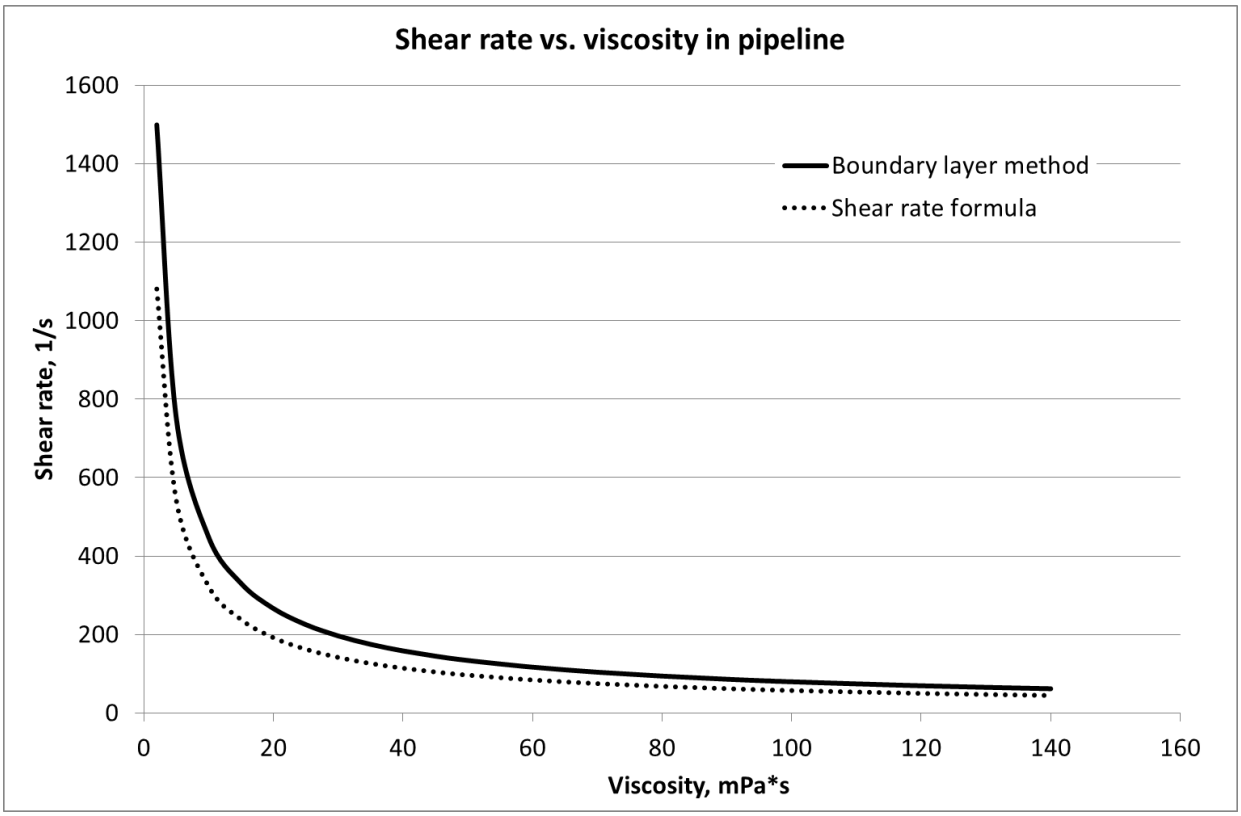

Figure 33: Shear rate calculated in two different ways as a function of viscosity.

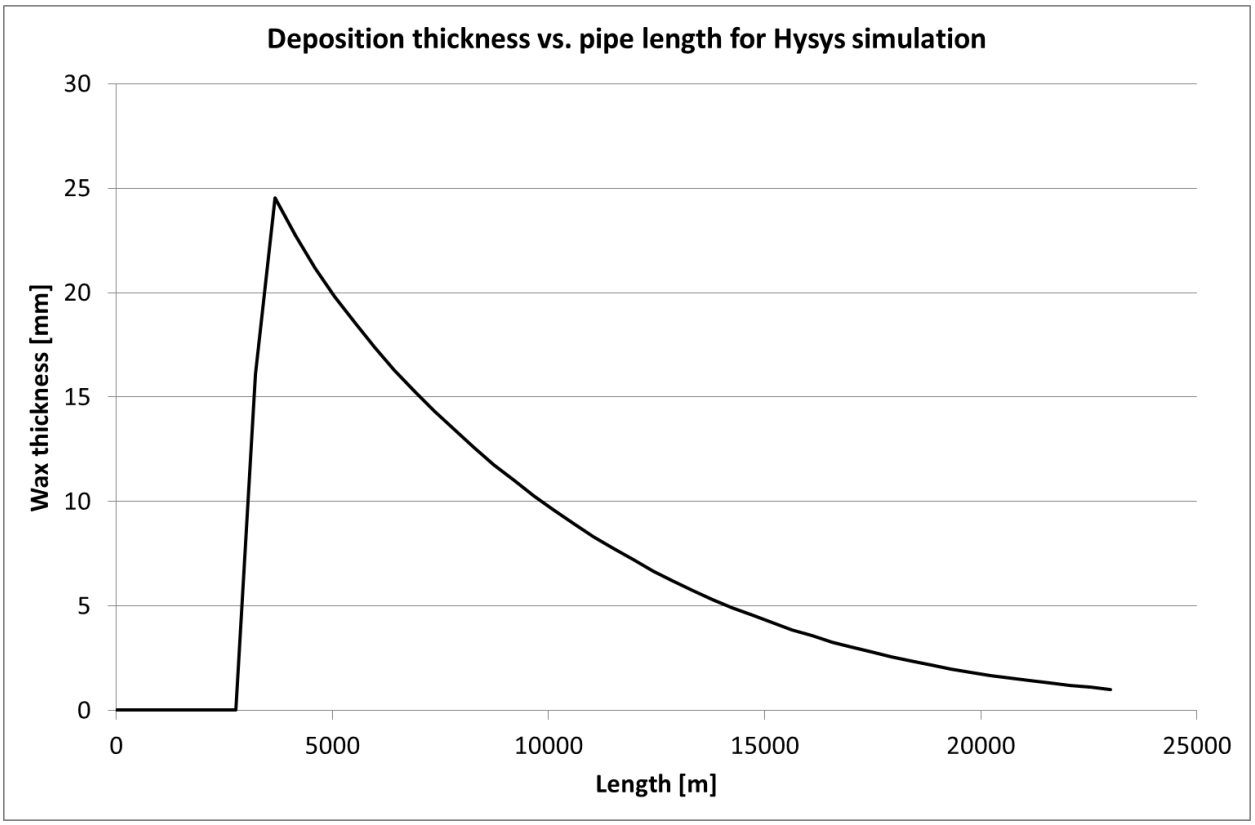

Figure 34: Wax thickness vs. pipe length for the HYSYS simulation.

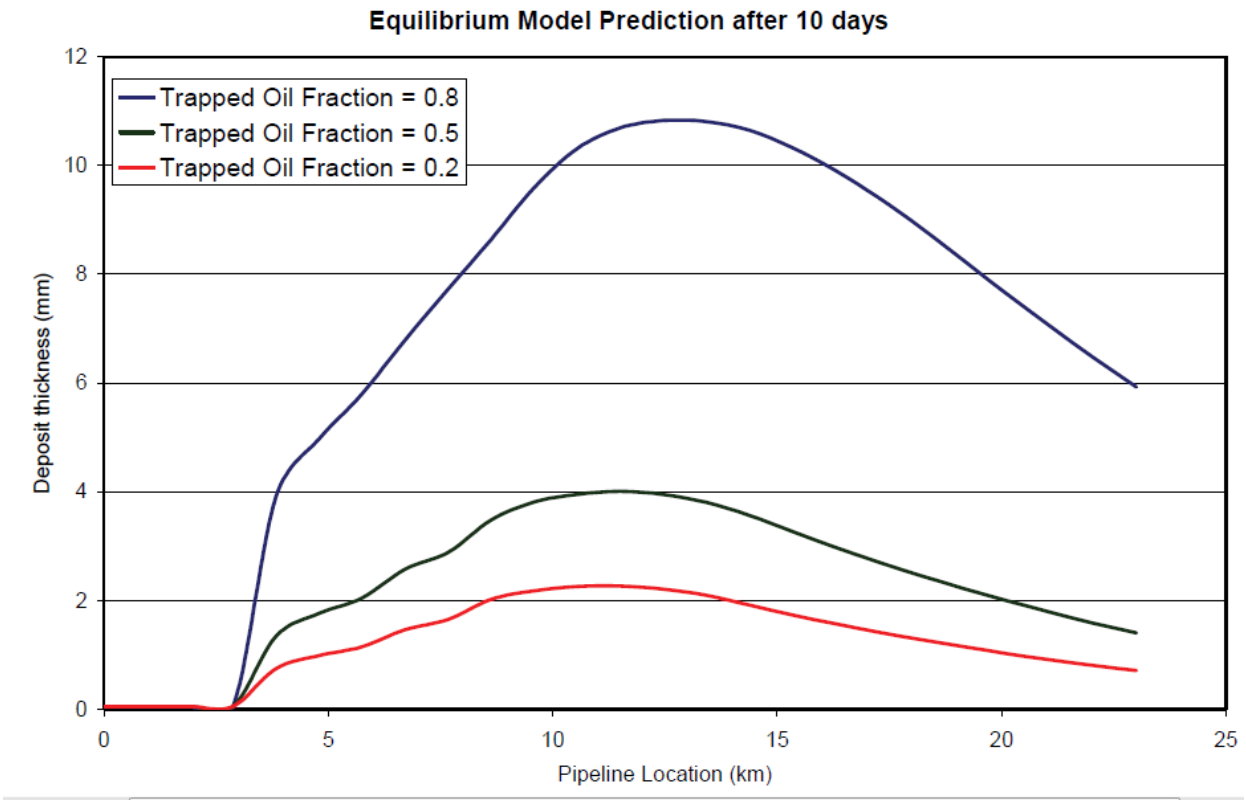

Figure 35: Wax thickness vs. pipe length from TUWAX simulation. Ref Singh et al. (2011)

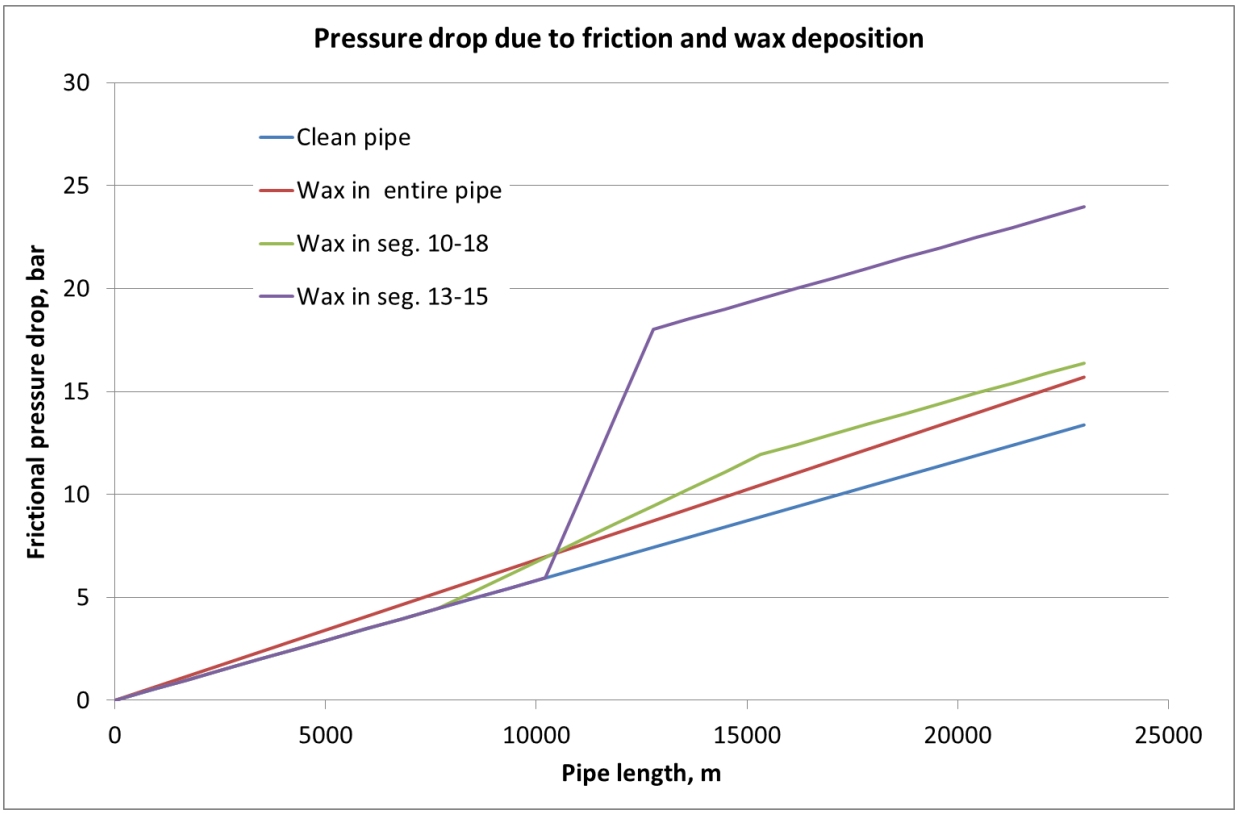

Figure 36: Pressure drop increase for non-evenly distributed deposits.

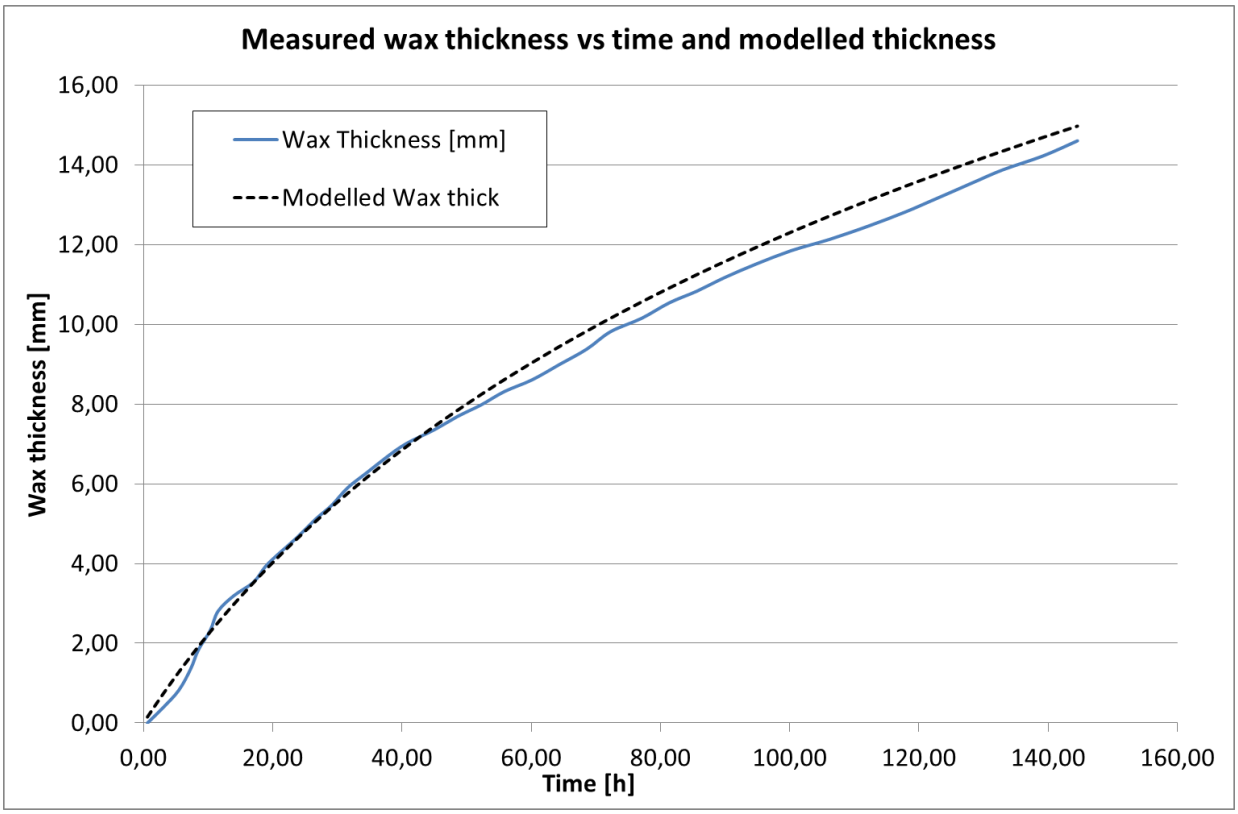

Figure 37: Calculated wax deposition in real pipeline and match with the deposition-release model.

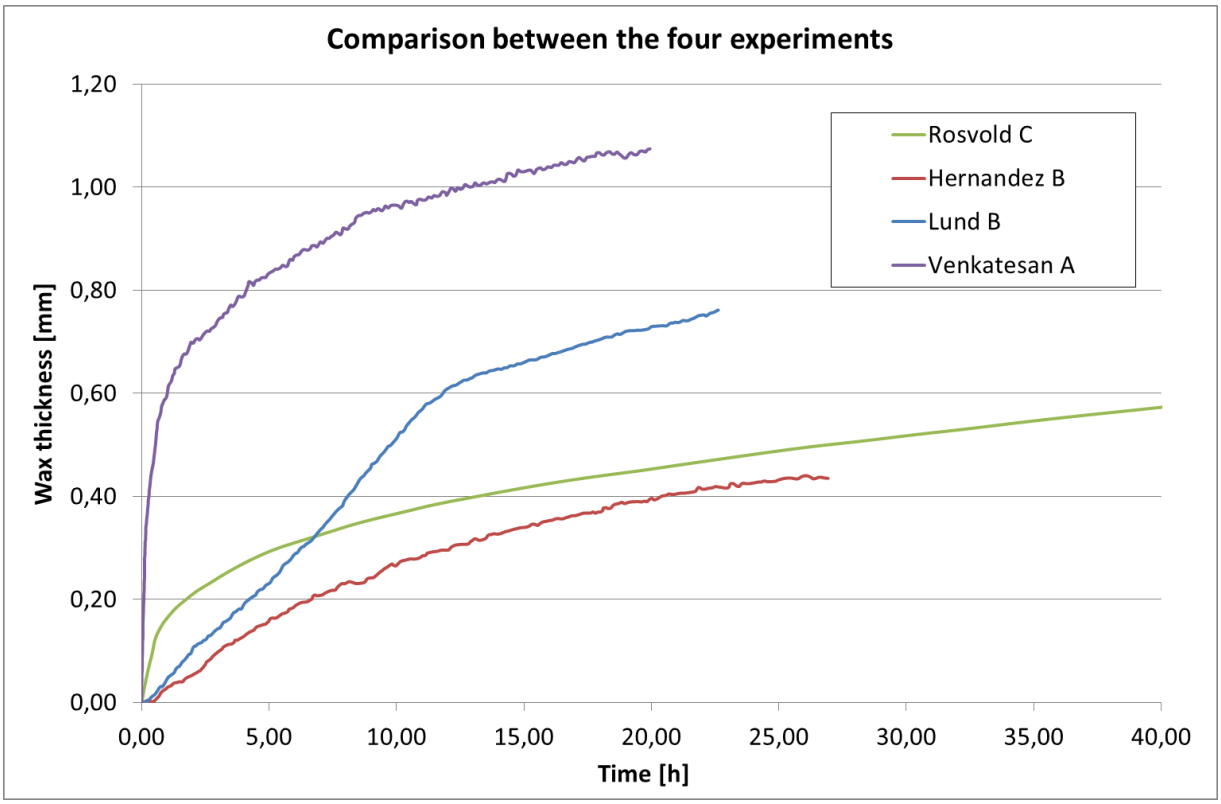

Figure 38: Comparison between four similar experiments from all theses.

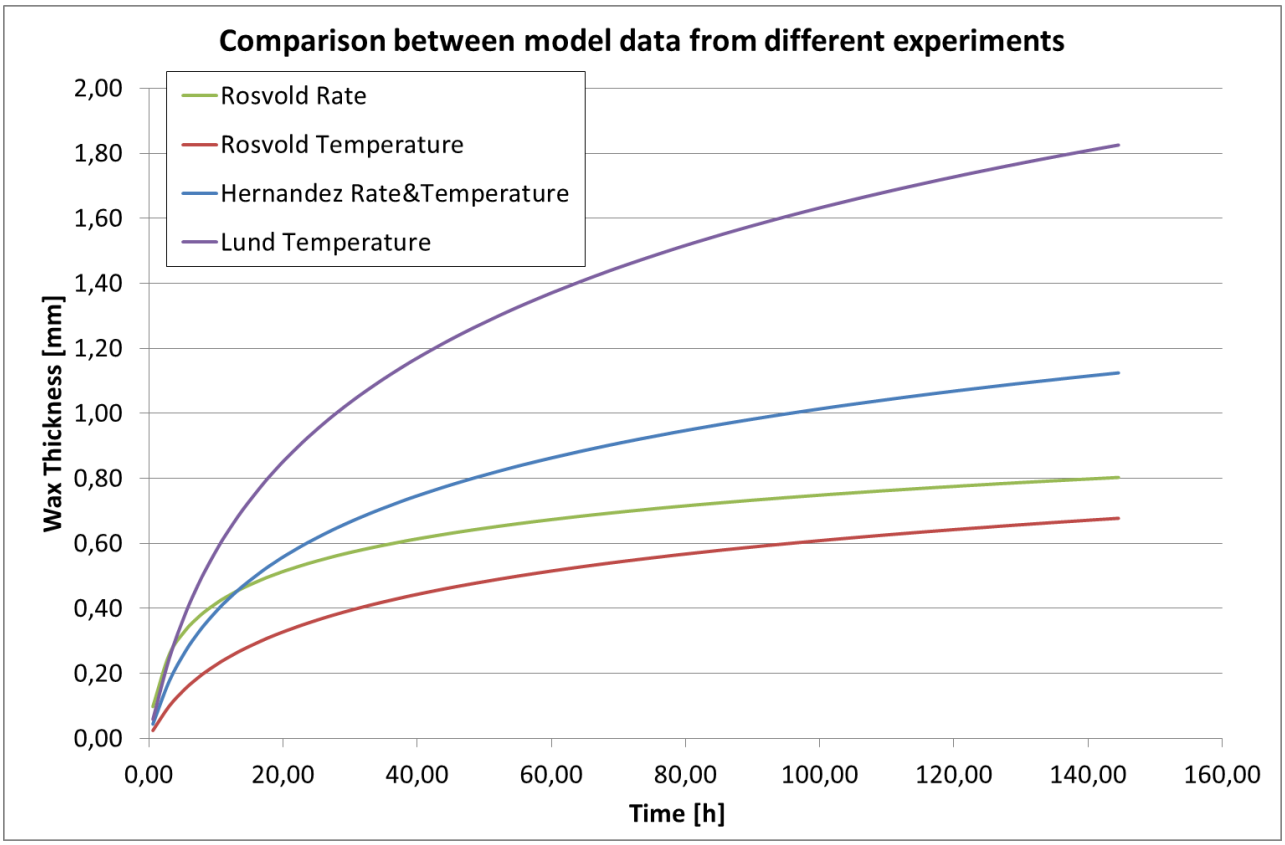

Figure 39: Comparison between model data from all experiments.

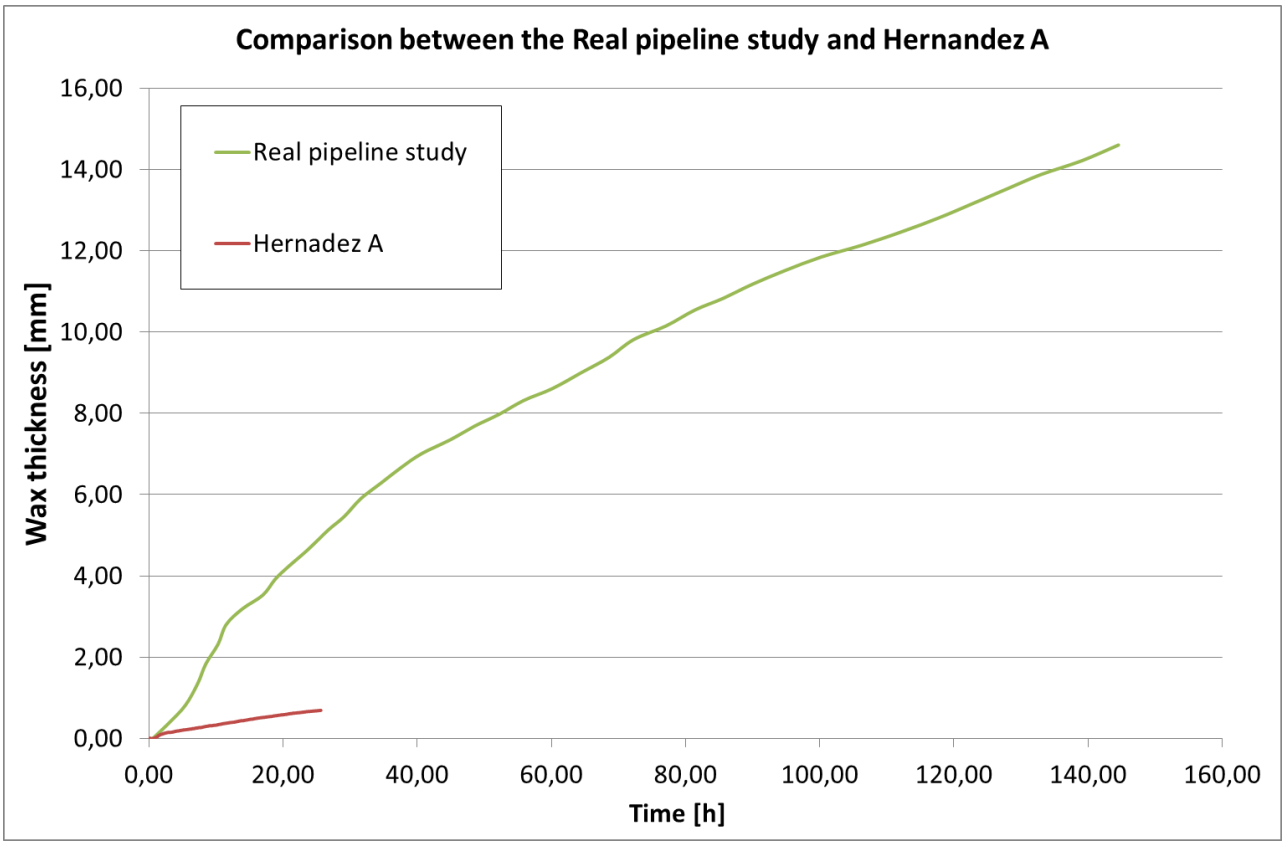

Figure 40: Comparison between the Real pipeline study and the Hernadez A experiment.

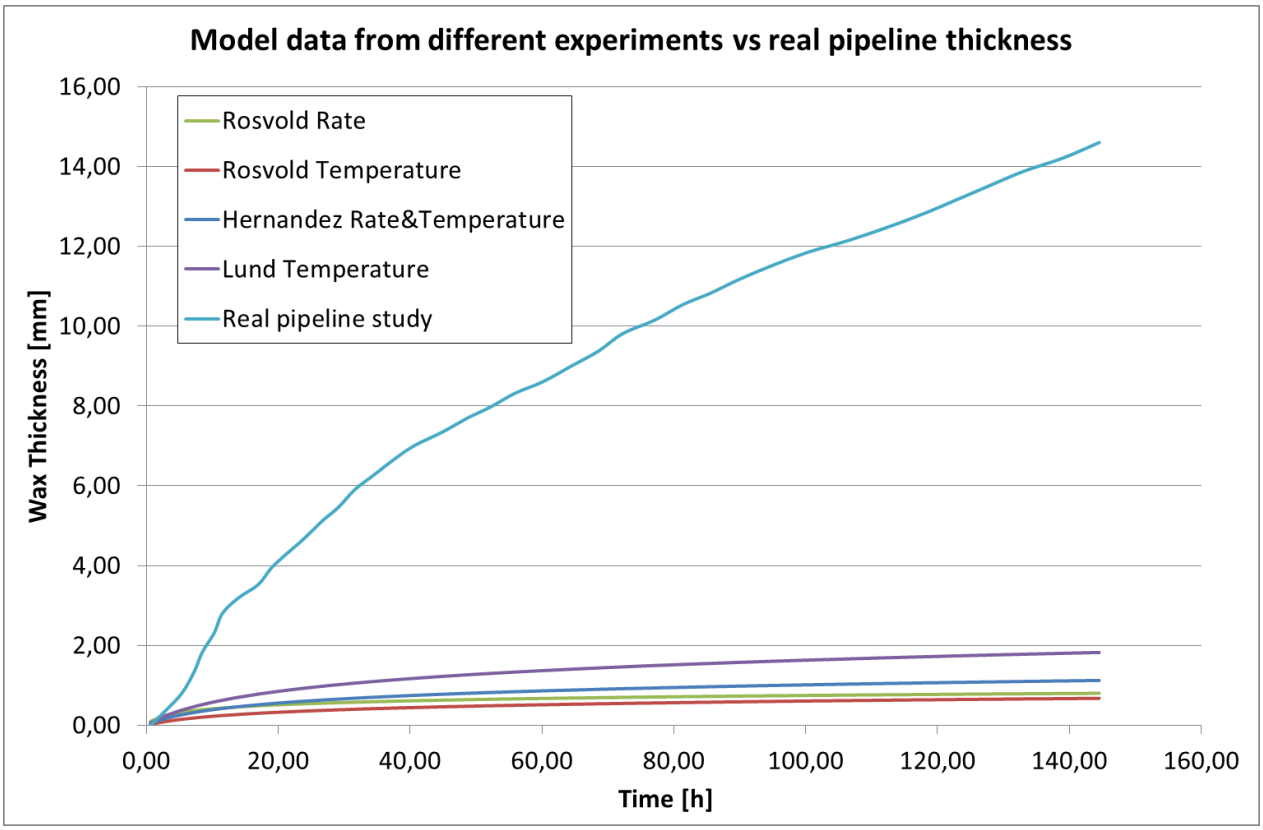

Figure 41: Comparison between the experimental models and the Real pipeline study.

Appendix

Appendix A: Digitizing graphical data

All experiments used in this thesis were performed and given by others. All experiments were plotted as wax thickness against time. In order to utilize these data properly the experiments were digitized. The software used to do this is called Didger (ver. 2). Here is a short presentation on how this was done.

1. The experiments were given in PDF files and plots from these files were saved as a picture file. The picture was then loaded into the Didger software.
2. First four points on each graph was manually selected as accurate as possible (using zoom). The coordinates for the selected point was typed in. For simplicity I used the four points (0, 0), (max x, 0), (0, max y) and (max x, max y). The value of max x and max y varied from graph to graph.
3. Using zoom the entire graph was identified as accurate as possible. Each graph was identified with 120 – 300 points. Any graphs with a big spread were digitized as good as possible by staying in the middle.
4. An output file was saved as a data file and opened in Microsoft Excel. This data file contained the x and y coordinates to all digitized points on a graph. The data was plotted using Excel and the plot was compared to the original from the thesis.

A total of 21 thickness plots were digitized. Most plots were easy to digitize. The original graph for one of Rosvold experiments (experiment A, q = 5 m3/h) had a big spread. A sort of an average line between all the points were used and digitized. The data from this series may not be very accurate, especially the part which shows the initial deposition. All other series showed a very good match with the original plots. Some of the plots from the real pipeline study were also digitized in order to do calculations.

Appendix B: Derivation of the logarithmic model:

$$\frac{dx}{dt} = k_1 {k_2}^{-x} \quad \left(= \frac{k_1}{{k_2}^{x}}\right)$$

Rewrite

$$\frac{{k_2}^{x} dx}{k_1} = dt$$

Integrate

$$\int_0^x \frac{{k_2}^{x} dx}{k_1} = \int_0^t dt$$

Fill in

$$\frac{1}{k_1}\left[\frac{{k_2}^{x}}{\ln k_2}\right]_0^x = [t]_0^t$$

Rewrite

$$\frac{{k_2}^{x}}{\ln k_2} - \frac{1}{\ln k_2} = k_1 t$$

Rewrite

$${k_2}^{x} - 1 = k_1 \ln k_2\, t$$

Rewrite

$${k_2}^{x} = 1 + k_1 \ln k_2\, t$$

Use natural logarithm (ln)

$$\ln {k_2}^{x} = \ln[1 + (k_1 \ln k_2)t]$$

Rewrite

$$x ln\, k_2 = \ln[1 + (k_1 \ln k_2)t]$$

The solution becomes

$$x = \frac{1}{ln\, k_2} \ln[1 + (k_1 \ln k_2)t]$$

Initial rate is given by

$$\frac{dx}{dt}_{x=0} = k_1$$

Appendix C: Estimating k_1 and k_2 in the model

This is a brief introduction to how I estimated the values for parameters k_1 and k_2 in the logarithmic deposition-release model.

$$\frac{dx}{dt}_{x=0} = k_1$$

Estimating k_1

Initial wax buildup is determined by k_1. It can be identified by drawing a tangent line to the start of a graph. I used Microsoft Excel and plotted the first 4-8 points as wax thickness vs. time. Then I used the trend line function through the origin and got an equation for the line. This equation was a linear function like y = ax. Then a [mm/h] is the k_1 value we are looking for. To ensure a good match the tangent was plotted against the entire graph. All tangents found had a good match to the experimental data (digitized data).

Estimating k_2

Values for k_2 in each model was found using tables from digitizing and values for k_1. The logaritmic function derived in Appendix B was used to estimate k_2.

$$x = \frac{1}{ln\ k_2} \ln[1 + (k_1 \ln k_2)t]$$

This function or equation is not solvable for k_2 in a regular way. I used the solver function in Excel to help me with this. Parameter k_2 was set equal to 1 and wax thickness (x_{calc}) was calculated using time (t) and already estimated values of k_1. The solver function was then used in order to find the k_2 that would give $x_{calc} = x_{real}$.

In order to match k_2 with all points in the experimental table this method was applied to all points. A macro was used so that Excel would perform this procedure automatically on all points. This produced a different value for k_2 in each point. A small range of values was selected from this table and used to make a wax thickness plot. This plot was then compared to the experimental plot showing different k_2 values against the digitized experiment. The k_2 value with the best fit to the experimental plot was selected as the best match.
A simple try and fail method from the start would probably produce the same result. But in order to save time I choose the procedure described here.

Appendix D: Calculating particle mass transfer

The individual particle size of wax crystals was reported to in the range between 1-10 µm. The smallest crystals were found in condensate while the larger crystals were found in crude oil. The fluid used in Rosvold's experiments was waxy gas condensate. A particle size below 10 µm seems like a reasonable assumption. Another assumption needed in these calculations was the density of the wax particles. A typical wax particle density of 930-970 kg/m^3 was given by Gudmundsson (2010). The density of 970 kg/m^3 was selected in these calculations.

The particle relaxation time were calculated and used to calculate the dimensionless particle relaxation time. Formulas used were (Gudmundsson 2010):

$$\tau_p = \frac{\rho_p d^2}{18\,\mu} \quad , \quad u^* = u * \sqrt{\frac{f}{8}} \quad \& \quad {\tau_p}^+ = \frac{\tau_p \rho {u^*}^2}{\mu}$$

Where τ_p is particle relaxation time, ρ_p is particle density, d is particle diameter, µ is viscosity, u* is friction velocity, u is average velocity, f is friction factor, ${\tau_p}^+$ is dimensionless particle relaxation time and ρ is oil density. Dimensionless particle relaxation times were calculated using crystal sizes of 1, 10 and 100 µm. The 100 µm is well above the expected size. The dimensionless particle relaxation times are given for different crystals sizes below (for Rosvold's q_o = 25 m^3/h series).

d [µm]	τ_p+
1	5,17E-05
10	0,00517
100	0,517

The flow regime of the particles is dependent on the dimensionless particle relaxation times. The regime gives the approximate value of the dimensionless particle mass transfer coefficient, h^+. The values determining the regime are specified below (Gudmundsson 2010).

Regime	τ_p+	h+
Diffusion	<0,1	10^{-3}-10^{-4}
Inertia	0,1-10	10^{-4}-10^{-1}
Impaction	>10	10^{-1}

With particle diameter between 1-10 µm the relaxation times values are well inside the limit for the diffusion regime. The diffusion regime gives a dimensionless mass transfer coefficient between 10^{-3} and 10^{-4}. The particle mass transfer coefficient is given by multiplying the friction velocity with the dimensionless mass transfer coefficient.

Appendix E: Derivation of pressured drop method

The study of the real subsea pipeline by Singh et al. (2011) calculates wax thickness from measured pressure drop. The method is derived and explained here. The basis for the calculations is the Darcy-Weisbach equation (Gudmundsson 2009).

$$\Delta p = \frac{f}{2}\frac{L}{d}\,\rho u^2$$

The friction factor is determined by the Blasius friction factor correlation $f = 0.316/Re^{0.25}$ and put into the equation.

$$\Delta p = \frac{0.316}{2Re^{0.25}}\frac{L}{d}\,\rho u^2$$

The diameter is replaced by the radius, d = 2r.

$$\Delta p = \frac{0.316}{2Re^{0.25}}\frac{L}{2r}\,\rho u^2$$

Rewrite

$$\frac{0.158L}{2r}\frac{\rho u^2}{Re^{0.25}}$$

Fill in for Reynolds number and rewrite, $Re = 2\rho ur/\mu$.

$$\Delta \mathrm{p} = \frac{0.158L}{2r}\left(\frac{\mu}{2r\rho u}\right)^{0.25}\,\rho u^2$$

Rewrite

$$\Delta \mathrm{p} = \frac{0.158L}{2r}\frac{\mu^{0.25}}{(2r)^{0.25}\rho^{0.25}u^{0.25}}\,\rho u^2$$

Rewrite

$$\Delta \mathrm{p} = \frac{0.158L\mu^{0.25}}{(2r)^{1.25}}\,\rho^{0.75}u^{1.75}$$

When wax deposits in the pipe the diameter of the pipe decreases and the velocity will increase. The radius given in the formula above will also change when wax is deposited. All other parameters are assumed constant when wax deposition decrease pipe diameter. The production rate stays constantan when wax deposits.

$$q_{no\ wax} = q_{with\ wax} =>$$

q = u*A:

$$u_0 A_0 = uA$$

The 0 denotes a clean pipe (no wax). Fill in for area in the equation above.

$$u_0\,\pi {r_0}^2 = u\,\pi r^2$$

Solve for u.

$$u = u_0 \left(\frac{r_0}{r}\right)^2 = u_0 \left(\frac{2r_0}{2r}\right)^2$$

Fill in for u in the pressure drop equation given above.

$$\Delta p = \frac{0.158 L \mu^{0.25}}{(2r)^{1.25}} \rho^{0.75} \left(u_0 \left(\frac{2r_0}{2r}\right)^2\right)^{1.75}$$

Rewrite

$$\Delta p = \frac{0.158 L \mu^{0.25}}{(2r)^{1.25}} \rho^{0.75} {u_0}^{1.75} \left(\frac{2r_0}{2r}\right)^{3.5}$$

Rewrite the equation above.

$$\Delta p = \frac{0.158 L \mu^{0.25}}{(2r)^{4.75}} \rho^{0.75} {u_0}^{1.75} (2r_0)^{3.5}$$

Singh et al. (2011) introduce a parameter called κ ($\kappa = \Delta P / {u_0}^{1.75}$). This parameter was introduced to normalize fluctuations in the pressure drop caused by flow rate changes. The κ parameter can be written like this.

$$\kappa = \frac{\Delta P}{{u_0}^{1.75}} = \frac{0.158 L \mu^{0.25}}{(2r)^{4.75}} \rho^{0.75} (2r_0)^{3.5}$$

When wax deposits the only parameters that will change in the equation above is the radius r. The wax thickness is calculated by comparing κ before and after deposition.

$$\frac{\kappa}{\kappa_0} = \frac{(2r_0)^{4.75}}{(2r)^{4.75}}$$

The R can also be specified as $r = r_0 - x$, where x is the wax thickness. Fill in for r in the equation above.

$$\frac{\kappa}{\kappa_0} = \frac{(2r_0)^{4.75}}{(2r_0 - 2x)^{4.75}}$$

Turn the equation.

$$\frac{\kappa_0}{\kappa} = \frac{(2r_0 - 2x)^{4.75}}{(2r_0)^{4.75}}$$

Rewrite.

$$\frac{2r_0 - 2x}{2r_0} = \left(\frac{\kappa_0}{\kappa}\right)^{\frac{1}{4.75}}$$

Rearrange

$$2r_0 - 2x = 2r_0 \left(\frac{\kappa_0}{\kappa}\right)^{1/4.75}$$

Solve for x and the final equation becomes.

$$x = r_o\left(1 - \left(\frac{\kappa_0}{\kappa}\right)^{1/4.75}\right)$$

Appendix F: Calculations of shear rate

The shear rate in the real subsea pipeline studied by Singh et al. (2011) was calculated in two different ways.

Boundary layer method

The velocity and the thickness of the boundary layer can be calculated using formulas given by Gudmundsson (2009). The dimensionless boundary layer thickness for viscous sub layer is $y^+ < 5$ (Gudmundsson 2009). The thickness of the viscous sub (y) layer is calculated by rearranging this formula.

$$y^+ = \frac{yu^*\rho}{\mu}$$

Rearrange.

$$y = \frac{y^+\mu}{u^*\rho}$$

Where u* is friction velocity and μ is the viscosity. The dimensionless sub layer viscosity (u^+) is set to $u^+ = y^+$. The velocity at the sub layer is calculated be rearing the formula.

$$u^+ = \frac{u}{u^*}$$

Rearrange

$$u = u^+u^*$$

Newtonian fluid in the viscous sub layer is assumed. A linear increase in velocity with distance from the wall is assumed. The shear rate (du/dy) is then calculated by.

$$\frac{du}{dy} \approx \frac{u}{y}$$

The shear rate is given in s^{-1}. Since the viscosity of a fluid change with temperature the shear rate is shown as a function of velocity in Figure 33.

Using viscosity definition

The viscosity definition given by White (2008) gives the relationship between shear stress and viscosity by using the shear rate.

$$\tau = \mu\frac{du}{dy}$$

The wall shear stress (Equation 3.1) is

$$\tau = \frac{1}{8} f \rho u^2$$

The two equations are put equal to each other and solved for shear rate.

$$\mu \frac{du}{dy} = \frac{1}{8} f \rho u^2$$

Solve for shear rate:

$$\frac{du}{dy} = \frac{1}{8} \frac{f \rho u^2}{\mu}$$

This equation is also solved for a range of viscosity as shown in Figure 33. The two methods give very similar shear rates as seen in Figure 33.